2015-09-11

ATP-Dependent Heterochromatin Remodeling: A Dissertation

Benjamin J. Manning
University of Massachusetts Medical School

ATP-DEPENDENT HETEROCHROMATIN REMODELING

A Dissertation Presented

By

BENJAMIN JON MANNING

Submitted to the Faculty of the

University of Massachusetts Graduate School of Biomedical Sciences, Worcester

In partial fulfillment of the requirements for the degree of

DOCTOR OF PHILOSOPHY

September 11th, 2015

Interdisciplinary Graduate Program

ATP-DEPENDENT HETEROCHROMATIN REMODELING

A Dissertation Presented By

BENJAMIN JON MANNING

The signatures of the Dissertation Defense Committee signify completion and approval as to style and content of the Dissertation

Craig Peterson, Ph. D., Thesis Advisor

Paul Kaufman, Ph. D., Member of Committee

Sharon Cantor, Ph. D., Member of Committee

Thomas Fazzio, Ph. D., Member of Committee

Danesh Moazed, Ph. D., Member of Committee

The signature of the Chair of the Committee signifies that the written dissertation meets the requirements of the Dissertation Committee

Kendall Knight, Ph. D., Chair of Committee

The signature of the Dean of the Graduate School of Biomedical Sciences signifies that the student has met all graduation requirements of the school.

Anthony Carruthers, Ph.D., Dean of the Graduate School of Biomedical Sciences

Interdisciplinary Graduate Program

September 11th, 2015

To education, independence, and basic science research.

Acknowledgements

First, I would like to thank my thesis mentor, Craig. Your wealth of knowledge, natural curiosity, rigorous skepticism, patience, and keen sense for both priority and perspective are inspiring. You provided plenty of independence for scientific exploration, yet your office/iPhone was always open/on, for 'preliminary' good results or for 'important control' bad results. I have learned a lot from you.

I thank every member of the Peterson lab for providing such an open, collaborative dynamic to my graduate career. I thank Nicholas, Mayuri, Shinya, and Kim for the vast amount of assistance and insight they've given me. I also thank Chris, Sarah, Sal, Marty, Welles, and Nate for making each day in lab fun.

I thank my TRAC members, Paul Kaufman, Kendall Knight, Sharon Cantor, and Anthony Imbalzano for their time, guidance, and constructive criticism—both from a science perspective, and from a career development perspective. I would also like to thank Thomas Fazzio and Danesh Moazed for dedicating their time to participate in my DEC. I thank Darla, IGP, and the GSBS for all the effort that they put forth for the students here at UMASS Medical.

Finally, I thank my family and friends for supporting me: my parents, Jen and Pete, for raising me; my brothers, Jer, Josh and Sam, for being there for me; my fiancée, Jen, for inspiring me to keep improving; and my close friends, Jake, Rick, Dan, Ben, Greg, Felix, Han, Nick, and Mayu, for helping me to keep on going.

ABSTRACT

Eukaryotic DNA is incorporated into the nucleoprotein structure of chromatin. This structure is essential for the proper storage, maintenance, regulation, and function of the genomes' constituent genes and genomic sequences. Importantly, cells generate discrete types of chromatin that impart distinct properties on genomic loci; euchromatin is an open and active compartment of the genome, and heterochromatin is a restricted and inactive compartment. Heterochromatin serves many purposes *in vivo*, from heritably silencing key gene loci during embryonic development, to preventing aberrant DNA repeat recombination. Despite this generally repressive role, the DNA contained within heterochromatin must still be repaired and replicated, creating a need for regulated dynamic access into silent heterochromatin. In this work, we discover and characterize activities that the ATP-dependent chromatin remodeling enzyme SWI/SNF uses to disrupt repressive heterochromatin structure.

First, we find two specific physical interactions between the SWI/SNF core subunit Swi2p and the heterochromatin structural protein Sir3p. We find that disrupting these physical interactions results in a SWI/SNF complex that can hydrolyze ATP and slide nucleosomes like normal, but is defective in its ability to evict Sir3p off of heterochromatin. *In vivo*, we find that this Sir3p eviction activity is required for proper DNA replication, and for establishment of silent chromatin,

but not for SWI/SNF's traditional roles in transcription. These data establish new roles for ATP-dependent chromatin remodeling in regulating heterochromatin.

Second, we discover that SWI/SNF can disrupt heterochromatin structures that contain all three Sir proteins: Sir2p, Sir3p and Sir4p. This new disruption activity requires nucleosomal contacts that are essential for silent chromatin formation *in vivo*. We find that SWI/SNF evicts all three heterochromatin proteins off of chromatin. Surprisingly, we also find that the presence of Sir2p and Sir4p on chromatin stimulates SWI/SNF to evict histone proteins H2A and H2B from nucleosomes. Apart from discovering a new potential mechanism of heterochromatin dynamics, these data also establish a new paradigm of chromatin remodeling enzyme regulation by nonhistone proteins present on the substrate.

Table of Contents

List of Figures:

List of Abbreviations

5-FOA	5-Fluoroorotic acid
AAA+	ATPases associated with diverse cellular activities
aa ##-##	Amino acids ## through ## (counted from the N-terminus)
Abf1	Autonomously replicating sequence binding factor 1
ACF	ATP-utilizing chromatin assembly and remodeling factor
ARID	AT-rich interactive domain
Arp	Actin-related protein
Ash1	Absent, small, or homeotic discs 1
ATP	Adenosine triphosphate
BAH	Bromo-adjacent homology (referencing regions in PBRM1)
BAHD1	BAH domain-containing protein 1
bp	(DNA) base pair
BSA	Bovine serum albumin
C/N-terminal	At the carboxy or amino terminus of the peptide molecule
CEN/ARS	Centromeric / autonomously replicating sequence
CHD	Chromodomain helicase DNA-binding
ChIP	Chromatin immunoprecipitation
ChIP-chip	ChIP hybridized to a tiling array chip
CTCF	CCCTC-binding factor
DEAD	Aspartate(D)–Glutamate(E)–Alanine(A)–Aspartate(D) motif
DNA	Deoxyribonucleic acid
DNMT1	DNA methyltransferase 1
(D)NTP	(Deoxy) ribonucleotide triphosphate

Dot1	Disruptor of telomeric silencing 1
DSB	(DNA) Double-strand break
DTT	Dithiothreitol
EDTA	Ethylenediaminetetraacetic acid
EGTA	Ethyleneglycoltetraacetic acid
Esc1	Establishes silent chromatin 1
GAL	Galactose metabolism
Gcn5	General control nonrepressible 5
GST	Glutathione S-transferase
HSA	Helicase SANT associated
HMG	High-mobility group
HMLα	Homothallic mating locus on the left arm of chromosome III, α-specific genes
HMRa	Homothallic mating locus on the right arm of chromosome III, a-specific genes
HO	Homothallic switching endonuclease
HP1	Heterochromatin protein 1
HU	Hydroxyurea
H#X#(ac/me)$_Y$	Histone H#, residue (X) #, acetylated or methylated y times
Ino80	Inositol requiring 80 complex
ISWI	Imitation switch
Itc1	Imitation switch two complex 1
kb	(DNA) kilobase
kDa	kilo Dalton

M (mM, nM etc.)	Concentration in molarity (moles molecule per liter volume)
m (μm, nm etc.)	Length in meters
MAT	Yeast mating type locus; encodes a- or α- specific genes
MTA	Metastasis-associated
Mot1	Modifier of transcription 1
min	minute
NAA	1-Napthalene-acetic acid
NuRD	Nucleosome remodeling and histone deacetylase
Orc1	Origin recognition complex 1
PAD	Partitioning and anchoring domain
(SDS)-PAGE	(Sodium dodecyl sulfate) polyacrylamide gel electrophoresis
PBRM1	Poly-bromodomain 1
PCR	Polymerase chain reaction
PMSF	Phenylmethylsulfonyl fluoride
Rap1	Repressor/activator site binding protein 1
RecA	Recombination gene A
RNR	Ribonucleotide reductase
rpm	Revolutions per minute
Rrm3	rDNA Recombination Mutation 3
RSC	Remodels structure of chromatin
Rtt102	Regulator of Ty1 transposition 102
Rvb	Resistance to ultraviolet radiation gene B
Sas2	Something about silencing 2
SANT	(present in) Swi3, Ada2, N-Cor, and TFIIB

SC	Synthetic complete media
SD	Synthetic dropout media
SF2	Superfamily 2
Sfh1	Snf five homolog 1
SHL	Superhelical location
Sir	Silent information regulator
SnAC	Snf2 ATP coupling
Sth1	Snf two homolog 1
SUC2	Sucrose fermentation 2
SWI/SNF	Mating type switching defective/sucrose non-fermenting
Swp	SWI/SNF-associated protein
SWR	Sick with Rat8
TAE	Tris acetate EDTA
TAP	Tandem affinity purification
TBE	Tris borate EDTA
TBP	TATA binding protein
TE	Tris + EDTA
TELVR	Telomere on chromosome V, right chromosome arm
TRIM28	Tripartite motif-containing 28
Ura	Uracil biosynthesis
wH	Winged helix-turn-helix
YEPD	Yeast extract peptone plus dextrose
yKu70	Yeast KU 70 protein
yKu80	Yeast KU 80 protein

List of External Datasets

Chapter II, Dataset 1

Chapter II contains a genome-wide dataset, derived from an RNA-seq experiment, that compares gene expression in wild-type and *swi2-Δ10R* yeast strains. Generation of this dataset is described in the methods and materials section of Chapter II.

These data cannot be easily adapted for inclusion in this thesis. If desired, please access this dataset online, through the online PNAS version of the article, or via the web address below.

http://www.pnas.org/content/suppl/2014/11/29/1420096111.DCSupplemental/pnas.1420096111.sd01.xlsx

Preface

Chapter II of this work was initially published in *Proceedings of the National Academy of Sciences* as:

Manning BJ, Peterson CL. Direct interactions promote eviction of the Sir3 heterochromatin protein by the SWI/SNF chromatin remodeling enzyme. *Proceedings of the National Academy of Sciences of the United States of America* 111(50):17827-17832 (2014). doi:10.1073/pnas.1420096111.

Chapter I: Introduction

Eukaryotic genomes and chromatin

Cells are the emergent properties of their genes. All of the information that a cell needs to survive and reproduce—all of its genes and gene regulatory elements—are encoded by the sequence of adenine, cytosine, guanine, and thymine bases within that cell's DNA molecules. Each cell bears a full set of these DNA molecules. For humans, this is a set of 46 polyanions comprising 6.4 billion base pairs of DNA, which stretched end-to-end would exceed one meter in length. Not only must each human cell fit all of that negative charge and genetic information within a nucleus that is 10 micrometers across, but the cell must also properly replicate and express that genetic information.

These tasks are all greatly facilitated by the storage of eukaryotic genomes within the regulatory nucleoprotein structure called chromatin. Over millions of years, eukaryotes have incorporated aspects of chromatin structure into the regulation of most cell processes, from transcription (Rando and Winston, 2012; Venkatesh and Workman, 2015), to regulation of cell fate and development (Brookes and Shi, 2014; Laugesen and Helin, 2014), to DNA replication and repair (Papamichos-Chronakis and Peterson, 2012; Rivera *et al.*, 2014; Sinha and Peterson, 2009). Two contradictory themes of chromatin structure are structural compaction and dynamic accessibility: the restricted accessibility of DNA that is stored within packed chromatin, and the ways cells

have evolved to actively circumvent this storage. In my thesis I will talk about work I have done to characterize a novel balance between these two themes. I will begin by talking about chromatin structure, then transition into ways that cells modulate this structure.

Features of the nucleosome

The basic unit of chromatin is the nucleosome, in which 147 base pairs of DNA is wrapped 1.67 times around an octamer of histone proteins (Figure 1A) (Luger *et al.*, 1997a). As ten base pairs of nucleosomal DNA results in one full superhelical turn of DNA, one nucleosome contains fifteen such turns. Counting these superhelical turns along the nucleosome (superhelical location, or SHL) provides a useful reference point for the following discussion of nucleosome structure. SHL0 is defined as the midpoint of the nucleosome. Nucleosomes are a symmetrical structure, thus starting at SHL0 and progressing the same distance in different directions along the DNA, e.g. one superhelical turn to SHL+1 and SHL-1, brings you to the same locations on the two symmetrical halves of the nucleosome.

As implied by its symmetry, each nucleosome contains two copies apiece of the highly conserved core histones H2A, H2B, H3 and H4. These histones are small proteins, each only ~100-140 amino acids in length, and they contain a high proportion of lysine (K) and arginine (R) residues, imparting a large positive charge on the histone protein at physiological pH (pH 7-8). This positive charge

Figure 1: Structure and composition of the nucleosome (PDB#1AOI) (Luger *et al.*, 1997a). **(A)** Crystal structure of the nucleosome at 2.8 Å resolution. See right key for colors; orange numbers correspond to SHL. **(B)** Histones contain core fold domains and unstructured tail domains. **(C)** Handshake interactions (purple highlight) hold histones together, and four-helix bundle interactions (orange highlight) hold histone heterodimers together.

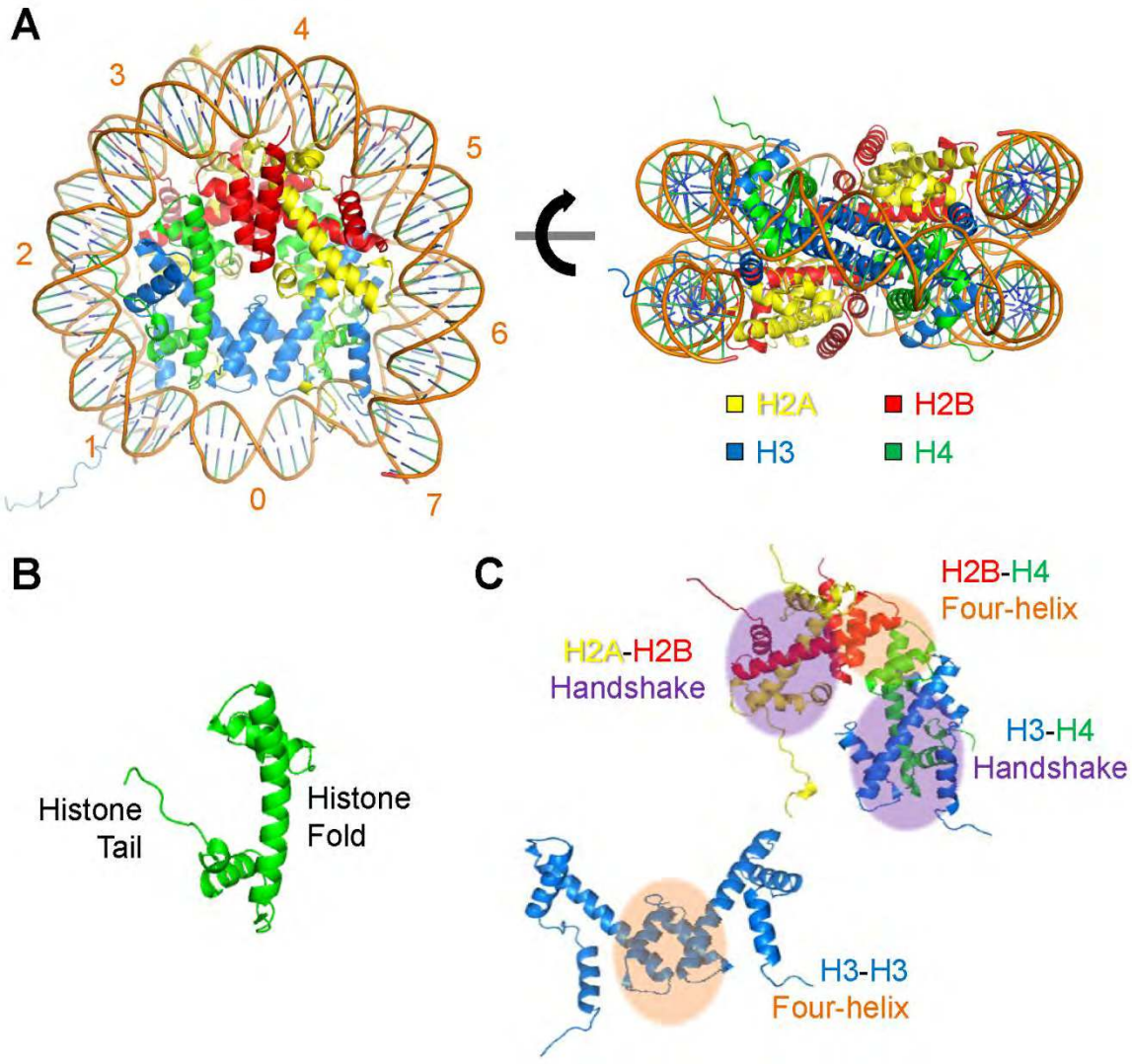
A
4
3
5
2
6
1
0
7
H2A
H2B
H3
H4
B
Histone
Tail
Histone
Fold
C
H2B-H4
Four-helix
H2A-H2B
Handshake
H3-H4
Handshake
H3-H3
Four-helix

helps to partially neutralize the strong negative charge of the DNA polyanion (Kornberg, 1977; Hansen, 2002).

At the core of each histone protein lies a ~70 amino acid-long histone fold domain (Figure 1B). This histone fold domain contains three alpha helices that are separated from one another by two loop domains. Hydrophobic interactions between histone fold domains of different histones ultimately guide the assembly of the histone octamer via two different modes of binding. The handshake mode of binding uses the length of the histone fold's middle helix to unite heterodimers of H2A/H2B and H3/H4 (Figure 1C) (Arents *et al.*, 1991). The four-helix bundle mode of binding combines two H3/H4 heterodimers into a tetramer that sits at SHL0, the center of the histone octamer. Additional four-helix bundles at SHL±3, between H4 and H2B, anchor H2A/H2B heterodimers on either side of the central H3/H4 tetramer (Arents *et al.*, 1991; Luger *et al.*, 1997a). Finally, interactions between the two H2A/H2B dimers in the nucleosome lend cooperative stability to dimer binding (Suto *et al.*, 2000).

Given the strong positive charge of each histone protein, histone octamers only assemble under conditions where the positive charge can be shielded, such as at high concentrations of salt (over 2M sodium chloride) or in the presence of sufficient DNA. On their own, histone octamers at physiological salt concentrations (150mM sodium chloride) dissociate into two H2A/H2B heterodimers and a tetramer of H3/H4. These ionic stability characteristics are commonly used to reassemble histone octamers and DNA into nucleosomes *in*

vitro, by step salt dialysis (Tatchell and Van Holde, 1977). Octamers and DNA are first mixed at high salt (2M sodium chloride) and gradually dialyzed or diluted into lower salt concentrations. By 1M sodium chloride, the histone octamer dissociates into an H3/H4 tetramer and two H2A/H2B dimers, and the H3/H4 tetramer binds to DNA. This tetrasome binds from SHL-3 to SHL+3, where the center of the nucleosome will ultimately be. At 0.8M sodium chloride, and again at 0.6M sodium chloride, H2A/H2B dimers bind, flanking the H3/H4 tetramer and occupying from SHL±3 to SHL±6. The final superhelical turns, SHL±7, are then held by H3 and H4 (Hansen *et al.*, 1991; Luger *et al.*, 1997a). This stepwise order of octamer assembly is similar to what occurs *in vivo* during DNA replication, except this process *in vivo* makes use of specialized chaperone proteins that stabilize the histone proteins away from DNA, instead of salt-based ionic shielding (Corpet and Almouzni, 2009).

In contrast with the structured histone fold domains, the rest of the histone protein consists of unstructured N-terminal (H2A, H2B, H3 and H4) and C-terminal (H2A) tails (Figure 1B). These tails exist outside of the confined nucleosome core and are generally more accessible, e.g. to proteases like trypsin, than the histone fold domains (Weintraub and Lente, 1974). Despite this accessibility, the high concentration of positive charges along the histone tails would suggest that the tails are regularly bound to negatively charged surfaces. Examples of negatively charged binding partners include nucleosomal DNA, linker DNA—the naked DNA that spans between adjacent nucleosomes—and

negatively charged regions on other proteins, including histone tail binding proteins and other nucleosomes (Hansen, 2002).

The histone tails emerge from diverse parts of the octamer core. The histone H2B and H3 N-terminal tails emerge from the sides of the core, passing between the two gyres of DNA. These tails fit out in spots where the minor grooves of the two DNA gyres align. The H2B tail sits between SHL±4.5 and the opposite SHL±3, and the H3 tail emerges between SHL±1 and the opposite SHL±7. Notably, the H3 N-terminal tail aligns with the entry and exit points of DNA from the nucleosome, implying a direct function for the H3 N-terminus in regulating the boundaries of the nucleosome. In contrast, the H4 N-terminal tail and the H2A C-terminal tail emerge from the top and bottom of the octamer core, at SHL±1.5 and SHL±0.5 respectively (Luger *et al.*, 1997a). The H4 tail specifically plays a key role in the organization of individual nucleosomes into higher-ordered structures (Hansen, 2002; Allahverdi *et al.*, 2011).

Higher-order chromatin structure

Eukaryotic genomes, depending on their size, contain from tens of thousands to millions of nucleosomes. Along a linear stretch of DNA, adjacent nucleosomes are separated from one another by twelve to seventy base pairs of linker DNA (Kornberg, 1977; Lohr and Holde, 1979). This simple one-dimensional starting point for chromatin structure, the 10nm-tall ‘beads-on-a-string’ chromatin fiber, is very open and lacks contacts between nucleosomes

(Olins and Olins, 1974). However, this structure is only known to exist *in vitro*, at salt concentrations lower than what is found physiologically.

Once salt is added and the strong negative charge of the DNA begins to be shielded, this 10nm fiber begins to undergo folding. If monovalent cations like sodium$^{(+)}$ are added, this folding proceeds to an intermediate state; if divalent cations like magnesium$^{(2+)}$ are added, you begin to see formation of a maximally folded state (Hansen *et al.*, 1989). This maximally folded state, the 30nm fiber, also occurs in the presence of the linker histones H1 and H5, which bind one per nucleosome at SHL0 and stabilize an additional 20bp of DNA within the nucleosome, turning it into a chromatosome (Hansen, 2002). The physical dimensions of the 30nm fiber depend upon the length of the linker DNA between the nucleosomes (Dorigo, 2004; Robinson *et al.*, 2006; Wong *et al.*, 2007). While the existence of this 30nm fiber has yet to be confirmed *in vivo*, one common feature of 30nm fiber computational and EM studies is that nucleosomes interact with neighboring nucleosomes both on their top/bottom sides, where the H4 and H2A tails reside, and side-to-side past the DNA. At yet higher concentrations of divalent cations, chromatin fibers will cooperatively aggregate (Schwarz *et al.*, 1996). All of these structural transitions have been shown to be reversible.

Histone tails also mediate higher-order chromatin structure, specifically the interactions between separate nucleosomes. Many solved crystal structures, including that of a tetranucleosome array, highlight the importance of interactions between the positively charged H4 tail of one nucleosome, and the negatively

charged H2A acidic patch of another nucleosome (Luger *et al.*, 1997a; Dorigo, 2004). The H4 tail is required for formation of 30nm fibers *in vitro*—even acetylation of one lysine on the H4 tail, lysine 16, is sufficient to disturb both 30nm fiber folding and inter-array cooperative aggregation (Shogren-Knaak, 2006).

On yet higher levels, these 30nm fibers are thought to be organized into loops whose physical dimensions are on the scale of hundreds of nanometers (Belmont, 1994; Horn and Peterson, 2002; Woodcock and Ghosh, 2010). Recent molecular biology approaches based on the chromosome conformation capture methodology, which crosslinks spatially close genomic loci together to derive information about overall genome packaging, imply the existence of large-scale topologically associated domains (TADs) in metazoan cells (Lieberman-Aiden *et al.*, 2009; Dixon *et al.*, 2012). These domains vary in size between organisms—from sixty thousand base pairs in flies (Sexton *et al.*, 2012), to hundreds of thousands of base pairs in human cells (Rao *et al.*, 2014; Sexton and Cavalli, 2015)—but they share common features. Nucleosomes within these domains show greater interaction frequency with each other than with nucleosomes outside of these domains. Also, the ends of these domains constitute insulators or "barriers" that block interaction between nucleosomes on opposite sides of the barriers. Interestingly, these domains interact with other domains in ways that correlate with the organization of genomes into active and repressed regions, or

euchromatin vs. heterochromatin (Lieberman-Aiden *et al.*, 2009; Rao *et al.*, 2014).

Euchromatin and heterochromatin

Despite sharing a common base subunit, there exist many different types of chromatin within the cell. These types of chromatin fall broadly into two categories based on overall transcriptional activity. The first type, euchromatin, contains genes that are actively expressed, such as housekeeping genes whose continuous activity is required for cell viability. In line with this activity, euchromatin is a more open and accessible structure—this has been found both observationally, by electron microscopy and intensity of DNA staining, and biochemically, by accessibility of its DNA to endogenous and ectopic proteins. Euchromatin also replicates earlier during S phase of the cell cycle (Woodcock and Ghosh, 2010).

The second type of chromatin, heterochromatin, generally occupies inactive genes, repetitive DNA, and structural DNA elements like centromeres and telomeres. First noted cytologically for the density of its staining relative to other chromatin (Heitz E., 1928), heterochromatin is a generally repressive mode of genetic storage. Cytologically, heterochromatin is found toward the periphery of cell nuclei, as well as abutting the nucleolus. Molecularly, gene loci within heterochromatin domains are generally transcribed at low levels, and the DNA sequences within these domains are less accessible to proteins. There are two

main types of heterochromatin in metazoans, defined empirically by whether they are silenced in all of an organism's cell types (constitutive heterochromatin) or only in particular cell types (facultative heterochromatin). Importantly, both facultative and constitutive heterochromatin are heritable—they represent genomic states that persist through generations of cell divisions—despite not being directly coded into the genome itself (Grewal and Jia, 2007).

The existence of facultative heterochromatin helps to explain how two cells that contain the same DNA can become different cell types, as different as one person's cardiac muscle cells and neurons. Indeed, many genes that are important for establishing facultative heterochromatin domains were first identified during genetic screens for developmental defects (Lewis, 1978; Simon and Kingston, 2009). Subsequent studies showed that heterochromatic silencing plays a key role in silencing development-sensitive gene loci to facilitate embryonic patterning. In agreement with this, the loss of key heterochromatin proteins in embryonic stem cells results in defective transition into differentiated cell types (Laugesen and Helin, 2014; Steffen and Ringrose, 2014).

As expected from a repressive domain, heterochromatin replicates late during S phase of the cell cycle, and is also repressed for DNA recombination. This recombinational repression seems intuitively palatable given that heterochromatin covers repetitive DNA loci. Recombination is a repair process that takes a damaged DNA locus, searches elsewhere in the genome for homologous DNA sequence, then uses the other locus it finds as a template to

repair the initial damaged locus. If the homology search step detects a homologous repeat on a different chromosome, then recombination can lead to chromosomal translocation, which is a hallmark phenotype of cancer. Consistent with this logic, disruption of heterochromatin structure by knockdown of key heterochromatin proteins results in repetitive DNA-associated genome instability (Peng and Karpen, 2007, 2009).

Counterintuitively, it has also been shown that heterochromatic loci are preferentially repaired by homologous recombination. This repair happens at slower rates in heterochromatin than in euchromatin, and the rate-limiting step appears to be association of the damaged locus with the protein that mediates homology search, Rad51p. The damaged locus must spatially exit the heterochromatin domain before it can associate with Rad51p and proceed with recombinational repair (Chiolo *et al.*, 2011). It has also been shown *in vitro* that Rad51p can mediate a search through euchromatin for homology (Sinha and Peterson, 2008), but inclusion of key heterochromatin proteins block homology search (Sinha *et al.*, 2009). Taken together, these data describe the role of repressive heterochromatin in establishing a chromatin context for the regulation of multiple nuclear processes.

The distinction between euchromatin and heterochromatin begins at the nucleosome. Histone proteins are extensively post-translationally modified—methylated, acetylated, phosphorylated, ubiquitylated, and more—on both their histone tails and on solvent-exposed parts of their core (Bannister and

Kouzarides, 2011). Only a few of these modifications affect chromatin higher-order structure by influencing chromatin folding (Shogren-Knaak, 2006; Lu *et al.*, 2008), as outlined above; most histone post-translational modifications function as recognition keys for chromatin-associated “reader” domains (Musselman *et al.*, 2012).

Euchromatic nucleosomes tend to bear active histone marks, like H3K9 and H4K16 acetylation, or H3K4 and H3K36 methylation. These marks vary as a function of the proteins around that nucleosome, and as an extension of that, they vary based on where that nucleosome sits within the gene body. Similarly, heterochromatic nucleosomes bear their own repertoire of post-translational modifications. Generally, these nucleosomes exhibit very low levels of acetylation, in combination with additional modifications that interact specifically with heterochromatin proteins (Grewal and Jia, 2007; Yang *et al.*, 2008; Gozani and Shi, 2014).

Heterochromatin formation has several evolutionarily conserved themes. First, its formation begins at a nucleation site, where proteins interacting with the nucleation site DNA also recruit enzymatic machinery that deposits heterochromatin-specific modifications on adjacent nucleosomes. In recent years, some noncoding RNA transcripts have also been shown to help in the recruitment step (Brockdorff, 2013). Second, these post-translationally modified nucleosomes are then specifically bound by other, structural heterochromatin proteins. These structural proteins recruit more of the post-translational

modification complex, creating more binding sites for the structural proteins. This cycle iterates, with the upshot being that the heterochromatin domain spreads outwards along the chromosome in a DNA sequence-independent manner (Grewal and Jia, 2007; Hathaway *et al.*, 2012; Grunstein and Gasser, 2013).

To set an outer limit for the spreading of a heterochromatin domain, boundary factors are needed. One such boundary factor that regulates heterochromatin is the incorporation of histone variants, alternate versions of the canonical core histones, into the nucleosome. An example of this is the incorporation of the histone variant H2A.Z, a variant of H2A associated with gene promoters, into loci on the border of heterochromatin; this acts as a barrier to prevent further spreading of silent heterochromatin (Bönisch and Hake, 2012; Meneghini *et al.*, 2003; Lu and Kobor, 2014). In contrast, the plant-specific H2A variant H2A.W is ubiquitously present in heterochromatic regions, playing key roles in gene silencing and compaction (Yelagandula *et al.*, 2014). Proteins other than histone variants also serve as key boundary factors. For example, the insulator protein CTCF regulates chromatin TAD boundaries as well as the extent of facultative heterochromatin at developmentally regulated gene loci (Rao *et al.*, 2014; Narendra *et al.*, 2015).

Sir heterochromatin

Currently, the most well-understood model system for heterochromatin has been described for the budding yeast *Saccharomyces cerevisiae*. This

heterochromatin, nucleated by the silent information regulator (Sir) proteins, exhibits all of the functional properties of heterochromatin found in higher eukaryotes, from transcriptional silencing to delayed replication (Grunstein and Gasser, 2013). While Sir heterochromatin itself is not perfectly conserved in higher eukaryotes, two of its three constituent proteins are conserved, and one is implicated in Drosophila facultative chromatin formation (Furuyama *et al.*, 2004).

Sir heterochromatin in yeast is found at transcriptionally silent loci—at subtelomeric regions on the ends of each chromosome, and also at the silent 'homothallic mating' loci *HMLα* and *HMRa* (Grunstein and Gasser, 2013). These two silent loci contain different coding copies of the transcriptionally active *MAT* locus. The *MAT* locus expresses genes that are required for haploid yeast to be either one of the two yeast mating types—α or a. Haploid yeast can switch mating types by expressing the HO endonuclease, which creates a double-strand break in the DNA at the *MAT* locus. This break is repaired by recombination, with the silent mating locus of the opposite mating type from the MAT locus being used as the preferred template (Herskowitz and Jensen, 1991; Pâques and Haber, 1999).

In order for haploid yeast to mate and form a diploid, one of the yeast must express *α* genes from its *MATα* locus, and the other must express *a* genes from its *MATa* locus. If yeast are defective for silencing *HMLα* or *HMRa*, then those pseudodiploid yeast express both *α*- and *a*-specific genes (like diploid *MATα/MATa* yeast) and are unable to mate. Identifying haploid yeast that were

unable to mate after mutagenic screening identified proteins that are important for heterochromatic silencing (Rine and Herskowitz, 1987). These proteins were also found to be involved in silencing in regions adjacent to telomeres (Aparicio *et al.*, 1991).

The Sir proteins

There are three main Sir proteins that are indispensable for silencing at both subtelomeres and *HMLα/HMRa*: Sir2p, Sir3p, and Sir4p (Figure 2A). There is one additional protein, Sir1p, whose presence is not absolutely required for silencing at telomeres. In the absence of Sir1p, the silent mating loci can exist in either transcriptionally active or inactive states, both of which are epigenetically heritable (Rine and Herskowitz, 1987). Sir1p binds to the BAH domain of Orc1p and to Sir4p (Triolo and Sternglanz, 1996; Hsu *et al.*, 2005).

The first Sir protein that will be described here is Sir4p. Sir4p is the largest and least well-conserved of the Sir proteins. It interacts with a large number of other proteins, including the N-terminal tails of histones H3 and H4 (Hecht, Andreas *et al.*, 1995). The amino terminus of Sir4p (aa1-270) appears to bind and protect linker DNA on reconstituted nucleosomes, a function that is important for telomeric but not HM silencing *in vivo* (Kueng *et al.*, 2012). This region of Sir4p also interacts with yKu80p (Roy *et al.*, 2004). Further down the protein, the PAD (aa950-1262) in the center of Sir4p is known to interact with Esc1p and yKu80p, thereby promoting the recruitment of silent heterochromatin to the

Figure 2: Sir heterochromatin. (A) Schematic representation of the Sir protein peptides, with their constituent domains as abbreviated in the text. **(B)** Crystal structure of the Sir3 BAH domain bound to a nucleosome at 3.0 Å resolution. Star denotes the H4 tail (PDB#3TU4) (Armache *et al.*, 2011). **(C)** Schematic representation of Sir heterochromatin spreading from an *HM* silencer, with inhibition from boundary factors. ORC is the ORC complex, R is Rap1p, A is Abf1p, numbers 1 through 4 are Sir1p through 4p

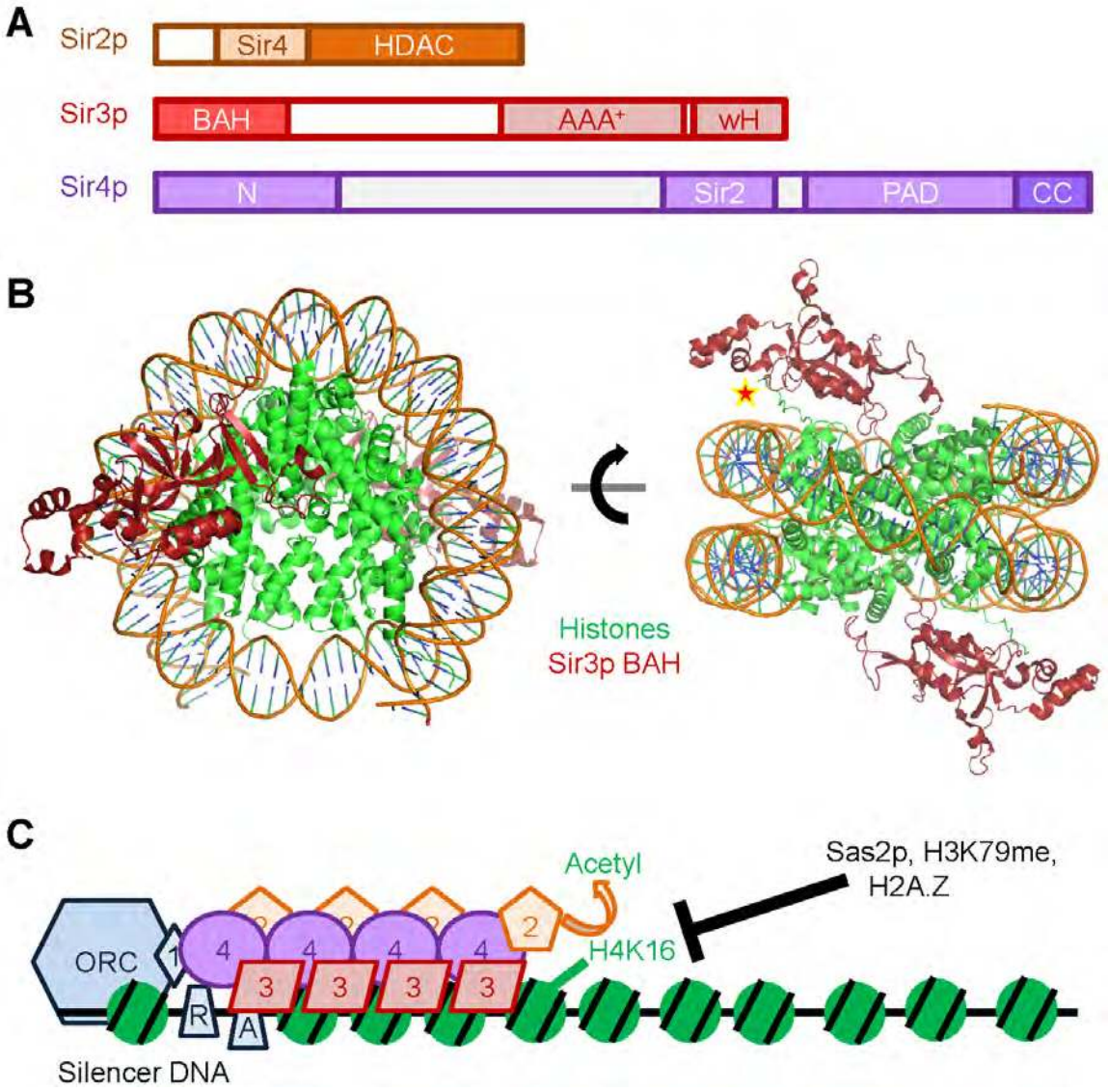
A
Sir2p
Sir4
HDAC
Sir3p
BAH
AAA+
wH
Sir4p
N
Sir2
PAD
CC
B
Histones
Sir3p BAH
C
Acetyl
Sas2p, H3K79me,
H2A.Z
ORC
1
4
3
2
H4K16
R
A
Silencer DNA

nuclear periphery (Taddei *et al.*, 2004). Sir4p also binds to yKu70p (Tsukamoto *et al.*, 1997) and Rap1p (Luo *et al.*, 2002), interactions that serve to anchor Sir4p to proper DNA elements at telomeres and *HM* loci. At the C-terminus (aa1262-1358) of Sir4p is a coiled-coil motif that has been shown to interact with Sir3p (Chang *et al.*, 2003; Rudner *et al.*, 2005) and other molecules of Sir4p (Chang *et al.*, 2003). Finally, aa737-839 of Sir4p forms a stable heterodimeric complex with, and stimulates the enzymatic activity of, the second Sir protein, Sir2p (Hsu *et al.*, 2013).

Sir2p is a histone deacetylase (Imai *et al.*, 2000). It is the eponymous, founding member of the sirtuin class of NAD-dependent histone deacetylases. Sirtuin deacetylases have been implicated in gene silencing and organism lifespan in various species, from yeast to man (Poulose and Raju, 2015). Unlike the other Sir proteins, Sir2p also plays a role at rDNA loci. There, Sir2p represses RNA polymerase II transcription and promotes rDNA repeat stability (Gottlieb and Esposito, 1989). The most well-characterized role of Sir2p in Sir silencing is the deacetylation of histone H4 at lysine 16 (H4K16) (Imai *et al.*, 2000). This deacetylation creates a high-affinity binding site for the third Sir protein, Sir3p.

Sir3p is thought to be the predominant structural protein of Sir heterochromatin (Hecht *et al.*, 1996; Strahl-Bolsinger *et al.*, 1997; Sinha *et al.*, 2009; Swygert *et al.*, 2014). It contains an N-terminal (aa1-214) nucleosome-binding BAH domain that is indispensable for proper silencing (Norris and Boeke,

2010). BAH domains are found in many other conserved chromatin-associated proteins, many of which are involved in transcriptional silencing (Callebaut *et al.*, 1999). Despite poor primary amino acid sequence conservation—particularly across BAH domains in different protein families—the core 'distorted β-barrel' fold of the BAH domain is ubiquitous (Oliver *et al.*, 2005; Kuo *et al.*, 2012).

In the few cases where these domains have been functionally characterized, they have been found to mediate protein-protein interactions with chromatin (Muller *et al.*, 2010; Armache *et al.*, 2011; Chambers *et al.*, 2013). Many of these interactions are also sensitive to post-translational modifications on histone proteins, an insight that bridges *in vitro* structural studies to *in vivo* transcriptional control. For example, Sir3p itself is a silencing-specialized paralog of the key origin recognition complex subunit Orc1p. Orc1p serves the purpose of Sir3 in other fungal species' silent heterochromatin (Hickman and Rusche, 2010; Hickman *et al.*, 2011). Furthermore, in metazoans, the BAH domain of Orc1 helps the origin recognition complex interact with chromatin *in vivo* in an H4K20me$_2$-dependent manner. Disruption of this specific interaction results in the primordial dwarfism of Meier-Gorlin Syndrome (Kuo *et al.*, 2012; Zhang *et al.*, 2015).

How do BAH domains read chromatin? The crystal structure of the Sir3p BAH domain bound to a nucleosome has recently been solved by several groups (Figure 2B) (Armache *et al.*, 2011; Wang *et al.*, 2013; Yang *et al.*, 2013). These structures give mechanistic bases to the genetic phenotypes of many histone

and Sir3p BAH domain mutants (Norris and Boeke, 2010). Spatially, the Sir3p BAH domain binds a swath across the face of the nucleosome, from SHL±2 on the DNA, over the H4 tail, the LRS region of H3 and H4, and terminating on a region of H2B that abuts the H2A acidic patch (Figure 2B, left). One such interaction happens entirely on one face of the nucleosome, and in the crystal structure two BAH domains are bound to opposite faces of each nucleosome. Per BAH, approximately thirty residues are involved in contacting the nucleosome surface, and many of these contacts are electrostatically mediated (Armache *et al.*, 2011).

One important contact occurs between a negatively charged 'pocket' on the Sir3p BAH domain and the positively-charged H4K16-R19 patch on the H4 tail (Figure 2B; red/yellow star). Disruption of the Sir3p BAH pocket-H4 tail interaction, specifically via charge-neutralizing acetylation of H4 at K16, abolishes both silencing *in vivo* as well as Sir3p BAH-nucleosome binding *in vitro* (Onishi *et al.*, 2007; Buchberger *et al.*, 2008; Armache *et al.*, 2011). This theme of H4 tail reading is also present in the crystal structure of mouse Orc1 BAH domain bound to an H4K20me$_2$ histone tail peptide; there, the methylation state of the lysine is read by a hydrophobic pocket (Kuo *et al.*, 2012).

As a result of this tail-pocket interaction, the H4 tail becomes structured and held in a particular configuration. Tight sequestration of the H4 tail by Sir3p could block interaction of the H4 tail with other proteins, changing chromatin fiber conformation and blocking access of transcriptional activation machinery to

chromatin. Another side effect of this mode of binding is that two arginine residues on the H4 tail, R17 and R19, are pushed into the DNA backbone. It is thought that this H4-DNA interaction helps establish a resilient heterochromatin structure. In line with his hypothesis, charge-neutralizing mutations of these arginines to alanines do not affect binding of Sir proteins to nucleosomes, but drastically inhibit transcriptional silencing (Wang *et al.*, 2013).

While the Sir3p BAH domain on its own is able to interact with nucleosomes, the remainder of the Sir3p protein is also involved in silencing. Following the N-terminal BAH domain is an unstructured region (aa214-532). This region is known to be post-translationally modified by phosphorylation at several serine residues in response to stress, thereby affecting expression of a subset of subtelomeric genes (Ai *et al.*, 2002).

The C-terminus of Sir3 contains a number of protein-protein interaction sites. Beginning after the unstructured region is a conserved domain related to the AAA+ family of ATPases. This domain is also present in Orc1p. However, the Sir3p AAA+-like domain (532-845) lacks the nucleotide binding pocket, and thereby the nucleotide hydrolysis activity, that is present in other AAA+ ATPases (Ehrentraut *et al.*, 2011). There is considerably less sequence identity between the AAA+ domains of Orc1p and Sir3p (~27%) than between their BAH domains (~50%)—as Orc1p and Sir3p that have swapped BAH domains are still functional, while swapped AAA+ chimeras are not functional (Bell *et al.*, 1995). The AAA+ domain also has the ability to interact with histones H3 and H4, as

well as bind to nucleosomes in a manner that is sensitive to methylation of H3K79 (Hecht, Andreas *et al.*, 1995; Ehrentraut *et al.*, 2011).

Other proteins known to interact with the Sir3 C-terminus include Rap1p (Moretti *et al.*, 1994), Sir4p (Chang *et al.*, 2003; Liou *et al.*, 2005; King *et al.*, 2006), and other molecules of Sir3p (King *et al.*, 2006; Oppikofer *et al.*, 2013a). Sir4 interacts with a complex surface on Sir3p, minimally requiring residues 464-728. This region encompasses the entire 'base' fold region of the Sir3p AAA+ domain, as well as an alpha helical stretch extending from the N-terminus of the AAA+ domain. Finally, the C-terminal 138 amino acids of Sir3p constitute a winged helix-turn-helix (wH) domain whose dimerization activity is required for silent chromatin formation. Inclusion of this dimerization domain with the aforementioned AAA+ domain results in increased nucleosome and DNA binding activity, presumably due to cooperative binding made possible by dimerization (King *et al.*, 2006; Oppikofer *et al.*, 2013a).

Establishment of Sir domains

As mentioned above, one hallmark of heterochromatin is the manner in which it forms regions of silent chromatin. This formation happens in two general phases: nucleation, and subsequent sequence-independent spreading. The nucleation step is generally controlled by DNA-sequence-specific binding factors, which ensure that heterochromatin occurs at the correct loci.

For Sir heterochromatin, these sequence-specific binding factors vary based on genomic location. At the *HM* loci, flanking silencer DNA elements "*E*" and "*I*" contain binding sites for Rap1p, Abf1p and the ORC (Rusche *et al.*, 2003). Here, Sir1p is known to interact with the BAH domain of Orc1p, a step important for silent chromatin establishment but not its maintenance (Rine and Herskowitz, 1987; Fox, 1997; Hsu *et al.*, 2005). Redundancy is key for these nucleation loci, both in terms of the presence of multiple binding sites for the same factor, and also the binding of multiple factors. Then, in a Sir2p activity-independent manner (Imai *et al.*, 2000), these factors bind and recruit the Sir proteins (Rusche *et al.*, 2003; Grunstein and Gasser, 2013).

At telomeres, more redundant nucleation factor interactions are seen. Rap1p binds to the TG-rich telomeric repeat sequence. The yKu70p/yKu80p heterodimer is also present at telomeres, and both the yKu heterodimer and Rap1p interact with Sir4p (Luo *et al.*, 2002; Roy *et al.*, 2004). These Sir4p interactions are key for the establishment of silent chromatin at subtelomeric regions, but are not as essential for *HM* silencing. *HM* Sir silencing is also much more resilient than subtelomeric Sir silencing. While *HM* loci are almost never expressed, genes in subtelomeres are generally less Sir-repressed the further one goes away from the telomere core. Additionally, reporter genes integrated at subtelomeric regions regularly become heritably expressed (Gottschling *et al.*, 1990; Kitada *et al.*, 2012). This gene-sequence-independent transcriptional variation is called "Telomere Position Effect," and it resembles the "Position

Effect Variegation" heterochromatin effect seen in Drosophila (Grunstein and Gasser, 2013).

There are also connections between heterochromatin nucleation and the process of DNA replication. In addition to the ORC binding sites present at the *HM* "*E*" and "*I*" silencers, earlier work demonstrated that passage through S phase was required for restoration of transcriptional silencing in temperature-sensitive Sir protein mutants (Lau *et al.*, 2002). This finding was expounded upon in more recent work, which showed that tightly bound DNA-protein complexes recruit Sir proteins and silence reporter genes in cis (Dubarry *et al.*, 2011). This phenomenon was found to also happen at replication pause sites in strains lacking the replication-assisting helicase Rrm3p. Taken together, these data suggest that DNA replication stress plays a key role in heterochromatin nucleation.

The second phase of heterochromatin establishment is the spreading of the heterochromatin domain from the nucleation site. Unlike other forms of transcriptional silencing, which occur primarily when repressor factors bind near gene promoters and preclude activator binding (Rando and Winston, 2012), heterochromatin establishes its silent domains by spreading outward from its nucleation sites. This spreading requires protein-protein and protein-DNA interactions between the chromatin fiber and heterochromatin proteins, as well as interactions between heterochromatin proteins themselves. The importance of heterochromatin self-interaction in silencing is evident in the numerous protein-

protein interactions listed above. Hypothetically, constraining the genome with self-associating groups of factors could be sufficient to explain the preferential interaction of chromosomal domains with similar distal chromosomal domains.

Therefore, two key cellular targets for regulating heterochromatin spreading are controlling the amount of available heterochromatin proteins, and regulating the chromatin surface to which they bind. Towards the first point, changing the level of Sir protein expression has multiple different effects on gene expression. Overexpression of Sir4p or Sir2p disrupts silencing (Cockell *et al.*, 1998), while overexpression of Sir3p leads to ectopic Sir spreading and larger clustering of telomeres and *HM* loci at the nuclear periphery (Hecht *et al.*, 1996; Strahl-Bolsinger *et al.*, 1997; Ruault *et al.*, 2011). These findings, along with *in vitro* evidence that Sir3p alone is sufficient to change the shape of the chromatin fiber and to inhibit recombination (Sinha *et al.*, 2009; Swygert *et al.*, 2014), are the arguments for Sir3p being the primary, limiting structural protein of Sir heterochromatin.

Heterochromatin proteins can also be post-translationally modified in such a way as to decrease the amount of protein available for binding. Examples of this are the aforementioned phosphorylation of Sir3p (Ai *et al.*, 2002), and the phosphorylation of the metazoan heterochromatin protein TRIM28 in response to DNA damage (Ziv *et al.*, 2006; Bolderson *et al.*, 2012). Finally, heterochromatin proteins might bind to partner proteins or ectopic loci away from their loci of

interest, thereby lowering the effective available amount of that protein (van Leeuwen *et al.*, 2002; Dror and Winston, 2004).

With regards to chromatin surface regulation, another common theme in heterochromatin spreading is the concomitant perpetuation of specific heterochromatin-associated post-translational modifications on the histone proteins themselves (Hathaway *et al.*, 2012). As mentioned before, deacetylation of H4K16 by Sir2p is essential for Sir3p to bind and establish repressive chromatin. This Sir3p can also interact with the Sir2p/Sir4p heterodimer (Liou *et al.*, 2005), providing a platform to increase the range of Sir2p's deacetylase activity (Figure 2C).

One factor curtailing Sir spreading is acetylation of H4K16. Mutation of H4K16 to glutamine, mimicking constitutive acetylation, totally ablates Sir silencing (Johnson *et al.*, 1990). H4K16 acetylation is performed in subtelomeric regions primarily by the SAS-I complex, whose core catalytic subunit is the MYST family histone acetyltransferase, Sas2p (Kimura *et al.*, 2002). H4 acetylation by NuA4 complex has also been proposed to direct incorporation of H2A.Z, another boundary factor briefly described above, at subtelomere boundaries (Altaf *et al.*, 2010). These data could imply a cooperative mode of boundary function.

Another histone mark, H3K79Me, is known to inhibit silent chromatin formation *in vivo* and *in vitro* (van Leeuwen *et al.*, 2002; Johnson *et al.*, 2009; Kitada *et al.*, 2012; Xue *et al.*, 2015). This mark, despite somehow having no

effect on Sir2/3/4 complex binding to chromatin *in vitro* or by ChIP assay, can block binding of either the Sir3p BAH domain or AAA+ domain to nucleosomes. This mark is deposited by Dot1p, an SAM-dependent histone methyltransferase. It only methylates H3K79 residues that are already within nucleosomes. While Dot1p is known to deposit H3K79Me in a transcription-associated manner, no enzyme is known that removes this mark. Therefore, establishment of silencing can only happen once H3K79Me nucleosomes have been diluted out by successive cell cycles.

The H3K79 residue is present at ±2 SHL on the surface of the histone core, within the LRS region of the nucleosome, and right underneath loop 3 of the Sir3p BAH domain. While the impact of H3K79 on Sir3p AAA+ binding is not currently understood, structural studies predict that H3K79 could form up to three hydrogen bonds with negatively charged residues on the Sir3p BAH domain (Armache *et al.*, 2011). This partially explains the influence of H3K79 methylation on Sir silencing—methylation of H3K79 removes hydrogens, increases the amine's Lewis basicity, and makes the residue larger and more hydrophobic. All of these effects impact both the hydrogen bonding of the amine and the sterics of its interaction with the BAH domain. Interestingly, totally removing not only H3K79 hydrogen bonding but also its charge, by mutating H3K79 to alanine, results in a much larger silencing loss than deletion of Dot1p alone (van Leeuwen *et al.*, 2002). While overexpression of Dot1p leads to decreased levels of Sir proteins at telomeres by ChIP, Dot1p deletion only results in minor Sir3p

relocalization by ChIP-chip and silencing phenotypes at some telomeres (Takahashi *et al.*, 2011). These data might hint at methylation-independent roles for H3K79 in silencing.

Recent studies have also shown that the Ino80 chromatin remodeling complex, which has been shown to evict H2A.Z from chromatin, functions as a boundary factor in yeast (Xue *et al.*, 2015). However, instead of preventing the spread of heterochromatin into euchromatin, Ino80 plays the opposite role: it prevents the spread of euchromatin into heterochromatin. The proposed model for this barrier function is that Ino80 inhibits the methylation of H3K79. Some potential mechanisms for this inhibition: Ino80 binding could sterically occlude Dot1p activity, or Ino80-mediated histone dynamics could influence Dot1p activity, or Ino80 could prevent transcription outside of normally transcribed regions thereby preventing transcription-associated H3K79 methylation.

Taking all of the above data into consideration, much is known about the nucleation, spreading, regulation, and confinement of inactive Sir heterochromatin (Figure 2C). However, less is known about the exact molecular superstructure of heterochromatin, and how this superstructure imposes dormancy on the underlying genetic information. Empirically, we know that heterochromatin is a refractory, inaccessible domain. However, it cannot remain permanently inaccessible—at least once per cell cycle, heterochromatic DNA must be replicated. Also, when heterochromatic DNA is damaged, as described above, a cell must access and faithfully repair that damage. Very little is known

about the manner by which cells can dynamically circumvent heterochromatin structure in times of need.

Comparatively more is known about strategies that cells use to regulate their euchromatin. The three paradigms of chromatin regulation are histone posttranslational modification, histone variant incorporation, and ATP-dependent chromatin remodeling. Extensive interplay exists between these paradigms, and they impact the control and mechanism of most nuclear processes (Clapier and Cairns, 2009; Bannister and Kouzarides, 2011; Swygert and Peterson, 2014; Venkatesh and Workman, 2015). The first two paradigms, as described above, have been explored with relation to regulating heterochromatin. The focus of this thesis is on the less explored third paradigm of chromatin regulation, which we will now introduce.

ATP-dependent chromatin remodeling enzymes

Dynamic accessibility of genetic information is a concern for even euchromatin. While linker DNA is free to bind transcription factors—when linker histones are not present—still, much of the genome lies within a nucleosome. DNA sequences on the interior of the nucleosome, facing the histone core, are more protected even from small molecules like hydroxyl radicals (Hayes *et al.*, 1990). Also, incorporation into a nucleosome bends the DNA backbone such that even DNA sequences away from the histone core assume a different conformation than free DNA in solution. There is a subset of “pioneer”

transcription factors that bind well even to chromatinized motifs (Iwafuchi-Doi and Zaret, 2014), but binding of many transcription factors and DNA processing enzymes is inhibited by nucleosomes (Rando and Winston, 2012).

Nucleosomes themselves can spontaneously unwrap their DNA and change positions along DNA *in vitro* (Li and Widom, 2004). However, this unwrapping of nucleosomal DNA happens at time scales that are prohibitive in a biological sense, especially for loci near the nucleosomal dyad. Iterative loading of DNA-binding proteins to kinetically trap spontaneous unwinding has been shown to separate DNA from nucleosomes (Javaid *et al.*, 2009), but the end product is a protein-occluded substrate. Finally, nucleosome dynamics can be slightly regulated *in vitro* by a subset of histone posttranslational modifications and histone variants (Thakar *et al.*, 2009; Watanabe *et al.*, 2010), but the primary tool used by cells for dynamic genome access is ATP-dependent chromatin remodeling (Clapier and Cairns, 2009).

The first ATP-dependent chromatin remodeling enzyme complex was discovered in yeast, via two genetic screens (Neigeborn and Carlson, 1984; Stern *et al.*, 1984). One screen searched for genes involved in the transcription of the aforementioned *HO* endonuclease; yeast bearing mutations in these genes were unable to switch (*swi*ˇ) mating types. The second screen identified sucrose non-fermenting (*snf*ˇ) yeast that were defective in transcribing the sucrose invertase *SUC2*. The first hint of these genes' function came from their common transcriptional phenotypes (Peterson and Herskowitz, 1992), and also by their

genetic interaction with mutant histone alleles (Peterson *et al.*, 1991; Kruger *et al.*, 1995). The products of five genes from these screens were found to co-purify as the SWI/SNF protein complex: Swi1p, Swi2p/Snf2p, Swi3p, Snf5p and Snf6p (Peterson *et al.*, 1994). This complex and its human homolog were shown to stimulate binding of a transcription factor to nucleosomal DNA (Cote *et al.*, 1994; Kwon *et al.*, 1994). Notably, this activity requires the energy of ATP hydrolysis.

After the discovery of SWI/SNF, a number of other distinct chromatin remodeling enzymes were found based on sequence homology with the Swi2p enzyme (Cairns *et al.*, 1996; Delmas *et al.*, 1993; Elfring *et al.*, 1994; Tsukiyama *et al.*, 1995; Tran *et al.*, 2000; Shen *et al.*, 2000; Mizuguchi, 2004). These ATP-dependent chromatin remodeling enzymes are generally megadalton-sized, multiprotein complexes, nucleated around a *SNF2*-family core subunit. While originally discovered and studied in the context of transcriptional regulation, these enzymes are involved in all aspects of genome regulation, from nucleosome positioning and DNA replication to DNA repair. There are four families of these enzymes, with each family named after its founding member: the ISWI family, the CHD family, the Ino80 family, and the SWI/SNF family. While these families have unique compositions, activities and regulation, they all share a common reaction mechanism: using the power of ATP hydrolysis to translocate DNA within a nucleosome. This hydrolysis and translocation mechanism is catalyzed by a conserved SF2 helicase domain present in the core subunit of each complex (Hauk and Bowman, 2011).

SF2 core domains in ATP-dependent chromatin remodeling enzymes, hereafter referred to as *SNF2* ATPase domains, consist of two RecA-like folds separated by an insertion of variable length. The two RecA-like folds interface with each other, and grip DNA in the cleft between them (Figure 3A) (Dürr *et al.*, 2005, 2006). This DNA-bound state is the active, hydrolysis-competent conformation of the ATPase core. With its grip, the ATPase domain uses ATP hydrolysis to translocate along the DNA, a process that generates superhelical torsion in the DNA. However, these enzymes do not generate enough torsion to match what would be seen if they perfectly tracked the DNA backbone, implying either an alternative mode of translocation or transient loss of torsion (Singleton *et al.*, 2007).

There are seven conserved motifs interspersed throughout *SNF2* ATPase domains. The N-terminal RecA fold, a Walker A-type fold, contains motifs I, Ia, II and III. This N-terminal half seems to coordinate ATP binding and hydrolysis. The C-terminal RecA fold, a Walker B-type or DEAD-box-type fold, contains motifs IV, V, VI and VII. This C-terminal half directs coupling of ATP hydrolysis to productive DNA translocation and nucleosome remodeling. In summary, these ATPase domains can bind to and hydrolyze ATP, bind to DNA, and translocate along DNA in what has been mostly shown to be the 3`->5` direction (Smith and Peterson, 2005; Singleton *et al.*, 2007). This translocation occurs at a rate of ~12bp*sec^{-1} of nucleosomal DNA in small 1-3bp steps, with a force of up to 12pN, for purified SWI/SNF complex (Zhang *et al.*, 2006; Sirinakis *et al.*, 2011).

Figure 3: Snf2-family ATPases. (A) Crystal structure of the *S. sulfataricus* Snf2-family ATPase domain bound to DNA at 3.0 Å resolution. The N-terminal RecA-like lobe is colored in light green; the C-terminal such lobe is colored in dark green (PDB#1Z63) (Dürr *et al.*, 2005). **(B)** Schematic representation of the ATPase subunits for each of the four families of chromatin remodeling enzymes.

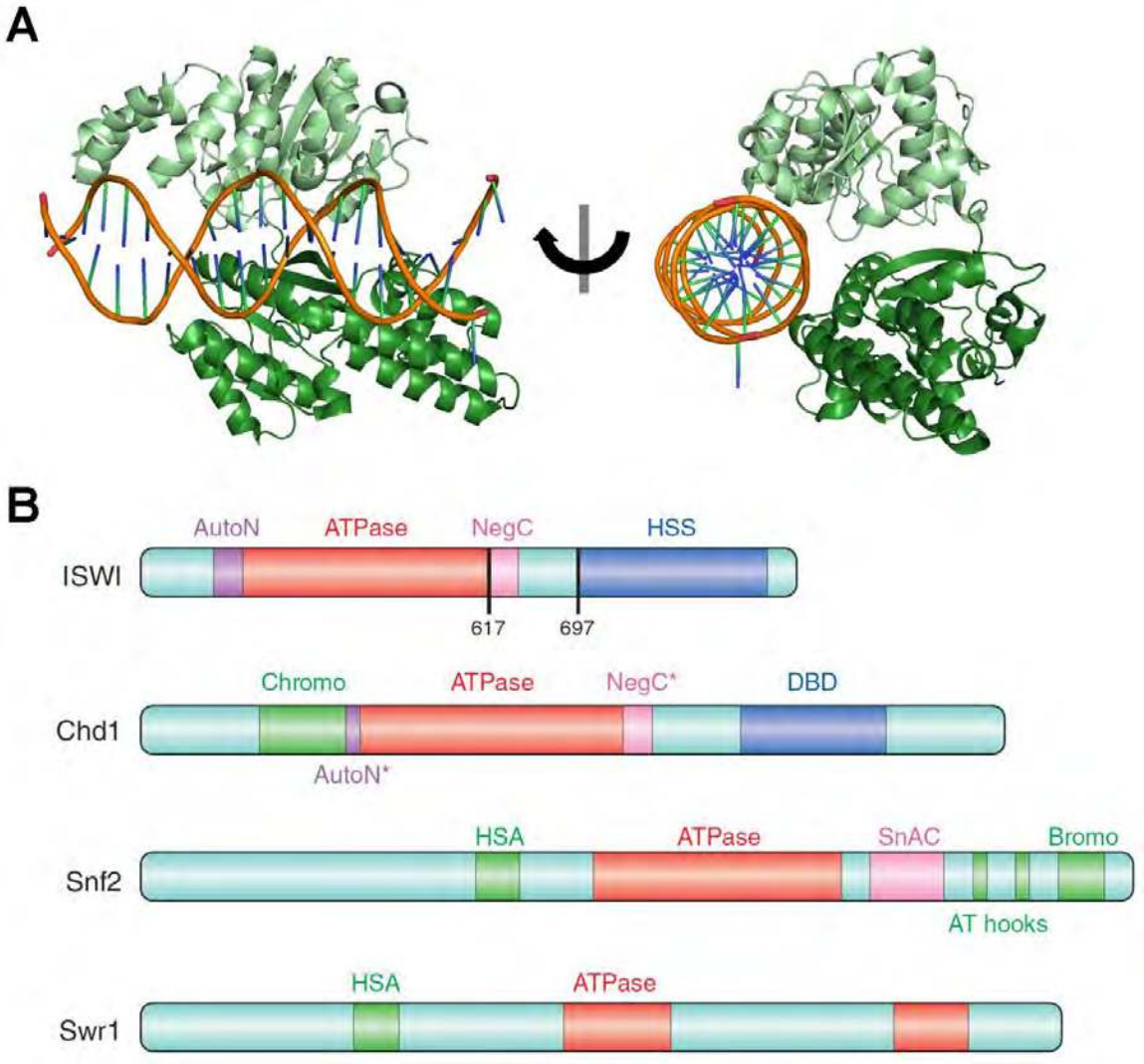
A
B
AutoN
ATPase
NegC
HSS
ISWI
617
697
Chromo
ATPase
NegC*
DBD
Chd1
AutoN*
HSA
ATPase
SnAC
Bromo
Snf2
AT hooks
HSA
ATPase
Swr1

While the ATPase translocates along DNA, the rest of the complex stays bound to the nucleosome. This anchored motion, together with superhelical torsion generated from translocation, pumps DNA into the nucleosome, ultimately destabilizing nucleosomal DNA as a loop off of the octamer surface (Bazett-Jones *et al.*, 1999; Zhang *et al.*, 2006). Chemical crosslinking experiments using SWI/SNF and ISWI complexes have defined a strong contact between their ATPase domains and nucleosomal DNA at ±2SHL. Creating substrates with nicks or gaps in the DNA around ±2SHL strongly inhibits nucleosome sliding by SWI/SNF and ISWI chromatin remodeling enzymes, suggesting that this particular region of the nucleosome is the focus of DNA translocation to drive DNA loop formation. This loop subsequently relaxes by repositioning nucleosomal DNA along the histone core (Zofall *et al.*, 2006; Dechassa *et al.*, 2008).

While this core ATPase motor is very well conserved between families of chromatin remodeling enzymes, the different families demonstrate different biological and biochemical activities when placed in the context of entire complexes. These differences can be attributed to regulatory domains and subunits that are also present in intact complexes (Figure 3B). Some of these domains, like acetyllysine-binding bromodomains or methyllysine-binding chromodomains, function purely to recognize and bind to specific histone posttranslational modifications, thereby decreasing the off-rate of the enzyme from a substrate locus. Some of these subunits function to interact with external

transcriptional activators in order to drive recruitment of these complexes to loci of interest (Rando and Winston, 2012). Some subunits purely function as a scaffold, to hold the components of the complex together.

However, there also exist a number of domains outside the ATPase core that serve to directly regulate the ATPase's activity, in order to drive the formation of a specific product (Manning and Peterson, 2013). Some of these domains are inhibitory, and some may act as chaperones for reaction intermediates. For example, research done on the ISWI complex catalytic core subunit identified an "AutoN" domain N-terminal of the ATPase domain that inhibits ATP hydrolysis. While the H4 tail is required for ISWI ATPase activity, AutoN is thought to mimic the H4 tail and compete with the H4 tail for binding to the ATPase domain, thereby inhibiting ISWI ATPase activity in the absence of its substrate (Clapier and Cairns, 2012; Mueller-Planitz *et al.*, 2012). Similarly, the chromodomains of CHD's core subunit have an acidic helix region that, in the absence of bound nucleosomes, binds to the Walker B motif of the CHD ATPase core. This binding sterically prevents the ATPase core from binding DNA and reaching its active, ATP-hydrolyzing conformation. However, these chromodomains also play a positive role in the CHD chromatin remodeling mechanism, as their deletion reduces the efficiency of nucleosome repositioning by two orders of magnitude (Hauk *et al.*, 2010; Patel *et al.*, 2011, 2013).

Ultimately, the emergent properties of each complex's different subunits grant that enzyme complex unique activities. The currently known range of ATP-

dependent chromatin remodeling enzyme activities includes nucleosome repositioning via sliding, histone dimer and histone octamer eviction, and histone dimer exchange (Clapier and Cairns, 2009; Swygert and Peterson, 2014). Members of the CHD and ISWI families can slide nucleosomes along DNA, and can homogenously space nucleosomes to make nucleosomal arrays with uniform linker length *in vitro* (Vary Jr. *et al.*, 2003). In the case of mononucleosome-length chromatin molecules, CHD and ISWI will reposition a nucleosome on the end of the DNA fragment to the middle of the DNA fragment. For ISWI, accessory subunits like Itc1p (ACF in metazoans) help act as a biochemical ruler to regulate DNA translocation in a way that is sensitive to linker DNA (Hwang *et al.*, 2014); for CHD, it has been proposed that the N-terminus of its core subunit may serve a similar role (Hughes and Rando, 2015).

The Ino80 enzyme can also centrally position nucleosomes on DNA fragments. In addition, the Ino80 family of enzymes possesses the ability to replace nucleosomal histone H2A/H2B dimers with different, free H2A/H2B dimers. SWR complex, another member of the Ino80 family, specifically replaces nucleosomal H2A/H2B dimers with H2AZ variant-containing dimers (Mizuguchi, 2004); Ino80 catalyzes the reverse reaction (Papamichos-Chronakis *et al.*, 2011). This activity appears to be catalyzed by subcomplexes associated with this enzyme family's elongated (200-300aa long) ATPase insertion domains. These subcomplexes contain the AAA+ ATPase Rvb helicase proteins, along with additional conserved subunits that are central to regulating both ATPase activity

and enzyme complex conformation. Interestingly, SWR appears to be specialized for histone dimer exchange—it lacks nucleosome sliding activity, and has a uniquely low ATP hydrolysis rate (Watanabe *et al.*, 2015).

SWI/SNF-family chromatin remodeling enzymes

The final family of ATP-dependent chromatin remodeling enzymes is named after the founding complex, SWI/SNF. The SWI/SNF enzyme family, which contains SWI/SNF, RSC (Figure 4A), and their respective human homologs SWI/SNF-A (BAF) and SWI/SNF-B (P-BAF) (Figure 4B), possess nucleosome sliding (Cote *et al.*, 1994; Kwon *et al.*, 1994), H2A/H2B dimer eviction (Vicent *et al.*, 2004), and octamer eviction (Dechassa *et al.*, 2010) activities *in vitro* (Figure 4C). When given a mononucleosome substrate that is positioned in the center of a DNA fragment, SWI/SNF enzymes will push the nucleosome to either end of the DNA (Jaskelioff *et al.*, 2000), in contrast to the spacing and centering activities of other enzyme families.

This spacing-insensitivity may also contribute to the octamer eviction activity of SWI/SNF enzymes. SWI/SNF has been shown *in vitro* to evict dimers from nucleosomes it remodels (Yang *et al.*, 2007), as well as dimers and octamers from nucleosomes that are adjacent to the nucleosome being remodeled by SWI/SNF (Dechassa *et al.*, 2010). One suggested mechanism for this eviction is the anchoring and committed remodeling of one nucleosome by SWI/SNF; after sufficient DNA is translocated into that nucleosome, the adjacent

Figure 4: SWI/SNF-family chromatin remodeling enzymes. (A) Equimolar amounts of SWI/SNF and RSC (Rsc2p-containing) complex were resolved on SDS-PAGE and visualized by silver staining. Subunits are listed next to their corresponding protein bands; names in red are the ATPase subunits, names in blue are the shared Arp submodule. **(B)** Table containing evolutionarily conserved SWI/SNF-family conserved subunits with their names in *S. cerevisiae* and *H. sapiens*. **(C)** Schematic representation of SWI/SNF family activities on chromatin, top: nucleosome sliding, middle: dimer eviction, bottom: octamer eviction.

A

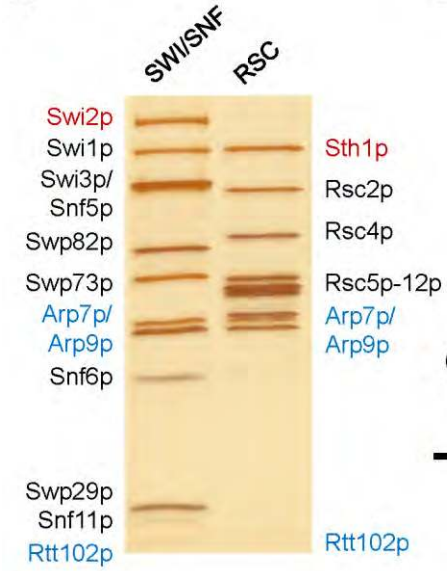

B

S. cerevisiae		*H. sapiens*	
SWI/SNF	RSC	SWI/SNF-A	SWI/SNF-B
Swi2p	Sth1p	Brg1, Brm	Brg1
Swi1p	-	BAF250	-
-	Rsc1p, 2p, 4p	-	PBRM1
Snf5p	Sfh1p	hSNF5	hSNF5
Swi3p	Rsc8p	BAF170/155	BAF170/155
Swp73p	Rsc6p	BAF60A/B/C	BAF60A/B/C
Arp7p Arp9p	Arp7p Arp9p	BAF53 β-actin	BAF53 β-actin

C

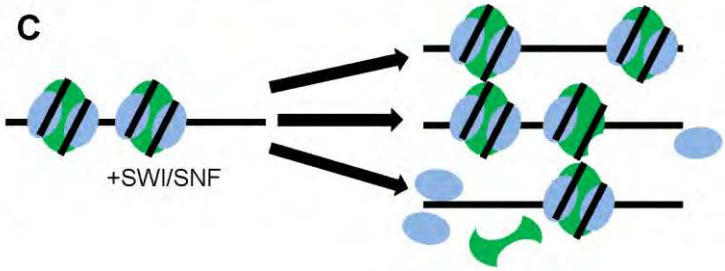

nucleosome becomes destabilized. This mechanism, however, cannot explain eviction of H2A/H2B dimers from mononucleosomes by SWI/SNF; a separate mechanism whereby the remodeled nucleosome is destabilized must happen in this case.

The SWI/SNF holoenzyme is a 1.15 megadalton protein complex containing twelve unique subunits: Swi1p, Swi2p/Snf2p, Swi3p, Snf5p, Snf6p, Snf11p, Swp82p, Swp73p, Arp7p, Arp9p, Swp29p and Rtt102p (Smith *et al.*, 2003). Of these subunits, Swi1p, Swi2p, Swi3p, Snf5p, Swp73p, Arp7p and Arp9p have homologs in mammalian SWI/SNF proteins (figure 4B). The core ATPase-containing subunit of SWI/SNF, Swi2p, is characterized by its C-terminal bromodomain and its HSA domain. The HSA domain is an extended alpha-helix that coordinates binding to the regulatory Arp7p/Arp9p/Rtt102p subcomplex (Szerlong *et al.*, 2003, 2008; Schubert *et al.*, 2013). Between the ATPase domain and the bromodomain of Swi2p are a SnAC domain, involved in coupling ATP hydrolysis to nucleosome repositioning, and an AT-hook DNA binding motif (Sen *et al.*, 2011, 2013). Toward the N-terminus of Snf2p is a conserved 40aa-long region that binds to the Snf11p subunit. The N-terminal half of SWI/SNF also interacts with Swi3p, which is thought to then scaffold interactions with the rest of the complex.

Deletion of the Swi3p SANT protein-protein interaction domain results in the dissolution of SWI/SNF into four subcomplexes: Swi2p/Arp7p/Arp9p/Rtt102p, Swi1p, Snf5p, and Swi3p/Swp73p/Snf6. Surprisingly, the Swi2p-containing

minimal subcomplex retains most of the ATPase and nucleosome sliding activity of full SWI/SNF complex, but lacks dimer eviction activity—that activity requires the Swi3p N-terminal acidic patch (Yang *et al.*, 2007). The biochemical sufficiency of the minimal subcomplex is surprising, primarily given how *swi1Δ* and *swi3Δ* yeast have similarly severe growth phenotypes as *swi2Δ* yeast, and how Snf5p and Swp82p crosslink to the nucleosome core (Dechassa *et al.*, 2008). One possible explanation is that the other SWI/SNF subunits primarily function to recruit the enzyme to loci of interest through interactions with transcriptional activators. An alternative, non-mutually-exclusive explanation is that SWI/SNF-catalyzed dimer eviction is a very important, albeit understudied, activity *in vivo*.

SWI/SNF family enzymes play important roles in DNA replication, DNA repair, and transcriptional regulation (Clapier and Cairns, 2009; Venkatesh and Workman, 2015). In line with this, human SWI/SNF family genes are key tumor suppressor genes, found to be mutated in up to 20% of sequenced cancer samples (Kadoch and Crabtree, 2013; Kadoch *et al.*, 2013; Morgan and Shilatifard, 2015). Similarly, budding yeast lacking a functional SWI/SNF complex have the aforementioned severe growth defects, and budding yeast lacking RSC complexes are inviable (Peterson and Herskowitz, 1992; Cairns *et al.*, 1996).

Biochemically, RSC and SWI/SNF are very similar. RSC subunits Sth1p, Sfh1p, Rsc8p, and Rsc6p are paralogs of Snf2p, Snf5p, Swi3p and Swp73p, respectively, and both complexes contain the Arp7p/Arp9p/Rtt102p subcomplex

(Figure 4A). However, these similar complexes have been adapted to serve different roles in the cell. Looking at the subunit composition of these complexes, the key general difference between SWI/SNF and RSC complexes are the mutually exclusive proteins Swi1p (ARID1 in humans) and Rsc1/2/4p (PBRM1 in humans). These components each have multiple domains that can mediate interaction with chromatin substrates. Swi1 contains a zinc finger motif and a conserved ARID DNA-interaction domain. Rsc1/2/4p, present as the single polypeptide PBRM1 in humans, contains six bromodomains, two BAH domains, a zinc finger motif, and a DNA-binding HMG box group domain. RSC and SWI/SNF complexes also differ in abundance—RSC complex (~2000 copies per cell) is more abundant *in vivo* than SWI/SNF (~200 copies per cell) in yeast (Ghaemmaghami *et al.*, 2003). While SWI/SNF is important for inducible gene transcription, RSC plays a crucial role in establishing proper chromatin architecture at promoter regions (Rando and Winston, 2012). The two remodeling enzymes are involved in different DNA repair pathways, as well (Chai *et al.*, 2005).

Interestingly, SWI/SNF complex has also been implicated in regulating heterochromatin. In development, SWI/SNF is part of the trithorax group of genes, genes that are known to counteract heterochromatic polycomb group genes at key homeotic loci (Steffen and Ringrose, 2014). Further work has been done showing that derepression of silent plant flowering genes requires SWI/SNF to antagonize polycomb heterochromatin (Wu *et al.*, 2012; Li *et al.*, 2015). In

yeast, artificially tethered SWI/SNF is sufficient to act as a barrier against Sir heterochromatin spreading (Oki *et al.*, 2004). Finally, SWI/SNF was previously shown to aid in DNA repair of Sir heterochromatin via NER and HR pathways (Chai *et al.*, 2005; Gong *et al.*, 2006; Sinha *et al.*, 2009). These myriad lines of evidence imply that SWI/SNF could dynamically regulate the accessibility of heterochromatin.

The most direct evidence for SWI/SNF interacting with heterochromatin came from *in vitro* homologous recombination studies. While Sir proteins are sufficient to block Rad51p-mediated homology search, the inclusion of SWI/SNF complex reversed this inhibition. No other chromatin remodeling complex studied was able to recapitulate this rescue, even the highly similar RSC complex. These studies also provided a putative mechanism for heterochromatin accessibility—a novel ATP-dependent Sir3p heterochromatin protein eviction activity present in SWI/SNF complex (Sinha *et al.*, 2009). However, the requirements, mechanism, and *in vivo* applications of this activity still remained unknown.

Concluding remarks

Heterochromatin is a repressive mode of storage for genetic information. However, a cell must possess means to dynamically access the DNA contained within heterochromatin, at the very least for DNA repair and replication purposes. ATP-dependent chromatin remodeling enzymes have been found to regulate chromatin structure and play roles in most DNA metabolic pathways, and

specifically the SWI/SNF enzyme may be implicated in dynamically regulating heterochromatin structure. This enzyme complex has a novel Sir3p eviction activity that is sufficient to rescue homologous recombination *in vitro*. However, the mechanism, scope, and applications of this heterochromatin remodeling activity are still largely unknown. This work aimed to address these remaining questions, and in so doing present a new paradigm for genomic regulation.

Chapter II: Binding Interactions Guide Sir3p Eviction by SWI/SNF

Summary

Heterochromatin is a specialized chromatin structure that is central to eukaryotic transcriptional regulation and genome stability. Despite its globally repressive role, heterochromatin must also be dynamic, allowing for its repair and replication. In budding yeast, heterochromatin formation requires Sir2p, Sir3p, and Sir4p, and these Sir proteins create specialized chromatin structures at telomeres and silent mating type loci. Previously, we found that the SWI/SNF chromatin remodeling enzyme can catalyze the ATP-dependent eviction of Sir3p from recombinant nucleosomal arrays, and this activity enhances early steps of recombinational repair *in vitro*. Here, we show that the ATPase subunit of SWI/SNF, Swi2p/Snf2p, interacts with the heterochromatin structural protein Sir3p. Two interaction surfaces are defined, including an interaction between the ATPase domain of Swi2p and the nucleosome binding, Bromo-Adjacent-Homology (BAH) domain of Sir3p. A SWI/SNF complex harboring a Swi2p subunit that lacks this Sir3p interaction surface is unable to evict Sir3p from nucleosomes, even though its ATPase and remodeling activities are intact. In addition, we find that the interaction between Swi2p and Sir3p is key for SWI/SNF to promote resistance to replication stress *in vivo* and for establishment of heterochromatin at telomeres.

Introduction

All eukaryotic genomes are stored within the nucleoprotein structure of chromatin, the core subunit of which, the nucleosome, consists of 147 base pairs of DNA wrapped ~1.7 times around an octamer of histone proteins (Luger *et al.*, 1997a). Over millions of years, eukaryotes have incorporated chromatin structure into the regulation of many aspects of DNA metabolism, from simple nuclear packaging to transcriptional control (Rando and Winston, 2012). This diversity of purpose is reflected in two general types of chromatin structures within the nucleus – euchromatin, which is decondensed and transcriptionally active, and heterochromatin, which is typically localized to the nuclear periphery and repressive for DNA recombination and transcription. Heterochromatin structures are commonly associated with centromeres and telomeres, and these domains package much of a genome's repetitive DNA (Grewal and Jia, 2007). Consequently, the maintenance of heterochromatin is key for genomic integrity, as it prevents illicit recombination among DNA repeats and promotes chromosome segregation during mitosis (Peng and Karpen, 2007, 2009).

On a molecular level, heterochromatic loci are marked by specific chromatin posttranslational modifications, which are recognized and bound by characteristic nonhistone proteins. In many vertebrates, heterochromatin is characterized by members of the heterochromatin protein 1 (HP1) family of proteins, whereas in budding yeast, the silent information regulator (Sir) proteins,

Sir2p, Sir3p, and Sir4p, create heterochromatin structures at telomeres and the silent mating type loci (Grunstein and Gasser, 2013; Canzio *et al.*, 2014). Sir3p is believed to be the key structural component of yeast heterochromatin—Sir3p contains numerous protein-protein interaction motifs (Norris and Boeke, 2010; Ehrentraut *et al.*, 2011; Oppikofer *et al.*, 2013a), including an N-terminal Bromo-Adjacent Homology (BAH) domain that interacts with the nucleosomal surface (Armache *et al.*, 2011; Arnaudo *et al.*, 2013; Wang *et al.*, 2013). BAH domains are found in many other chromatin associated factors, including the Rsc2p subunit of the RSC remodeling enzyme and the Orc1p subunit of the Origin Recognition Complex (Callebaut *et al.*, 1999). The stability of the Sir3p BAH-nucleosome complex requires deacetylated histone H4 lysine 16 (Johnson *et al.*, 1990); consequently, amino acid substitutions at H4-K16 disrupt Sir3p-nucleosome binding and eliminate heterochromatin assembly *in vivo* (Johnson *et al.*, 1990; Onishi *et al.*, 2007; Johnson *et al.*, 2009).

In spite of the repressive structure of heterochromatin, these domains must be replicated and repaired, implying that mechanisms exist to regulate heterochromatin disassembly. Previously, we described an *in vitro* assay to monitor early steps of recombinational repair with recombinant nucleosomal array substrates (Sinha and Peterson, 2008). Whereas the repair machinery was not hindered by the simple presence of nucleosomes, we reported that the binding of the Sir proteins, or even Sir3p by itself, led to dramatic repression of recombinational repair events on nucleosomal arrays (Sinha and Peterson, 2008;

Sinha *et al.*, 2009). Surprisingly, we discovered that the ATP-dependent chromatin remodeling enzyme, SWI/SNF, was able to counteract these repressive effects of heterochromatin *in vitro*, stimulating early steps of homologous recombination. Intriguingly, these assays uncovered that SWI/SNF catalyzed the ATP-dependent eviction of Sir3p from nucleosomes, an activity not shared by several other remodeling enzymes (Sinha *et al.*, 2009). Thus, these studies suggested that the SWI/SNF enzyme may have a unique ability to disrupt heterochromatin structures.

In this paper, we identify a physical interaction between SWI/SNF and the heterochromatin protein Sir3p. We identify a pair of interactions—between the Swi2p Helicase SANT Adjacent (HSA) domain and the Sir3p AAA^+ domain, and between the Swi2p ATPase domain and the Sir3p BAH domain. Surprisingly, the ATPase-BAH interaction is conserved between many Swi2p/Snf2p ATPase family members and between two classes of BAH domains, suggesting a common mode of binding between these domains. Mutations are generated that ablate the interaction between Swi2p and Sir3p, and we find that the Swi2p-Sir3p interaction surfaces are required for SWI/SNF to evict Sir3p from nucleosomal arrays *in vitro*. Furthermore, *in vivo* studies indicate that SWI/SNF-Sir3p interactions are important both for resistance to replication stress and for establishment of silenced heterochromatic domains.

Results

SWI/SNF binds Sir3p

To investigate the unique ability of SWI/SNF to displace Sir3p from nucleosomes, we began by asking whether SWI/SNF and Sir3p physically interact. First, Sir3p-FLAG was affinity purified from yeast and immobilized on anti-FLAG antibody resin. Purified SWI/SNF and RSC remodeling enzymes were incubated with Sir3p-bound beads, and bound and free fractions were analyzed by western blotting (Figure 5A). Strikingly, SWI/SNF, but not the highly related RSC complex, was able to interact with bead-bound Sir3p (Figure 5A). This interaction was also apparent if SWI/SNF was immobilized on beads and incubated with purified Sir3p (Figure 6A). In order to confirm the interaction and to gain insight into which SWI/SNF subunit might be involved, we used far western analysis. Purified SWI/SNF, RSC, and Sir2p/Sir4p complexes were separated on an SDS-PAGE gel and transferred to a membrane. The membrane was incubated in buffer to stimulate protein renaturation, then incubated with purified Sir3p (Fig. 5B). Proteins bound to Sir3p were then detected by western blotting, using antisera to Sir3p. As expected, Sir3p interacted strongly with Sir4p in this assay, but little interaction was detected with subunits of RSC (Fig. 5B, right lanes). In contrast, Sir3p interacted well with two polypeptides from SWI/SNF. The largest species co-migrated with the Swi2p ATPase subunit

Figure 5: SWI/SNF interacts with Sir3p. (A) SWI/SNF, but not RSC, interacts with resin-bound Sir3p. Purified remodeling enzyme was incubated with anti-FLAG resin that was pre-bound with (+) or without (-) Sir3p. 'U', unbound supernatant; 'B', bound fraction. **(B)** Subunits of SWI/SNF, but not RSC, interact with Sir3p by far western. Equimolar amounts of SWI/SNF, RSC and Sir2p/4p complex were separated on SDS-PAGE, electro-blotted, renatured, and incubated with Sir3-FLAG. Sir3p-bound protein bands were visualized by anti-FLAG immunoblotting.

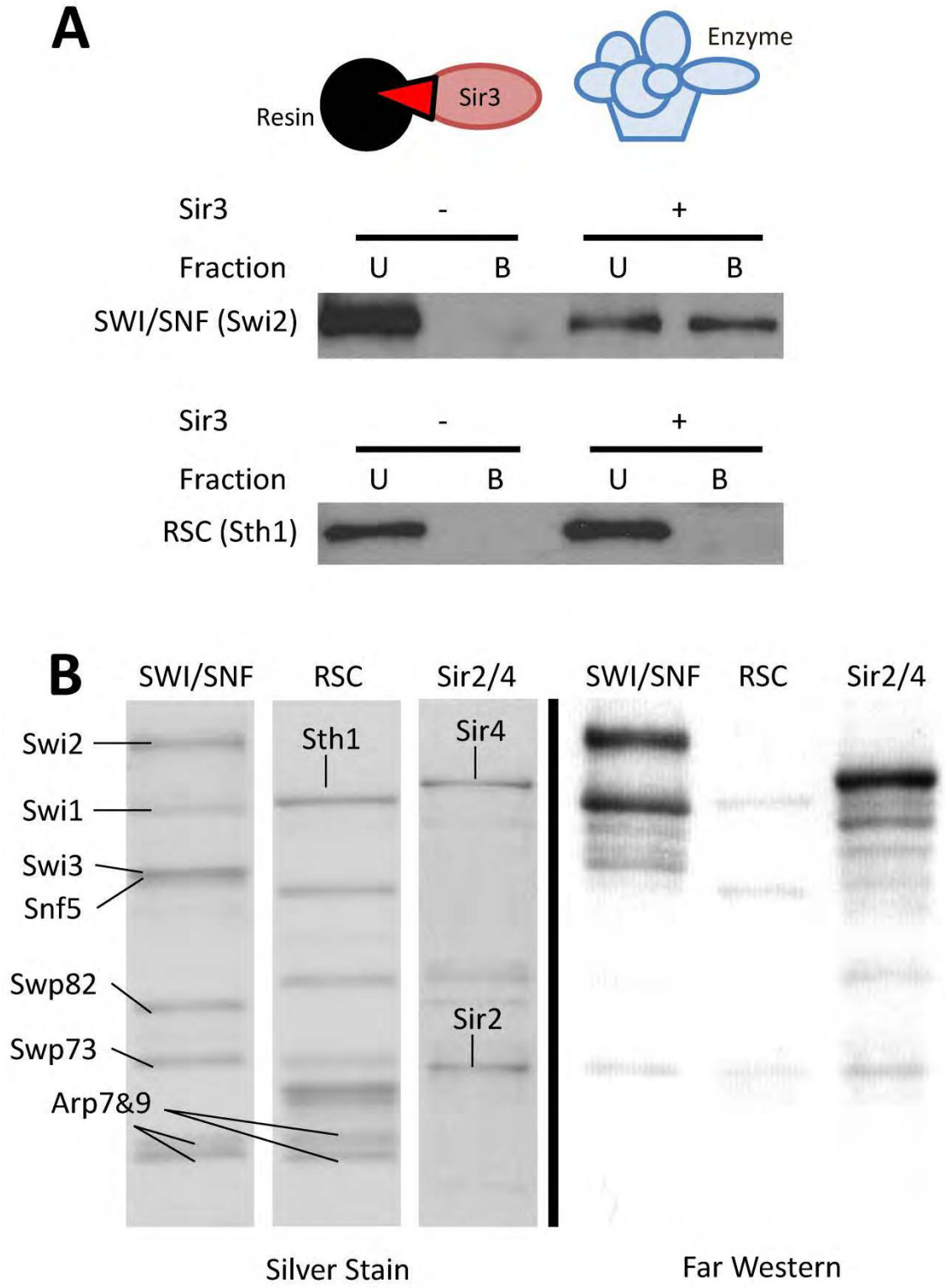
A
Enzyme
Resin
Sir3
Sir3
-
+
Fraction
U
B
U
B
SWI/SNF (Swi2)
Sir3
-
+
Fraction
U
B
U
B
RSC (Sth1)
B
SWI/SNF
RSC
Sir2/4
SWI/SNF
RSC
Sir2/4
Swi2
Swi1
Swi3
Snf5
Swp82
Swp73
Arp7&9
Sth1
Sir4
Sir2
Silver Stain
Far Western

Figure 6: Characterizing Swi2p subdomains that bind Sir3p. (A) Sir3p binds to immobilized SWI/SNF. Calmodulin affinity resin-bound SWI/SNF was incubated with increasing concentrations of Sir3p. **(B)** A central 10 amino acid stretch of the Swi2p HSA domain is required for Sir3p binding. GST fusions of the Swi2p HSA and progressive N-terminal truncations (C1 through C4) and C-terminal truncations (N1 through N4) of it were assayed for ability to bind Sir3p. **(C)** The N-terminal lobe of the Swi2 ATPase is able to bind Sir3p. Pieces of the Swi2p ATPase were assayed as GST fusions for ability to interact with free Sir3p. Bottom: Phyre2 predicted structure (http://www.sbg.bio.ic.ac.uk/phyre2/html/page.cgi?id=index) of the Swi2p ATPase domain, with different colors representing the corresponding regions of the ATPase domain. **(D)** SWI/SNF and RSC complexes interact with *H. sapiens* Orc1 BAH domain.

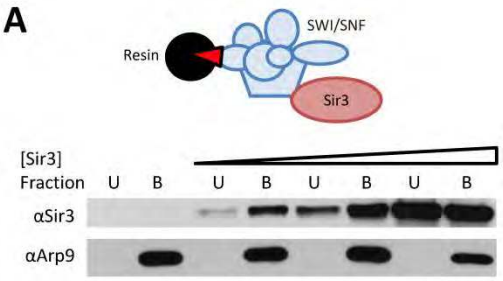
A
SWI/SNF
Resin
Sir3
[Sir3]
Fraction U B U B U B U B
αSir3
αArp9

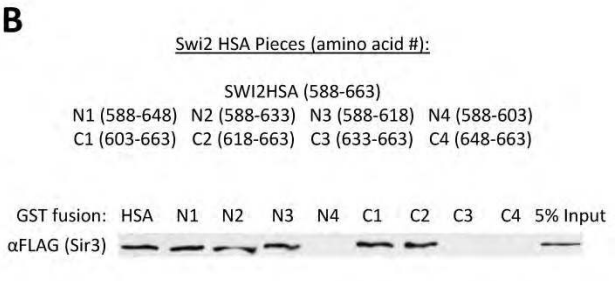
B
Swi2 HSA Pieces (amino acid #):
SWI2HSA (588-663)
N1 (588-648) N2 (588-633) N3 (588-618) N4 (588-603)
C1 (603-663) C2 (618-663) C3 (633-663) C4 (648-663)
GST fusion: HSA N1 N2 N3 N4 C1 C2 C3 C4 5% Input
αFLAG (Sir3)

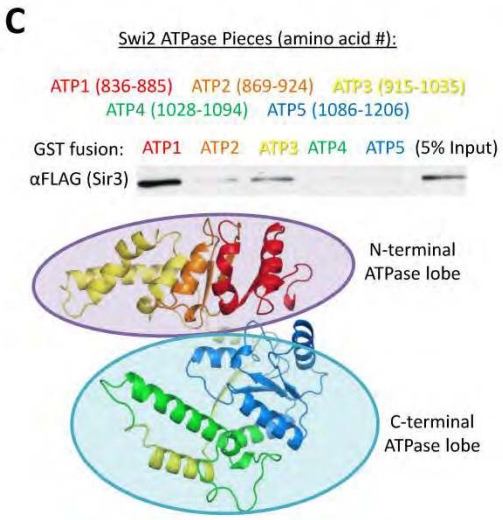
C
Swi2 ATPase Pieces (amino acid #):
ATP1 (836-885) ATP2 (869-924) ATP3 (915-1035)
ATP4 (1028-1094) ATP5 (1086-1206)
GST fusion: ATP1 ATP2 ATP3 ATP4 ATP5 (5% Input)
αFLAG (Sir3)
N-terminal ATPase lobe
C-terminal ATPase lobe

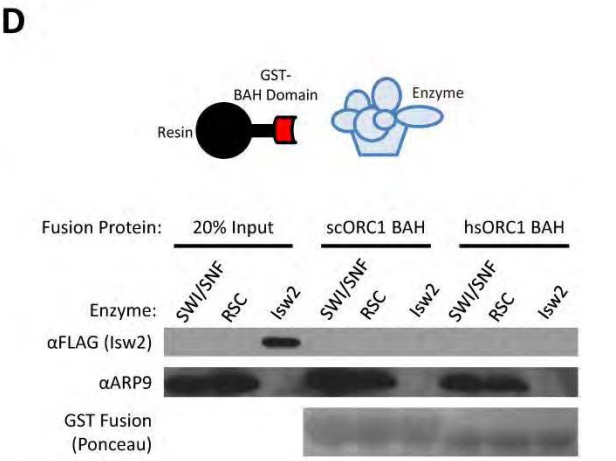
D
GST-BAH Domain
Enzyme
Resin
Fusion Protein: 20% Input scORC1 BAH hsORC1 BAH
Enzyme: SWI/SNF RSC Isw2 SWI/SNF RSC Isw2 SWI/SNF RSC Isw2
αFLAG (Isw2)
αARP9
GST Fusion (Ponceau)

(~250kDa), and the smaller species is either a proteolytic fragment of Swi2p or the Swi1p subunit (~150 kDa).

To directly monitor interactions between Swi2p and Sir3p, each protein was divided into several domains, expressed as GST fusion proteins in bacteria, and used in interaction studies (Fig. 7). First, GST-Swi2p fusions were tested for binding to full-length, purified Sir3p (Fig. 7A). Two regions of Swi2p were found to interact with Sir3p, the HSA domain and the central ATPase domain (Szerlong *et al.*, 2008). Likewise, two regions of Sir3p bound to SWI/SNF complex, the N-terminal BAH domain and a region at the C-terminus of the AAA^+ domain (Fig. 7B). Each domain was then expressed as a FLAG fusion protein and used in GST interaction assays. Interestingly, these domains were found to interact in a pairwise manner -- the Swi2p ATPase domain bound the Sir3p BAH domain, and the Swi2p HSA domain bound the Sir3p AAA^+ domain (Fig. 7C). Progressive N-terminal and C-terminal truncations of the GST-HSA fusion protein (Fig. 6B) defined a region of ten amino acids in the Swi2p HSA domain that is required for interaction with Sir3p (Fig. 7D). Likewise, dissection of the Swi2p ATPase domain identified a 49 amino acid fragment within the first RecA-like fold that retained Sir3p binding activity (Fig. 6C). Interestingly, the analogous residues from the ATPase domain of the RSC catalytic subunit, Sth1p, were unable to bind to Sir3p (Fig. 7D).

Figure 7: Swi2p and Sir3p have multiple interaction domains. (A) Schematic shows Swi2p domains. GST-Swi2 fusion proteins were used in pulldown assays with full-length Sir3p. GST-bound fractions were analyzed by western blot. 10% of Input is shown. **(B)** Schematic shows Sir3p domains. GST-Sir3 fusions were used in pulldown studies with SWI/SNF complex. Bound fractions were assayed by western blot as in (A). **(C)** GST-Swi2 or GST-Sir3 fusion proteins were incubated with FLAG-tagged Swi2p or Sir3p domains, and interactions were identified by GST pulldown and western analyses. **(D)** Swi2p alterations that disrupt Sir3p interactions. Schematic depicts alterations within either the Swi2p HSA or ATPase domain. The Δ10 derivative removes Swi2p residues 613-622; the Sth1(R) derivative replaces Swi2p residues 836-885 with the homologous region from Sth1 (residues 539-588). GST-Swi2 fusions harboring the indicated alterations were used in GST pulldowns with full-length Sir3p. Note that these binding assays used the individual HSA and ATPase regions of Swi2p.

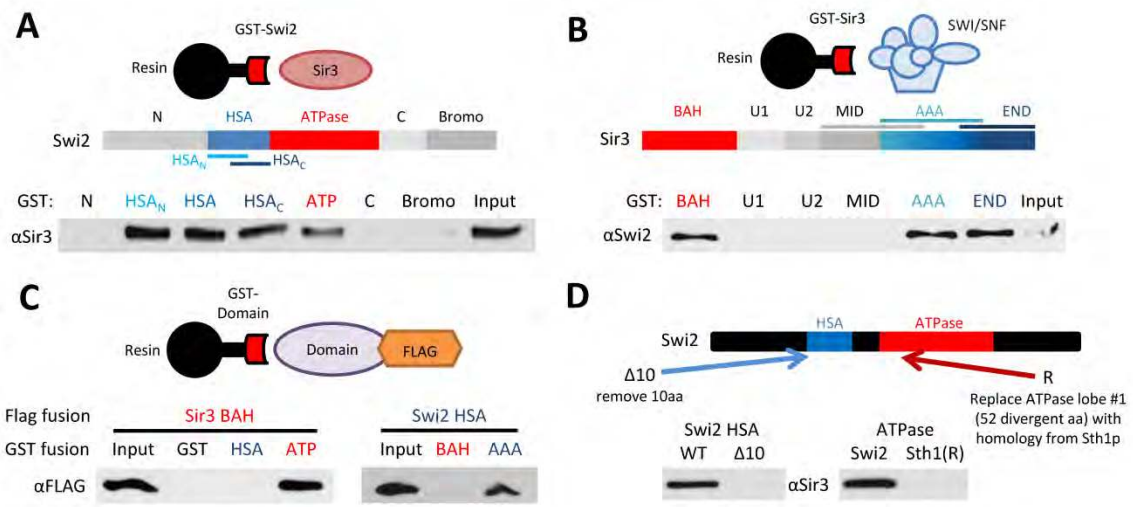
A
GST-Swi2
Resin
Sir3
N
HSA
ATPase
C
Bromo
Swi2
HSA_N
HSA_C
GST: N HSA_N HSA HSA_C ATP C Bromo Input
αSir3
B
GST-Sir3
SWI/SNF
Resin
BAH
U1
U2
MID
AAA
END
Sir3
GST: BAH U1 U2 MID AAA END Input
αSwi2
C
GST-Domain
Resin
Domain
FLAG
Flag fusion
Sir3 BAH
Swi2 HSA
GST fusion
Input GST HSA ATP
Input BAH AAA
αFLAG
D
HSA
ATPase
Swi2
Δ10
remove 10aa
R
Replace ATPase lobe #1 (52 divergent aa) with homology from Sth1p
Swi2 HSA
WT Δ10
ATPase
Swi2 Sth1(R)
αSir3

SWI/SNF and RSC interact with core BAH domains

Progressive C-terminal truncations were used to delimit the SWI/SNF-interacting sequences within the Sir3p BAH domain (Fig. 8A). Each deletion construct retained SWI/SNF binding, and a GST fusion that contained only the 97-amino acid core BAH domain was sufficient to interact with SWI/SNF. Surprisingly, this core BAH domain also interacted strongly with the RSC remodeling enzyme, whereas larger BAH-containing fragments were either unable to interact or interacted only weakly with RSC (Fig. 8A). To test if a BAH core domain might generally be sufficient for interaction with SWI/SNF-like enzymes, the core BAH domain of Rsc2p was assayed for interactions. Indeed, both SWI/SNF and RSC interacted well with the Rsc2p BAH core domain; however, inclusion of the conserved C-terminal (CT-1) domain eliminated interactions with both SWI/SNF and RSC (Chambers *et al.*, 2013). Furthermore, SWI/SNF also bound to the BAH domain from Orc1p, a subunit of the Origin Recognition Complex (ORC) (Fig. 8B). The RSC remodeling enzyme was also able to bind to the Orc1p BAH, despite being unable to interact with Sir3p BAH. Both SWI/SNF and RSC were also competent to bind to the human ORC1 BAH (Fig. 6D). In contrast, the Isw2 remodeling enzyme did not interact at detectable levels with either the Sir3 or yORC1 BAH domain, suggesting that BAH interactions may be a general feature of only the SWI/SNF subfamily of chromatin remodeling enzymes (Fig. 8B). These data also suggest that

Figure 8: SWI/SNF ATPases interact with BAH core domains. (A) Schematic shows C-terminal truncations within the Sir3p BAH domain. The indicated GST-BAH fusion proteins were incubated with either SWI/SNF or RSC, and bound fractions were assayed by western. The Rsc2p BAH fusion contains only the core BAH domain; the BAHCT-1 fusion also contains the C-terminal conserved CT-1 domain from Rsc2p. Western analyses used sera to the Arp9p subunit, common to both remodeling enzymes. **(B)** SWI/SNF, RSC or Isw2 complexes were incubated with GST- BAH fusions from yeast Orc1p or Sir3p. Bound fractions assayed by western to the indicated subunits. Bottom panel shows ponceau-stained membrane, depicting levels of GST fusions.

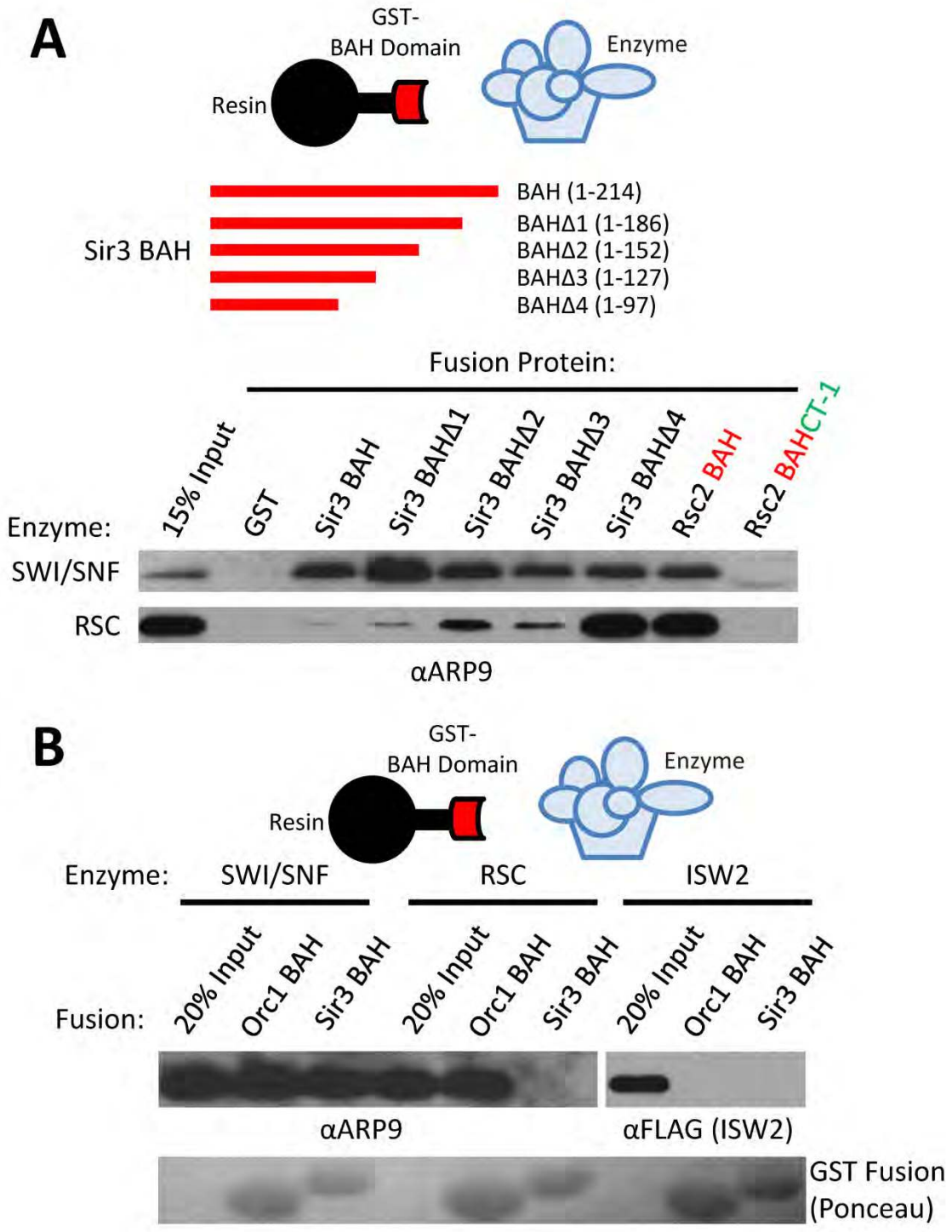
A
GST-
BAH Domain
Resin
Enzyme
Sir3 BAH
BAH (1-214)
BAHΔ1 (1-186)
BAHΔ2 (1-152)
BAHΔ3 (1-127)
BAHΔ4 (1-97)
Fusion Protein:
15% Input
GST
Sir3 BAH
Sir3 BAHΔ1
Sir3 BAHΔ2
Sir3 BAHΔ3
Sir3 BAHΔ4
Rsc2 BAH
Rsc2 BAHCT-1
Enzyme:
SWI/SNF
RSC
αARP9
B
GST-
BAH Domain
Resin
Enzyme
Enzyme:
SWI/SNF
RSC
ISW2
Fusion:
20% Input
Orc1 BAH
Sir3 BAH
20% Input
Orc1 BAH
Sir3 BAH
20% Input
Orc1 BAH
Sir3 BAH
αARP9
αFLAG (ISW2)
GST Fusion
(Ponceau)

sequences C-terminal to BAH core domains may govern the specificity of remodeling enzyme interactions.

Swi2/Snf2-Sir3p interactions are required for Sir3p eviction *in vitro*

Having identified Sir3p-interaction domains within Swi2p, we asked if they were required for the ATP-dependent eviction of Sir3p by SWI/SNF. To this end, a *SWI2* gene was created that contains a 10 amino acid deletion within the HSA domain (Δ10) as well as a 197 amino acid swap between the Sth1p and Swi2p ATPase domains (Sth1[R]) (termed *swi2-Δ10R*; see Figure 7D). This region of Sth1p encompasses the first RecA-like lobe of the ATPase domain. This region is nearly homologous to that of Swi2p, with the exception of a central, 52 amino acid divergent region. A C-terminal, TAP-tagged version of Swi2-Δ10R was then expressed in yeast from its normal promoter on a low-copy CEN/ARS plasmid, and SWI/SNF complex (SWI/SNF-Δ10R) that harbors Swi2p-Δ10R was isolated by tandem affinity purification. The concentration of active enzyme was determined by ATPase assays, and equal ATPase units of wild-type and SWI/SNF-Δ10R complexes were analyzed by SDS-PAGE and silver staining. The subunit composition of the SWI/SNF-Δ10R complex was nearly identical to that of wild-type SWI/SNF, with the exception of a ~2-fold depletion of the Arp7p and Arp9p subunits (Figure 9A). Since Arp subunits have been implicated in the regulation of ATPase kinetic parameters (Shen *et al.*, 2003), we characterized the ATPase activity of the SWI/SNF-Δ10R complex. Importantly, the SWI/SNF-

Figure 9: Swi2p-Sir3p contacts are required for eviction of Sir3p from nucleosomes. (A) SDS PAGE analysis of SWI/SNF and SWI/SNF-Δ10R complexes, visualized by silver staining. Equal levels of ATPase activity were loaded for each enzyme. **(B)** DNA-stimulated ATPase kinetics of SWI/SNF and SWI/SNF-Δ10R are equivalent. ATPase reactions were performed with varying concentrations of DNA cofactor, and hydrolysis rates were fit to Michaelis-Menten kinetic parameters. **(C)** Mononucleosome mobilization by SWI/SNF and SWI/SNF-Δ10R enzymes is equivalent. Varying concentrations of enzymes were incubated with a mononucleosome positioned in the center of a radiolabeled, 282bp DNA fragment harboring a 601 positioning sequence. Predicted positions of mononucleosomes are indicated to the left. Top: gel; bottom: quantification (error bars reflect standard deviation). **(D)** Schematic of the chromatin capture assay. Biotinylated nucleosomal arrays are bound to Sir3p, incubated with chromatin remodeling enzyme and ATP, and captured on streptavidin-coated magnetic beads. Chromatin-bound 'B' and unbound 'U' are assayed by western blotting. **(E)** SWI/SNF-Δ10R is defective for Sir3p eviction from nucleosomes. Increasing amounts of chromatin remodeling enzyme were incubated with Sir3p-bound nucleosomal array, and Sir3p eviction into the chromatin-unbound fraction 'U' was measured by western blotting. Left: representative blots; right: quantification.

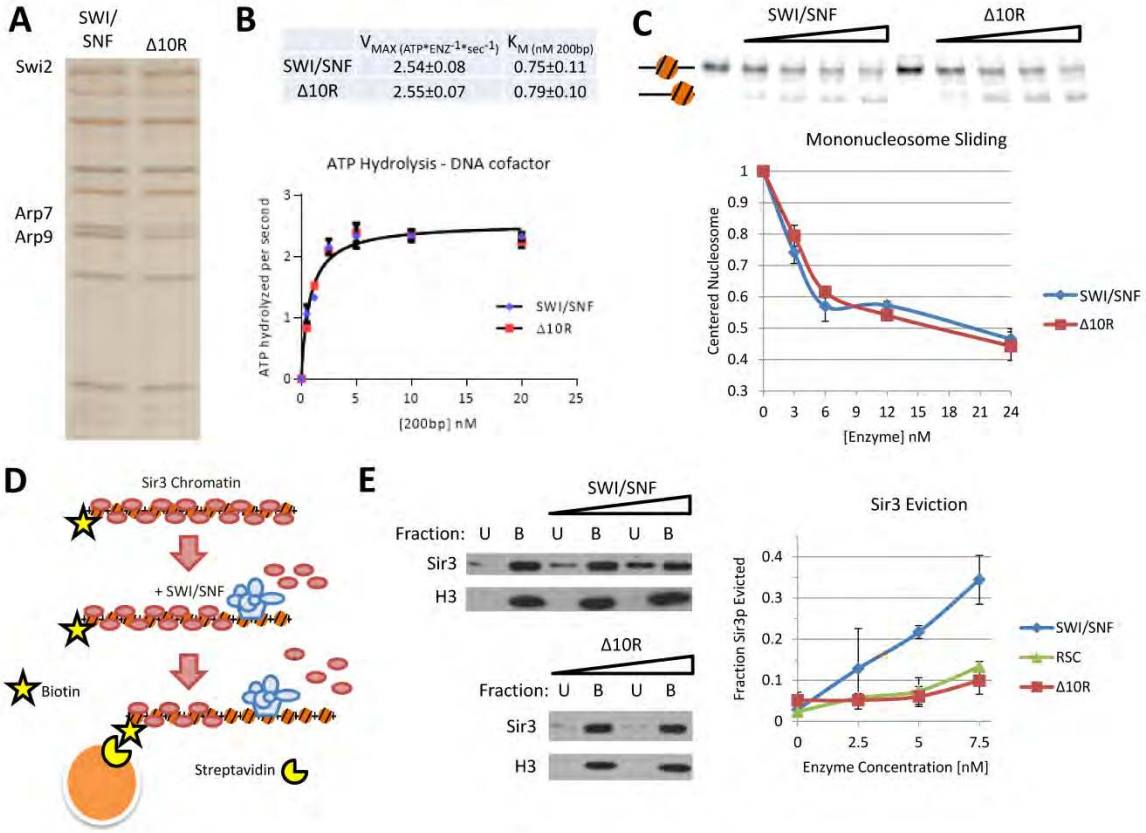
A
SWI/SNF
Δ10R
Swi2
Arp7
Arp9
B
V MAX (ATP*ENZ-1*sec-1)
K M (nM 200bp)
SWI/SNF 2.54±0.08 0.75±0.11
Δ10R 2.55±0.07 0.79±0.10
ATP Hydrolysis - DNA cofactor
ATP hydrolyzed per second
[200bp] nM
SWI/SNF
Δ10R
C
SWI/SNF
Δ10R
Mononucleosome Sliding
Centered Nucleosome
[Enzyme] nM
SWI/SNF
Δ10R
D
Sir3 Chromatin
+ SWI/SNF
Biotin
Streptavidin
E
SWI/SNF
Fraction: U B U B U B
Sir3
H3
Δ10R
Fraction: U B U B
Sir3
H3
Sir3 Eviction
Fraction Sir3p Evicted
Enzyme Concentration [nM]
SWI/SNF
RSC
Δ10R

Δ10R complex exhibited kinetic parameters for DNA-stimulated ATPase activity indistinguishable from the wild-type complex (Figure 9B).

The activity of the SWI/SNF-Δ10R complex was also monitored in several chromatin remodeling assays. First, equal ATPase units of wild-type and SWI/SNF-Δ10R complexes were incubated with mononucleosomes positioned in the center of a radiolabelled 282bp DNA fragment by a 601 nucleosome positioning sequence. The ATP-dependent movement of the nucleosome towards the DNA ends leads to faster mobility on native PAGE, and in this assay, the SWI/SNF-Δ10R enzyme was equivalent to wild-type (Fig. 9C). Chromatin remodeling was also assessed by a nucleosomal array accessibility assay (Logie and Peterson, 1997). This quantitative assay uses a positioned array of 11 nucleosomes, where the central nucleosome of the array occludes a unique SalI restriction enzyme recognition site. As the array is remodeled by SWI/SNF, this central nucleosome is repositioned or removed, increasing the rate of SalI cleavage. Similar to the ATPase and mononucleosome remodeling assays, the SWI/SNF-Δ10R enzyme showed equivalent activity compared to the wild-type complex (Figure 10).

Finally, we assayed the ability of the SWI/SNF-Δ10R enzyme to catalyze the ATP-dependent eviction of Sir3p protein from nucleosomal arrays (Fig. 9D). In this assay, 12-mer nucleosomal arrays were assembled with recombinant histone octamers, and ~15% of the octamers contained histone H2A biotinylated at an engineered cysteine within the exposed C-terminal domain

Figure 10: SWI/SNF-Sir3p contact disruption does not influence array remodeling. SWI/SNF and SWI/SNF-Δ10R were assayed for nucleosome array remodeling activity via the restriction enzyme accessibility assay. Experiment was done in triplicate; error bars denote sample standard deviation.

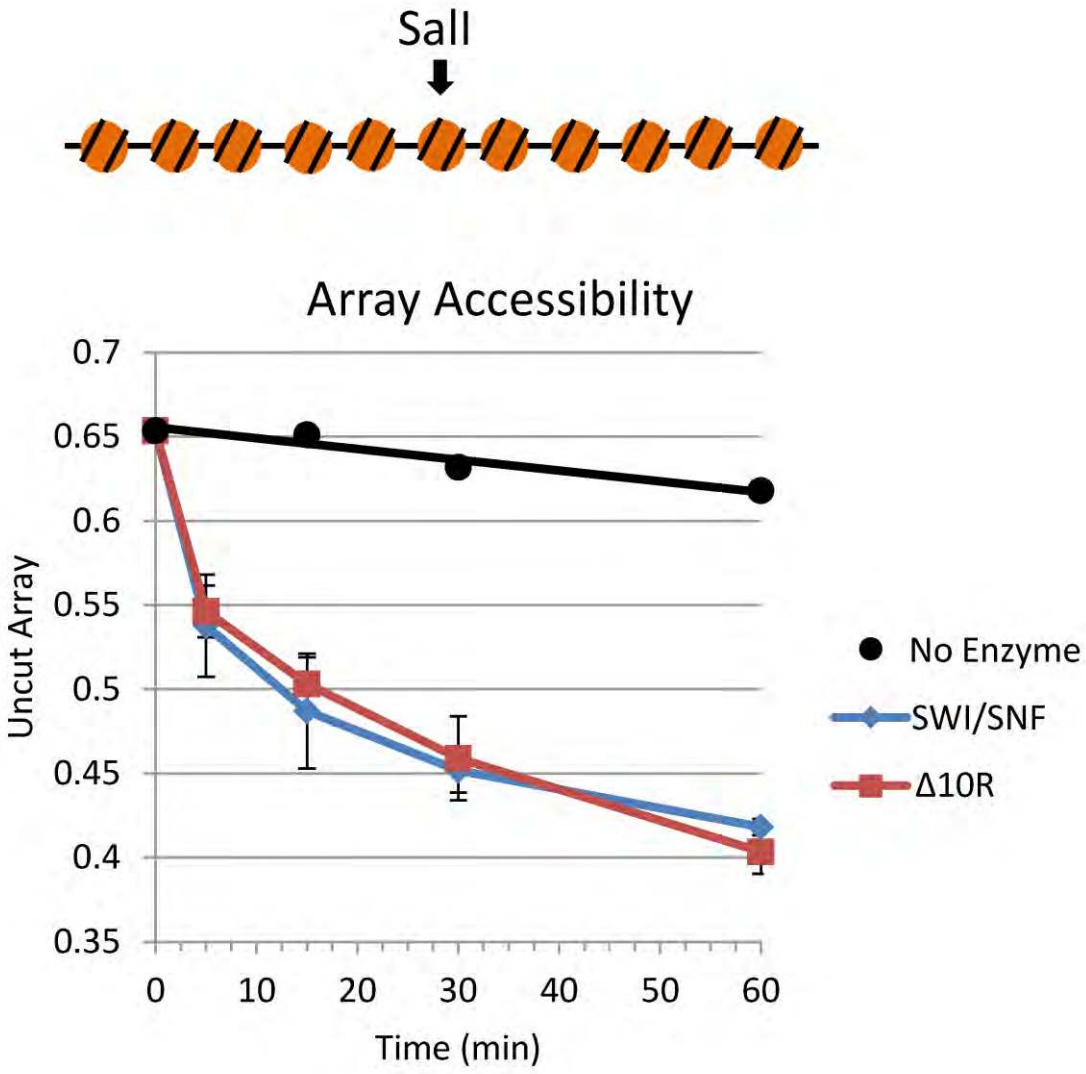
SalI
Array Accessibility
Uncut Array
0.7
0.65
0.6
0.55
0.5
0.45
0.4
0.35
0
10
20
30
40
50
60
Time (min)
No Enzyme
SWI/SNF
Δ10R

(Sinha and Peterson, 2008). Purified Sir3p protein was bound to these arrays at a ratio of two Sir3p monomers per nucleosome (Swygert *et al.*, 2014), and then incubated with chromatin remodeling enzyme in the presence of ATP. Reactions were captured on streptavidin-coated magnetic beads, and chromatin-bound (B) and unbound (U) fractions were subjected to western blotting, probing for both histone H3 and Sir3p. In these reactions, wild-type SWI/SNF was able to evict ~35% of the Sir3p into the unbound fraction, whereas the SWI/SNF-Δ10R complex was defective at Sir3p eviction (Fig. 9E). Indeed, the SWI/SNF-Δ10R complex resembled the activity of RSC, in that it only evicted small amounts of Sir3p at high concentrations (Fig. 9E). We conclude that the Sir3p interaction surfaces within Swi2p are dispensable for chromatin remodeling, but they are required for Sir3p eviction.

SWI/SNF-Sir3p Interactions are important *in vivo*

To identify potential phenotypes for the *swi2-Δ10R* allele that might be linked to Sir3p function, a plasmid-borne copy of *swi2-Δ10R* was introduced into *swi2Δ* and *swi2Δ sir3Δ* strains, and growth was assayed by spot dilution on several media. In the absence of *SWI2*, cells grow poorly on rich media or on media containing galactose or raffinose as carbon sources (Neigeborn and Carlson, 1984). In these cases, the *swi2-Δ10R* allele fully complemented these phenotypes, behaving like a wild-type strain (Fig. 11A). In contrast, the *swi2-Δ10R* allele showed a marked sensitivity to the replication stress agent

Figure 11: SWI/SNF-Sir3p interactions regulate resistance to replication stress and the establishment of telomeric silencing. (A) Growth assays. CEN/ARS plasmids containing either *SWI2* (CP1410), *swi2-Δ10R* (CP1413), or no insert (CP1250; pRS410) were introduced into *swi2Δ* or *swi2Δ sir3Δ* strains. WT and *swi2-Δ10R* complement *swi2Δ* growth and transcriptional defects, but *swi2-Δ10R* does not complement HU sensitivity. Five-fold serial dilutions of yeast cultures were spotted onto the indicated plates and allowed to grow for three days (YPD) or six days (all others) at 30°C. **(B)** Schematic of the subtelomeric silencing establishment assay. CY1755 (L1088; *swi2Δ TELVR::URA3*) was transformed with plasmids containing either *SWI2* (CP1410) or *swi2-Δ10R* (CP1413), and transformant colonies were grown on SD-URA$^+$G418 plates to select for Ura$^+$ cells. Colonies were then cultured in media lacking uracil for the indicated times, and then plated on 5-FOA plates to score establishment of silencing (Ura$^-$). Right: representative 5-FOA plates after 24 hours of growth on 5-FOA. **(C)** Quantitation of the assay from (B); five independent transformants were analyzed; error bars reflect standard deviation.

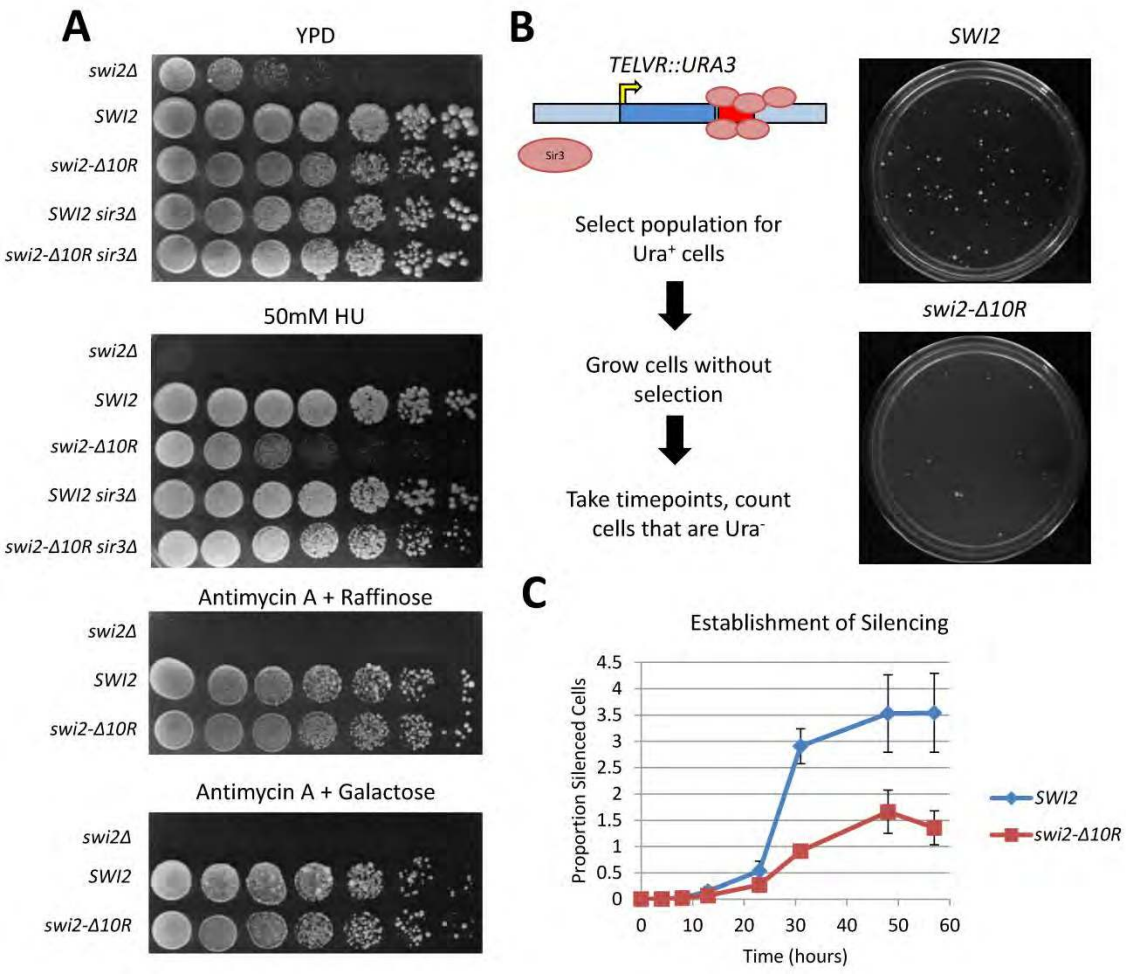
A
YPD
swi2Δ
SWI2
swi2-Δ10R
SWI2 sir3Δ
swi2-Δ10R sir3Δ
50mM HU
swi2Δ
SWI2
swi2-Δ10R
SWI2 sir3Δ
swi2-Δ10R sir3Δ
Antimycin A + Raffinose
swi2Δ
SWI2
swi2-Δ10R
Antimycin A + Galactose
swi2Δ
SWI2
swi2-Δ10R
B
TELVR::URA3
Sir3
Select population for Ura+ cells
Grow cells without selection
Take timepoints, count cells that are Ura-
SWI2
swi2-Δ10R
C
Establishment of Silencing
Proportion Silenced Cells
4.5
4
3.5
3
2.5
2
1.5
1
0.5
0
0
10
20
30
40
50
60
Time (hours)
SWI2
swi2-Δ10R

hydroxyurea (HU; Fig. 11A). Previous studies have suggested that the HU^s phenotype of *swi/snf* mutants may be due to a defect in transcriptional induction of ribonucleotide reductase (*RNR*) genes (Sharma and Reese, 2003); however, the *swi2-Δ10R* strain exhibited wild-type levels of *RNR3* transcriptional induction (Fig. 12A). Indeed, no significant changes in RNA expression were observed between wild-type and *swi2-Δ10R* strains when assayed by RNA-seq (Figs. 12B, 12C, Dataset 1). Consistent with previous work (Lenstra *et al.*, 2011), *swi2-Δ10R* did not affect *SIR2* or *SIR3* expression (Fig. 12D, Dataset 1). Interestingly, the HU^S phenotype of the *swi2-Δ10R* is suppressed by deletion of *SIR3*, consistent with a functional interaction between SWI/SNF and Sir3p during replication stress.

To test whether SWI/SNF regulates the dynamics of heterochromatin assembly, wild-type and *swi2-Δ10R* strains were assayed in a transcriptional silencing establishment assay (Dror and Winston, 2004). This assay was performed in strains with a *URA3* gene integrated adjacent to the telomere on right arm of chromosome V (*TELVR::URA3*). In this location, *URA3* expression is repressed by the spreading of adjacent subtelomeric heterochromatin, creating a biphasic population of Ura^- and Ura^+ cells. To monitor the establishment of the silenced state, cells were first grown in media lacking uracil, to enrich for cells in which *URA3* is in the ON state (Ura^+). Cells were then grown in the presence of uracil for increasing time, then plated onto plates that contain 5-FOA, scoring for cells that have silenced *URA3* (Ura^-). Compared to the wild-type, the *swi2-Δ10R*

Figure 12: *swi2-Δ10R* has no major transcriptional effects. (A) *swi2Δ* yeast, with either *SWI2* (CP1410) or *swi2-Δ10R*(CP1413), and with or without *SIR3* (labels as in Fig. 5A), was exposed to 200mM HU. Expression of *RNR3* relative to *ACT1* expression in each strain was quantified by RT-qPCR before and after exposure to HU. Experiment was done in biological triplicate; error bars represent sample standard deviation. **(B)** Scatterplot of gene expression in *SWI2* and *swi2-Δ10R* as measured by RNA-seq. Each gene is represented by a point. **(C)** Jensen-Shannon distance between *SWI2* and *swi2-Δ10R* RNA-seq replicates. **(D)** *SIR2* and *SIR3* transcript levels are not affected in the *swi2-Δ10R* mutant strain.

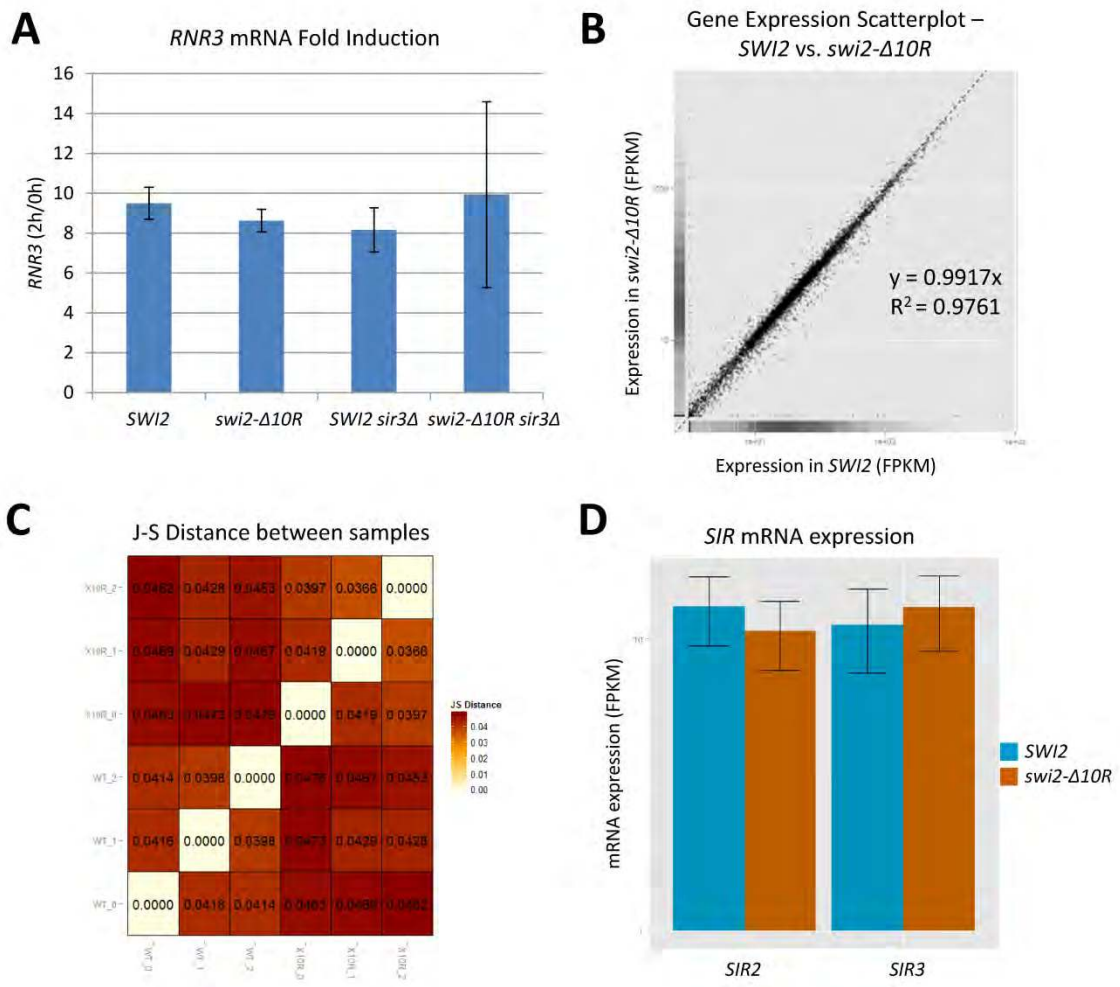
A
RNR3 mRNA Fold Induction
RNR3 (2h/0h)
16
14
12
10
8
6
4
2
0
SWI2
swi2-Δ10R
SWI2 sir3Δ
swi2-Δ10R sir3Δ
B
Gene Expression Scatterplot –
SWI2 vs. swi2-Δ10R
Expression in swi2-Δ10R (FPKM)
y = 0.9917x
R2 = 0.9761
Expression in SWI2 (FPKM)
C
J-S Distance between samples
0.0462 0.0428 0.0453 0.0397 0.0366 0.0000
0.0429 0.0419 0.0000 0.0366
0.0000 0.0397
0.0414 0.0398 0.0000
0.0416 0.0000 0.0398 0.0428
0.0000 0.0418 0.0414
JS Distance
0.04
0.03
0.02
0.01
0.00
D
SIR mRNA expression
mRNA expression (FPKM)
SWI2
swi2-Δ10R
SIR2
SIR3

mutant had a delayed onset of silencing and achieved a lower final level of silencing (Fig. 11D). Furthermore, the *swi2-Δ10R* strain formed much smaller colonies, suggesting that silencing is inherited less stably (Fig. 11D). Thus, these results suggest that interactions between SWI/SNF and Sir3p impact heterochromatin dynamics *in vivo*.

SWI/SNF is not required for heterochromatic recombinational repair

Yeast mating type switching requires that a double strand break (DSB) induced at the *MAT* locus is repaired by homologous recombination with sequences from a heterochromatic *HM* locus (Pâques and Haber, 1999). Previously, *in vivo* studies suggested that SWI/SNF is essential for mating type switching, and that SWI/SNF promotes repair only when the donor sequences are heterochromatic (Chai *et al.*, 2005; Sinha *et al.*, 2009). As an initial test for whether the *swi2-Δ10R* allele impacts heterochromatic mating type switching, a plasmid expressing a galactose-inducible HO endonuclease was introduced into isogenic wild-type, *swi2Δ*, and *swi2-Δ10R* strains. The strand invasion step of mating type switching was then assayed by a PCR-based assay following a switch to galactose media (Sugawara and Haber, 2012). Surprisingly, neither the *swi2-Δ10R* or *swi2Δ* strains showed a significant defect in strand invasion (Fig. 13A).

To confirm this observation, a *swi2Δ* strain was created by tetrad dissection in a strain harboring a chromosomal, galactose-inducible HO gene.

Figure 13: *SWI2* is dispensible for yeast mating type switching. (A) *swi2Δ* yeast (CY2041) were transformed with *pGAL-HO* and either pRS410 alone, CP1410 or CP1413. HO endonuclease expression was induced with galactose, then repressed with glucose to allow repair. Kinetics of HO-induced DSB formation and HR strand invasion were measured by qPCR. Averages of biological duplicates are shown. **(B)** Diploid yeast heterozygous for *SWI2* were sporulated and the resultant tetrads were dissected into haploid spores. Of the spores shown, 1C, 1D, 2B, 2C, 3A, and 3C are *SWI2*; the rest (triangles) are *swi2Δ*. **(C)** *swi2Δ* strains as from panel B were shifted into galactose to induce mating-type switching, then diluted, plated on rich media, and subjected to mating type testing. Shown are representative plates where before galactose, all yeast are MAT_{α}, and after galactose, approximately 60% of yeast have become MAT_{A}. **(D)** Top: a timecourse showing degradation of AID-tagged Swi2p by *A. thaliana* Tir1 E3 ligase in the presence of a synthetic auxin analog. Bottom: kinetics of DSB formation and repair; experiments done as in (A), but galactose was only added after cultures had been treated with or without 1-NAA.

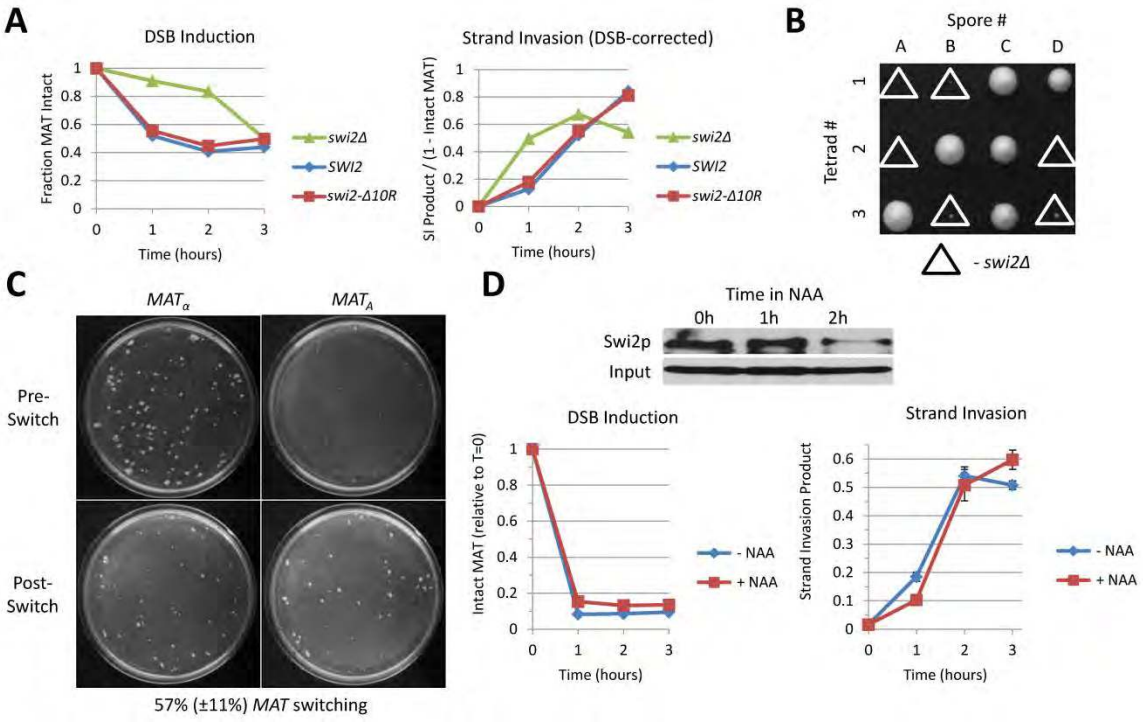
A
DSB Induction
Fraction MAT Intact
Time (hours)
swi2Δ
SWI2
swi2-Δ10R
Strand Invasion (DSB-corrected)
SI Product / (1 - Intact MAT)
Time (hours)
swi2Δ
SWI2
swi2-Δ10R
B
Spore #
A B C D
Tetrad #
1 2 3
- swi2Δ
C
MAT$_\alpha$
MAT$_A$
Pre-Switch
Post-Switch
57% (±11%) MAT switching
D
Time in NAA
0h 1h 2h
Swi2p
Input
DSB Induction
Intact MAT (relative to T=0)
Time (hours)
- NAA
+ NAA
Strand Invasion
Strand Invasion Product
Time (hours)
- NAA
+ NAA

Notably, this is the same background as used in previous studies (Chai *et al.*, 2005). Multiple *swi2Δ* segregants from independently created diploids showed severe growth defects (Fig. 13B) and delayed galactose induction kinetics that precluded kinetic analyses of strand invasion. However, following growth for 4 hours in galactose media, *swi2Δ* strains were competent to switch mating types with efficiencies similar to the wild-type strain (Fig. 13C). To circumvent the galactose induction defects of a *swi2Δ* and to study the kinetics of strain invasion, an auxin-inducible degron system was used to conditionally deplete Swi2p (Nishimura *et al.*, 2009). Following a 2-hour treatment with synthetic auxin (NAA) to deplete Swi2p, galactose was added to cultures, and PCR was used to monitor DSB formation and strand invasion. Consistent with the results from the *swi2Δ* strain, depletion of Swi2p did not alter DSB repair kinetics (Fig. 13D). Since the Swi2p ATPase is essential for SWI/SNF function, these results indicate that SWI/SNF is dispensable for mating type switching, even with a heterochromatic donor.

Discussion

Here, we have defined two distinct protein-protein interfaces between the Sir3p heterochromatin protein and the Swi2p subunit of the SWI/SNF chromatin remodeling enzyme. The HSA domain from Swi2p interacts with a region of Sir3p that contains its AAA^+ domain, and an N-terminal portion of the Swi2p

ATPase domain interacts with the nucleosome binding, BAH domain of Sir3p. Intriguingly, Sth1p, the related ATPase from the RSC remodeling enzyme, can also bind to the Sir3p BAH domain, but only after elimination of flanking sequence elements. Furthermore, both Swi2p and Sth1p are able to bind to the central core of the Rsc2p and Orc1p BAH domains, suggesting that SWI/SNF-like ATPase domains may harbor a general affinity for BAH domains. Importantly, elimination of Sir3p interaction surfaces within Swi2p (Swi2p-Δ10R) disrupts the ability of SWI/SNF to catalyze the ATP-dependent eviction of Sir3p from nucleosomal arrays *in vitro*, without impairing its ATPase or more canonical chromatin remodeling activities. Furthermore, these alterations led to specific phenotypes *in vivo*, consistent with functional interactions between SWI/SNF and Sir3p-dependent heterochromatin structures.

What is the functional role for Sir3p eviction by SWI/SNF? A previous study from Laurent and colleagues (Chai *et al.*, 2005) was consistent with this activity playing an essential role in recombinational repair events that involve heterochromatin. Specifically, they used strains harboring a galactose-inducible HO endonuclease to create a single DNA double strand break (DSB) at the euchromatic *MAT* locus. The recombinational repair of this DSB requires a successful homology search and strand invasion of a homologous, but heterochromatic, *HM* locus. In these assays, they reported that inactivation of the Snf5p subunit of SWI/SNF had no effect on early steps of HR, but that *snf5Δ* eliminated capture of the heterochromatic donor sequences, and repair was

blocked (Chai *et al.*, 2005). Subsequently, we showed that SWI/SNF is not required for recombinational repair of these same sequences when they are euchromatic, suggesting that this role for SWI/SNF might be specific for the heterochromatic context (Sinha *et al.*, 2009). To our surprise, however, our studies presented here do not support this key role for SWI/SNF in heterochromatic recombinational repair. We created *swi2Δ* strains that harbor a *GAL-HO* gene by tetrad dissection, and we find that these strains are competent to repair an HO-induced DSB, leading to mating type switching with efficiencies similar to wild-type. Furthermore, we employed an inducible degron strategy to remove Swi2p from these *GAL-HO* strains, but in this case as well, the loss of Swi2p, and thus SWI/SNF, had no impact on repair of a DSB at the *MAT* locus. Why our results differ from that of Laurent and colleagues in not clear. Unfortunately, the original *snf5Δ* strain is no longer available (B. Laurent, personal communication). The most likely explanation is that the previously observed phenotype was specific to this particular *snf5Δ* isolate that was created by direct cell transformation, rather than tetrad dissection. Alternatively, it could represent a phenotype that is unique to a *snf5Δ* mutant and does not reflect a role for SWI/SNF *per se*.

Yeast strains that lack SWI/SNF show a variety of phenotypes, including growth defects on rich media or media containing alternative carbon sources (e.g. galactose or raffinose), inositol auxotrophy (Neigeborn and Carlson, 1984; Peterson and Herskowitz, 1992), and sensitivity to DNA damaging and

replication stress agents (Chai *et al.*, 2005; Sharma and Reese, 2003). Consistent with the intact chromatin remodeling activities of the SWI/SNF-Δ10R enzyme, strains harboring the *swi2-Δ10R* allele showed normal growth on nearly every condition tested. The lone exception, however, was sensitivity to the replication stress agent, hydroxyurea. Furthermore, this phenotype was suppressed by deletion of the *SIR3* gene, consistent with a role for ATP-dependent Sir3p eviction during replicative stress. This phenotype was not due to a defect in transcriptional induction of the *RNR* genes, nor did the *swi2-Δ10R* allele lead to significant transcriptional changes that could be detected by RNA-seq. Thus, this HU phenotype is likely to reflect a transcription-independent role of SWI/SNF action in antagonizing Sir3p during DNA replication. One simple model posits that SWI/SNF is required for efficient replication through SIR heterochromatin, and that HU-induced fork stress heightens the need for SWI/SNF to remove Sir3p. Alternatively, work from Taddei and colleagues have shown that Sir proteins can be recruited to stalled replication forks (Dubarry *et al.*, 2011). Perhaps SWI/SNF plays a role in removing Sir proteins from stalled forks, alleviating the negative consequences of this Sir recruitment. This model may also provide an explanation for the defect in heterochromatin establishment observed in the *swi2-Δ10R* strain, as an accumulation of Sir3p at stalled forks may titrate Sir proteins from heterochromatic domains, interfering with heterochromatin assembly.

The ATP-dependent eviction of Sir3p from chromatin is reminiscent of the ability of the yeast Mot1p ATPase to catalyze the eviction of the general transcription factor, TBP from DNA. Mot1p is a member of the Swi2p/Snf2p family of DNA-stimulated ATPases and DNA translocases, and the ability of Mot1p to disrupt TBP-DNA interactions appears to be key for re-distributing TBP from TATA-containing binding sites to less preferred, TATA-less promoter elements (Auble, 2009; Zentner and Henikoff, 2013). Similar to SWI/SNF-dependent eviction of Sir3p from nucleosomes, Mot1p evicts TBP from a preformed TBP-DNA complex in an ATP-dependent reaction. Mot1p binds to TBP using two distinct interaction domains—a region containing multiple HEAT domains binds to the convex surface of the TBP-DNA complex, whereas a distinct “latch” domain interacts with the surface of TBP that is bound to DNA (Wollmann *et al.*, 2011). These structural studies have led to a model in which Mot1p binds to DNA adjacent to the TBP-DNA complex, allowing its HEAT domain to make extensive contacts with the exposed, convex surface of TBP. As Mot1p hydrolyzes ATP, DNA translocation leads to removal of TBP from DNA, and the latch domain of Mot1p interacts with the DNA-binding surface of TBP, preventing re-association with promoter DNA (Wollmann *et al.*, 2011). By analogy, we propose that the HSA domain of Swi2p may interact with the Sir3p-nucleosome complex, facilitating Sir3p removal during the DNA translocation reaction. Likewise, sequences within the N-terminal lobe of the ATPase domain

Figure 14: Model for eviction of Sir3p from nucleosomes by SWI/SNF. See text for description. Sir3p is in red, Swi2p is in blue.

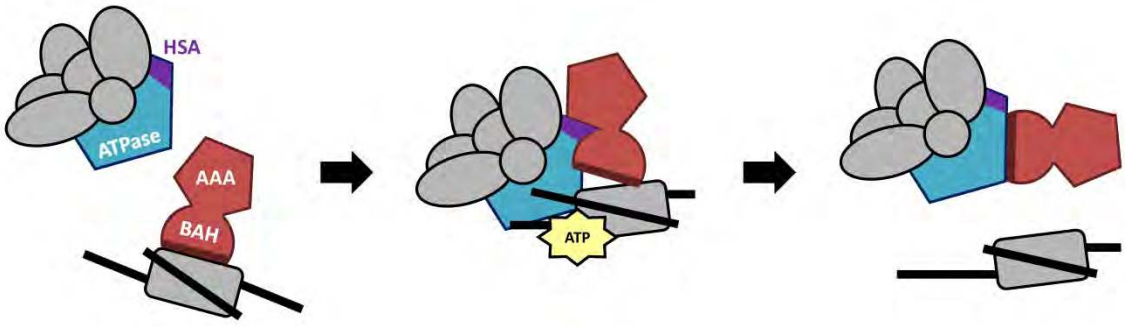
HSA
ATPase
AAA
BAH
ATP

may function as a “latch” that binds the Sir3 BAH domain, preventing re-association with the nucleosome (Fig. 14).

Although the Swi2 ATPase domain is uniquely able to interact with the Sir3p BAH, the ATPase domains from both Swi2p and Sth1p can interact with the yeast Orc1p BAH domain. Likewise, both the SWI/SNF and RSC complexes can bind to the BAH domain of human Orc1. These latter interactions are surprising given that the primary sequence of the yeast and human Orc1 BAH domains have diverged considerably, though the overall structures are homologous (Fig. 15A). Orc1p is a highly conserved member of the Origin Recognition Complex that is essential for cell viability and important for DNA replication (Fox *et al.*, 1995; Klemm *et al.*, 1997; Bell, 2002). Orc1p and Sir3p are paralogs, and as such they display domain and primary sequence conservation, particularly in their N-terminal BAH domains (47% identical sequence). In *K. lactis*, Orc1p has been shown to function analogously to the role of Sir3 in heterochromatin formation, in addition to its traditional role in replication (Hickman and Rusche, 2010). We postulate that the binding interaction between SWI/SNF-family enzymes and Orc1-like BAH domains is ancestral, and that specificity for Sir3p and Swi2p arose following the silencing sub-functionalization of Sir3p. Indeed, the sequences within the Swi2p ATPase domain that diverge from Sth1p, and that appear to provide specificity for Sir3p, are not well conserved in mammalian Swi2p/Snf2p homologs (Fig. 15B). The specificity for different BAH domains seems to be imparted by regions within BAH domains that

Figure 15: Conservation of Orc1 BAH domains and SWI/SNF ATPase domains. (A) Primary sequence alignment of *S. cerevisiae* Orc1p and *H. sapiens* Orc1 BAH domains (left). Structural alignment of *M. musculus* (4DOV) and *S. cerevisiae* (1M4Z) Orc1 BAH domains (right). **(B)** Top: sequence alignment of the N-terminal ATPase lobes of Snf2p, Sth1p, hBRM and BRG1. The Snf2p variable region highlighted in red is also colored red in the structural prediction of the Snf2p N-terminal ATPase lobe below.

A

```
Orc1p     1 MAKTLKDLQGWEIITTDEQGNIIDGG--QKRLRRRGAKTEHYLKRSSDGI 48
            ||.....|:.:.:...:. ::|..  .:..|....|||.    .|..|
hsOrc1    1 MAHYPTRLKTRKTYSWVGRP-LLDRKLHYQTYREMCVKTEG----CSTEI 45

Orc1p    49 KLGRGDSVVMHNEAAGTYSVYMIQELRLNTLNNVVELWALTYLRWFEVNP 98
            .:..|..|::  |.....:.|:.:.|.|...::.........::||
hsOrc1   46 HIQIGQFVLI--EGDDDENPYVAKLLELFEDDSDPPPKKRARVQWF---- 89

Orc1p    99 LAHYRQFNPDANILNRPLNYYNKLFSETANKNELYLTAELAELQLFNFIR 148
            :..........::|.|.... .::|.......:.:.||       ..|.
hsOrc1   90 VRFCEVPACKRHLLGRKPGA-QEIFWYDYPACDSNINAE-------TIIG 131

Orc1p   149 VANVMDGSKWEVLKGNVDPERDFTVRYICEPTGEKFVDINIEDVKAYIKK 198
            :..|:..:..:|:..|:..|:...|:.....  :||..:.|..
hsOrc1  132 LVRVIPLAPKDVVPTNLKNEKTLFVKLSWNE--KKFRPLSSELF------ 173

Orc1p   199 VEPREAQEYLKDLTLP 214
            .|..:.||.......|
hsOrc1  174 AELNKPQESAAKCQKP 189
```

S. cerevisiae Orc1p BAH
M. musculus Orc1 BAH

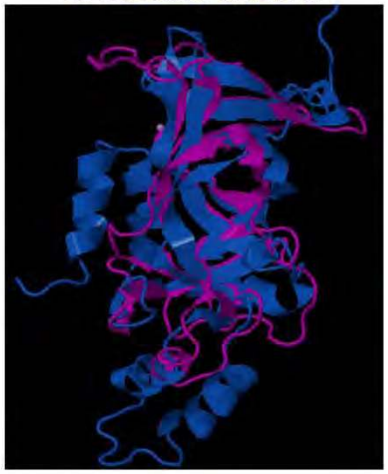

B

```
Swi2p  GTLKDYQIKGLQWMVSLFNNHLNGILADEMGLGKTIQTISLLTYLYEMKNIRGPYLVIVPLSTLSNWSSEFAKWAPTLRTISFKGSPNERKAKQAKIRA
Sth1p  GTLKEYQLRGLEWMVSLYNNHLNGILADEMGLGKTIQSISLITYLYEVKKDIGPFLVIVPLSTITNWTLEFEKWAPSLNTIIYKGTPNQRHSLQHQIRV
hBRM   GTLKHYQLQGLEWMVSLYNNNLNGILADEMGLGKTIQTIALITYLMEHKRLNGPYLIIVPLSTLSNWTYEFDKWAPSVVKISYKGTPAMRRSLVPQLRS
BRG1   GVLKQYQIKGLEWLVSLYNNNLNGILADEMGLGKTIQTIALITYLMEHKRINGPFLIIVPLSTLSNWAYEFDKWAPSVVKVSYKGSPAARRAFVPQLRS

Swi2p  GEFDVVLTTFEYIIKERALLSKVKWVHMIIDEGHRMKNAQSKLSLTLNTHYHADYRLILTGTPLQNNLPELWALLNFVLPKIFNSVKSFDEWFNTPFAN
Sth1p  GNFDVLLTTYEYIIKDKSLLSKHDWAHMIIDEGHRMKNAQSKLSFTISHYYRTRNRLILTGTPLQNNLPELWALLNFVLPKIFNSAKTFEDWFNTPFAN
hBRM   GKFNVLLTTYEYIIKDKHILAKIRWKYMIVDEGHRMKNHHCKLTQVLNTHYVAPRRILLTGTPLQNKLPELWALLNFLLPTIFKSCSTFEQWFNAPFAM
BRG1   GKFNVLLTTYEYIIKDKHILAKIRWKYMIVDEGHRMKNHHCKLTQVLNTHYVAPRRLLLTGTPLQNKLPELWALLNFLLPTIFKSCSTFEQWFNAPFAM
```

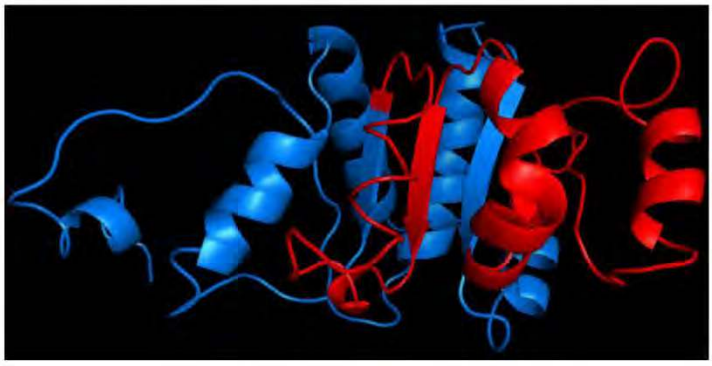

surround and regulate access to the core BAH fold. In line with this hypothesis, we found that the truncated, core BAH domains of Rsc2p and Sir3p were able to interact with both the SWI/SNF and RSC enzymes, but inclusion of C-terminal regions that wrap about the folds inhibited RSC and SWI/SNF binding. Given the plethora of BAH domains associated with chromatin (Callebaut *et al.*, 1999), this theme of BAH accessibility and gating might help regulate ATP-dependent chromatin remodeling enzyme activities in a context-dependent manner.

Materials and Methods

Protein Purification

Tandem affinity purification of SWI/SNF, RSC, SWI/SNF-Δ10R and Sir2p/Sir4p was performed as described previously (Smith *et al.*, 2003; Buchberger *et al.*, 2008). FLAG purification of Isw2 and Sir3p was performed as described previously for Sir3p-FLAG (Buchberger *et al.*, 2008), except that 350mM NaCl (no KCl) was used during the entire purification, and that following elution with 3XFLAG peptide, the protein was concentrated to ~3μM with a 10,000 PES MWCO Vivaspin 500 concentrator (Sartorius #VS0101). Concentrated Sir3p was dialyzed (Pierce #69570) for two hours at 4°C into storage buffer (20mM Hepes pH=7.5, 80mM NaCl, 10% glycerol, 0.1% TWEEN-20) and frozen in liquid nitrogen.

Concentrations of Sir3p and Sir2p/4p were calculated by ImageJ quantification (http://imagej.nih.gov/ij/) of coomassie-stained SDS-PAGE gel image intensities, using purified fraction V BSA for known protein mass standards. Concentration of active chromatin remodeling enzyme was calculated by measuring rates of ATP hydrolysis (see below) at saturating concentrations of dsDNA nucleic acid cofactor. These ATPase concentrations and Sir2p/Sir4p concentrations were used to load equimolar amounts of protein for SDS-PAGE analysis. Silver stain, immunodetection of Arp9p (for RSC and SWI/SNF), and immunodetection of the TAP tag, resulted in intensities that were equivalent between complexes.

GST fusion proteins were expressed using the pGEX-3X vector in Rosetta^{TM} 2 BL-21 (DE3) cells (EMD #71397). *E. coli* were grown at 28°C to an OD_{600} of 0.5, in 50mL LB with 50µg/mL carbenicillin and 17µg/mL chloramphenicol, then protein expression was induced by addition of IPTG to a final concentration of 0.2mM. After one hour of protein expression, *E. coli* were harvested by centrifugation at 2500g at 4°C for 15 minutes, in a Beckman J-6B centrifuge with a JS-4.2 rotor. Cell pellet was stored at -80°C, then thawed on ice and resuspended in 7.5mL lysis buffer (1x PBS with 1% Triton, 1mM DTT, and protease inhibitors [.17µg/mL aprotinin, 2µg/mL leupeptin, 2µg/mL pepstatin, 100µg/mL PMSF, and 1mM benzamidine]). After transfer to a 40mL centrifuge tube, cells were lysed via four fifteen-second pulses of sonication (setting 5, Fisher 550 sonic dismembrator) interspersed with incubations on ice to prevent

heat accumulation. Lysed cells were incubated on ice for 15 minutes, then bacterial debris was removed by centrifugation for 25 minutes at 27000g, at 4°C, in a Beckman J2-HC centrifuge with a JA-17 rotor. Clear supernatant lysate was frozen in liquid nitrogen and stored at -80°C.

Prior to each experiment, lysate aliquots were thawed on ice, and volumes of lysate containing equivalent amounts of each fusion protein (judged from lysate SDS-PAGE) were each brought to a final volume of 1.2 mL by addition of lysis buffer in a 1.5mL eppendorf microcentrifuge tube. These lysates were incubated with 15µL of glutathione sepharose 4B resin slurry (GE # 17-0756-01) at 4°C on a nutator for 1 hour. The resin was washed once in lysis buffer, twice in wash-350 buffer (1xPBS with [NaCl] @ 350mM, 0.1% TWEEN-20, 1mM DTT, 100µg/mL PMSF), and twice in wash buffer (1xPBS, 0.1% TWEEN-20, 1mM DTT, 100µg/mL PMSF). Each wash consisted of a five-minute incubation at 4°C on a nutator with 1mL of the appropriate buffer. Resin was collected by centrifugation for two minutes at 2000g, and supernatant was removed. Fusion protein concentration and purity was verified by SDS-PAGE, as for Sir3p and Sir2p/Sir4p above.

FLAG-fusion domains were purified from *E. coli* in a manner similar to GST fusion proteins, except post-clarification lysate was directly incubated with M2 anti-flag affinity resin (Sigma A2220). Once the resin was washed, protein was eluted with 0.2mg/mL 3xFLAG peptide (Sigma F4799) in 1xPBS. Fusion protein concentration and purity was verified by SDS-PAGE, as above.

Analysis of Enzyme ATP Hydrolysis Kinetics

ATP hydrolysis assays were performed as described previously (Yang *et al.*, 2007), except that quantification of images was performed using ImageJ (see the radiolabel quantification section below). For experiments to measure enzyme K_m, 10nM enzyme was used. As a nucleic acid cofactor, supercoiled pUC19 (NEB #N3041S) plasmid DNA was present, at appropriate concentrations of calculated 200bp DNA equivalent (13.43 per 2686bp plasmid). Microsoft Excel 2010 linear regression was used to calculate the initial velocity of each ATP hydrolysis reaction. This velocity was plotted as a function of 200bp-mer concentration via Graphpad Prism 6. Nonlinear fitting to the Michaelis-Menten equation yielded V_{max} and K_m parameters. Experiments were performed in triplicate, and error bars represent sample standard deviation.

Chromatin Reconstitution and Remodeling Assays

Recombinant *X. laevis* H2A, H2AS113C, H2B, H3 and H4 histones were expressed from pET vectors in BL-21(DE3) *E. coli*. Histones were purified and reassembled into octamers as described previously (Luger *et al.*, 1997b). Octamer containing H2AS113C was biotinylated as described previously (Swygert *et al.*, 2014), and biotinylation was confirmed by western blot analysis with HRP-Streptavidin. Histone octamers were reconstituted onto purified template DNA by the step salt dialysis method (Hansen *et al.*, 1991) at a

nucleosome positioning sequence (NPS) to octamer molar ratio of ~0.94-1.0. For biotinylated chromatin, one sixth of the octamer added to the reconstitution contained biotinylated H2AS113C—the rest of the octamer was wild-type. After reconstitution, a fraction of each array was digested with *Eco*RI and electrophoresed on a 4% Native PAGE gel, in 0.5xTBE buffer, to resolve nucleosomal and free DNA and estimate nucleosomal saturation.

Milligram quantities of 208-11 and 208-12 *L. variegatus* 5S NPS array-containing plasmid DNA (CP589 and CP426, respectively) were purified from *E. coli* (QIAGEN #12191). DNA was digested with a combination of *Hha*I, *Not*I, and *Hin*dIII restriction enzymes, and the array DNA molecule was subsequently separated and purified via a 120mL Sephacryl S-500 gel filtration column (GE #17-0613-01). 282bp-Mid601 DNA was amplified via PCR using Taq polymerase (NEB #M0273L) from plasmid pGEM-3Z lower strand 601 (CP1024) using primers GATCCTCTAGAGTCGGGAGCTC and TGACCAAGGAAAGCATGATTCTTCAC. DNA was purified by phenol/chloroform extraction and ethanol precipitation, then digested with *Xba*I restriction endonuclease. 208-11 array DNA and 282bp-Mid601 DNA were radiolabeled by an end fill-in reaction using Klenow Fragment (NEB #M0212S) with alpha-^{32}P dCTP, then purified by phenol/chloroform extraction and G-25 resin spin columns.

Mononucleosome sliding assays were performed in 25mM Hepes pH=7.5, 50mM NaCl, 5mM $MgCl_2$, 0.05% Tween-20, 1mM ATP, 1% glycerol, 100µg/mL

BSA and 1mM DTT. Given amounts of chromatin remodeling enzyme were incubated with 12nM 282bp-Mid601 mononucleosome at 30°C for 10 minutes. To stop the reaction, 10μL of the reaction was added to 2.4μL of stop buffer (50mM EDTA, 20% glycerol, 1mg/mL supercoiled plasmid DNA), mixed, and quenched on ice. These quenched aliquots were subjected to native PAGE for 45 minutes at 120V, in a 4% gel, in 0.5xTBE. Prior to visualization, these gels were dried under vacuum for 45 minutes at 80°C on a Bio-Rad model 583 gel dryer.

Restriction enzyme accessibility assays were performed as described (Logie and Peterson, 1997), except that 0.5U/mL *Sal*I-HF (NEB #R3138T) was used in place of *Hin*cII enzyme, and that 5nM chromatin remodeling enzyme and 1.25nM radiolabeled 208-11 array were used. After phenol/chloroform extraction, cut and uncut DNA were separated by electrophoresis in a 1% agarose gel. Prior to visualization, these gels were dried under vacuum for 90 minutes at 60°C.

Radiolabeled Gel and TLC Plate Quantification

Dried TLC plates, acrylamide gels, and agarose gels were exposed to Molecular Dynamics storage phosphor screens (generally, 3 hours for ATPase assays, and overnight for mononucleosome sliding or restriction enzyme accessibility assay gels). The screens were scanned on a Storm 820 scanner, then quantitated in ImageJ after processing with the Linearize GelData plugin (http://rsb.info.nih.gov/ij/plugins/linearize-gel-data.html). For ATPase assays, intensity of free phosphate signal was measured and normalized to the sum of

free phosphate plus unhydrolyzed ATP signal. For mononucleosome sliding assays, the intensity of the band corresponding to a centrally positioned nucleosome was measured and normalized to whole-lane intensity. For restriction enzyme accessibility assays, intensity of uncut array DNA signal was normalized to the sum of cut and uncut DNA signal. Experiments were performed in triplicate, and error bars represent sample standard deviation.

Sir3 Eviction Assay

8nM biotinylated nucleosomal array (96nM nucleosomes) was incubated with 96nM Sir3p (unless experimentally varied) in binding buffer (25mM Hepes pH=7.5, 50mM NaCl, 1.75mM $MgCl_2$, 0.05% Tween-20, 1mM DTT) for 25 minutes at 22°C. Then, an equal volume of 2x enzyme mix (double concentration of chromatin remodeling enzyme listed in figure; 2mM MgATP, 25mM Hepes pH=7.5, 100mM NaCl, 1.75mM $MgCl_2$, 0.05% Tween-20, 1mM DTT) was added, and the reaction proceeded for 10 minutes at 22°C.

This reaction was then incubated with 10µg/µl Streptavidin-coated magnetic beads (Invitrogen™ Cat# 11205D) for 5 minutes at 22°C. The magnetic beads had been washed twice in pulldown buffer and blocked for 15 minutes at 22°C in pulldown buffer supplemented with 100µg/mL BSA. During blocking and array binding, beads were kept continually suspended by constant rotation. After binding the array to beads, the beads were magnetically captured and the supernatant “unbound” fraction was removed. The beads were resuspended in

1x SDS-PAGE sample buffer, heated for 5’ at 95°C, and care was taken to magnetically extract the stripped beads from the supernatant “bound” fraction. These fractions were subjected to SDS-PAGE, electroblotted onto nitrocellulose membrane. Sir3 was immunodetected by HRP-FLAG (Sigma-Aldrich® Cat# A8592) immunoblotting, and H3 was detected by immunoblotting with Abcam antibody #1791. For quantification, the blot in ECL was photographed on a Fujifilm LAS 3000 CCD apparatus, and quantified with ImageJ using the ISAC plugin (http://rsb.info.nih.gov/ij/plugins/isac.html). Experiments were performed in triplicate, and error bars represent sample standard deviation.

Protein Capture Assays

2-10µg of resin-bound protein (equal masses were used of all proteins within the same experiment) of either Sir3p-FLAG (on anti-FLAG resin, from right after the wash steps in the purification protocol), SWI/SNF (on calmodulin affinity resin) or recombinant GST fusion protein (on glutathione sepharose resin) was incubated with 20µL free partner protein (20nM SWI/SNF, RSC, or ISW2; 100nM Sir3; ~100µM domain flag fusion) in wash buffer (1xPBS with 0.1% TWEEN-20, 1mM DTT, 100µg/mL PMSF) for 30’at 22°C with continuous gentle rotation. Resin was washed twice with 200µL wash buffer, then resuspended in 12uL 1xSDS-PAGE sample buffer, heated to 95°C for 5’, centrifuged at 14krpm in a tabletop microcentrifuge; the resultant supernatant was subjected to SDS-PAGE. These gels were electroblotted onto a nitrocellulose membrane, and equal resin-

bound protein loading was confirmed by Ponceau staining. Protein was detected by western analysis with the denoted antibodies. αArp9p Santa Cruz yN-19 goat polyclonal IgG was used to detect Arp9p in westerns, and tap-tagged proteins were detected by probing for CBP (Millipore #07-482).

Far Western Assays

~300nmol each of each purified complex was subjected to SDS-PAGE and electroblotting via wet transfer onto PVDF membrane. Insufficient protein was loaded to visualize by Ponceau staining, so an identical gel was visualized by silver stain (Life Technologies #LC6070) to confirm equal amounts of complex were used. Far western analysis was performed as previously described (Edmondson and Dent, 2001), with 3mL 10nM purified Sir3p-FLAG solution in 1xPBS and 3mg/mL BSA as the probe solution. Sir3p-bound peptide bands were subsequently detected with HRP-conjugated anti-FLAG antibody (Sigma #A8592) and visualized with ECL (Thermo #34087).

Structural Modeling

A predicted structure for the SWI/SNF ATPase domain was created by the Phyre2 protein fold prediction server (http://www.sbg.bio.ic.ac.uk/phyre2/html/page.cgi?id=index) (Kelley and Sternberg, 2009). PDB files were visualized for figures using PyMOL 1.3 (http://www.pymol.org/). For structural alignment, crystal structures of *S.*

cerevisiae (1M4Z) and *M. musculus* (4DOV)Orc1 (Connelly *et al.*, 2006; Kuo *et al.*, 2012) were aligned using the RCSB PDB Protein Comparison Tool (http://www.rcsb.org/pdb/workbench/workbench.do?action=menu) and visualized in Jmol (http://jmol.sourceforge.net/). Orc1 BAH domain sequences were aligned using EMBOSS Needle (http://www.ebi.ac.uk/Tools/psa/emboss_needle/), and Snf2p homolog N-terminal ATPase lobes were aligned using Clustal Omega (http://www.ebi.ac.uk/Tools/msa/clustalo/).

Plasmids

Plasmid for expressing GST-fusion human Orc1 BAH domain was a kind gift of Dr. Or Gozani (Kuo *et al.*, 2012). Molecular cloning via PCR, restriction digestion, plasmid ligation and transformation into *E. coli* was performed by standard methods. Phusion polymerase was used for PCR amplification during cloning (NEB #M0530S). For GST fusion protein cloning, coding sequences were cloned into the *Bam*HI and *Eco*RI restriction sites on pGEX-3X; recombinant flag-domains were cloned into pET expression vectors. Site-directed mutagenesis was used to generate the HSAΔ10 mutation (Agilent #200523). Oligonucleotides used in cloning are listed on the supplemental oligonucleotide table (Appendix 1). For cloning details, see the supplemental plasmid table (Appendix 2).

Yeast Strains and Genetic Methods

For yeast strains used, see the supplementary yeast strains table (Appendix 3). Standard genetic methods were used for yeast sporulation and tetrad dissection. One copy of the *SWI2* gene was deleted in a diploid strain by standard PCR-based method (Goldstein and McCusker, 1999).

Yeast transformations were performed using the lithium acetate/PEG/ssDNA carrier method (Schiestl and Gietz, 1989). Oligonucleotides and plasmids used for deletion cassette amplification and deletion confirmation are listed in the supplementary oligonucleotide (Appendix 1) and plasmid (Appendix 2) tables. Yeast genomic DNA preparations were performed using the glass bead/phenol method (Sugawara and Haber, 2012). Yeast protein extracts were prepared by the standard TCA/glass beads method. Ab5154 and ab1791 antibodies (Abcam) were used for western blots to detect Swi2p-AID and H3 (input), respectively, according to manufacturer recommendations.

For galactose-induced HO endonuclease expression and mating type switching assays, cells were incubated in appropriate lactate/glycerol medium to maintain selective pressure (synthetic URA dropout media for CY2041 + pGal-HO experiments in fig. 13A, and YP otherwise; both contained 3% glycerol, 2% lactate, .05% dextose, G418, media at pH=6.6). At mid-log phase (OD_{600}~0.4), galactose was added to a final concentration of 2% to induce HO expression, leading to double-strand break formation at the *MAT* locus. After one hour (four hours for *swi2Δ* in the plate-based mating type switching assay in fig. S4C), glucose was added to a final concentration of 2% to begin glucose repression of

HO transcription. For plate-based mating type switching, cells were diluted at this point to yield 100-200 colonies per plate (dilution empirically determined), and plated onto YPD. After five days of growth at 22°C, colonies were replica plated onto YPD plates with mating type tester lawns. After growth overnight at 22°C, mating plates were replica plated onto synthetic total dropout plates to score colonies with successful mating events.

For yeast genomic DNA preparations to assay DSB formation and repair kinetics via qPCR, samples were taken by collecting ~10^7 cells at the appropriate time intervals and centrifuging them at 2500g for 5 minutes, 4°C, in a Beckman J6-B (JS-4.2 rotor). Cell pellets were washed once with ice-cold dH_2O before storing at -80°C, until processing as above. For inducible degradation of Swi2p-AID, CY1766 yeast culture was grown at 25°C in YP-lactate until it reached an OD_{600} of 0.25. At that point, the culture was split in half, and either 1-Naphthalene Acetic Acid (1-NAA; dissolved at a concentration of 100mM in 100% ethanol) was added to a final concentration of 1mM, or an equal amount of just 100% ethanol. After two hours, galactose was added to induce *MAT* locus DSBs, and the experimental timecourse was started (see above). Once added, cells were kept in 1-NAA throughout the experiment.

For serial dilution spot plate assays, CY57 background yeast cells were cultured to saturation at 30°C in 5mL YPD + G418 (two overnights for *SWI2* and *swi2-Δ10R* cells, three overnights for *swi2Δ* cells). Yeast were diluted to an OD_{600} of 1.0 in sterile dH2O, and serially 4.64-fold diluted six times more. 7µL of

each of these seven dilutions was spotted onto plates of the indicated media. Where used, raffinose was at 2% w/v, galactose was 2% w/v, hydroxyurea was at 50mM, and antimycin A was at 2µg/mL.

For the silencing establishment assay, single colonies of CY1755 (*swi2Δ TELVR::URA3*) that were freshly transformed with either CP1410 or CP1413 were picked off of transformation plates and streaked out onto SD-URA+G418 plates. Biological replicates were performed from separate CP1410/CP1413 transformant colonies. After two days at 30°C, colonies were picked off the -URA plate and inoculated into SC+G418. Cells were kept at an OD_{600} between 0.05 and 0.60 at 30°C for three days by repeated dilution into fresh, prewarmed SC+G418. Timepoints were taken during those three days by diluting cells to an OD_{600} where 200µL of the cell dilution yielded ~150-400 colonies when plated on 5-FOA+G418. These dilutions were determined empirically, both for strain, and for time since beginning growth in SC+G418 (prior to five population doublings, undiluted culture was used). Another portion of the cell culture was contemporally diluted 1:3000 and plated on SC+G418 to count total cells. After three days, colonies were counted. The number of colonies for each strain and for each timepoint was normalized both to dilution (above) and to the number of cells that grew on SC+G418. The experiment was biologically repeated five times, and error bars are sample standard deviation.

For RNR induction, yeast cells were grown to mid-log, a 0 hour timepoint was taken, then hydroxyurea was added to a final concentration of 200mM. After two hours, the 2 hour timepoint was taken.

qPCR

Primers were designed with Primer3Plus (http://primer3plus.com/cgi-bin/dev/primer3plus.cgi) with qPCR server settings enabled, except primers for monitoring *MAT* locus breakage and repair, which were obtained from prior literature (Sugawara and Haber, 2012). Reactions were carried out at 25U/mL NEB Taq (NEB #M0273), in NEB Standard TAQ buffer (10mM Tris, 50mM KCl, 1.5mM $MgCl_2$, pH=8.3 @ RT) supplemented with an additional 1.5mM $MgCl_2$, 200µM of each dNTP, 200nM of each primer, SYBR Green (Invitrogen S-7563; diluted 1:2000 from stock into DMSO, then diluted 33.33-fold into reaction), and 50-fold diluted Rox dye (BIO-RAD #172-5858). Thermocycling was performed in an Applied Biosystems 7300 RT-PCR system, using Rox as the passive reference dye. Plates were held at 50°C for 2 minutes, then held at 95°C for 10 minutes, then cycled forty times between 95°C for 15 seconds and 61°C for 1 minute, and finally subjected to dissociation curve analysis. CT values were obtained via the “auto analyze” feature of the AB 7300 software. Standard curves for each primer pair were used to derive slope and intercept values that were subsequently used to calculate quantities of nucleic acid from CTs. Locus quantities were normalized to the ACT1 quantity for their respective nucleic acid

prep. All qPCRs were performed in technical duplicate and averaged to give a value for each biological replicate. Three biological replicates were performed for all experiments, except for figure 13A, which was performed in biological duplicate and averaged. All error bars represent standard deviation of the sample calculated from the three biological replicate values.

RNA Isolation

RNA was extracted and purified by the hot phenol method, as previously described (Collart and Oliviero, 2001), from 10-50mL CY57 background cultures (at OD~0.4-0.6) grown in YEPD , followed by contaminant DNA removal using RNAse-free DNAseI (Ambion #1907). RNA concentration and purity was measured on a Nanodrop spectrophotometer. For qRT-PCR analysis, 100ng of total RNA was subjected to reverse transcription (Invitrogen #11746) with locus-specific qPCR primers for 30 minutes at 50°C, prior to qPCR as above.

For RNA-seq analysis, three biological replicates each of CY57-background yeast cultures, containing either CP1410 or CP1413, were grown to mid-log and processed as above. Each replicate was derived from a different transformant colony. 25µg samples of RNA were processed for 90bp paired-end sequencing by BGI International (HK). Data was filtered to remove adaptors, contamination, and low-quality reads from the raw reads. Each sample yielded 28.8-36.4 million reads. These reads were all mapped to the Ensembl EF4 *Saccharomyces cerevisiae* genome build via Tophat 2.0.9 and Bowtie 2.1.0.0,

using Samtools 0.1.18.0. Relative gene expression was quantified by Cufflinks 2.1.1, and the resultant data was visualized by CummeRbund 2.6.1 in R 2.15.1 (all as in (Trapnell *et al.*, 2012)).

Chapter III: Sir2p/Sir4p-Dependent Histone Eviction by SWI/SNF

Summary

Heterochromatin has many roles *in vivo*, from transcriptional silencing to recombinational repression. In spite of being contained within such a repressive structure, heterochromatic DNA must at the least still be repaired and replicated, creating a need for regulated dynamic access into silent heterochromatin. In prior work, we characterized activities used by SWI/SNF complex to displace the Sir3p heterochromatin protein. Here, we discover that SWI/SNF can also disrupt heterochromatin structures containing all three Sir proteins: Sir2p, Sir3p and Sir4p. This new disruption activity requires nucleosomal contacts that are essential for silent chromatin formation *in vivo*. We find that SWI/SNF evicts all three heterochromatin proteins off of chromatin. Surprisingly, we also find that the presence of Sir2p and Sir4p on chromatin stimulates SWI/SNF to evict histone proteins H2A and H2B from nucleosomes. Apart from discovering a new potential mechanism of heterochromatin dynamics, these data establish a new paradigm of chromatin remodeling enzyme regulation by nonhistone proteins present on the substrate.

Introduction

Incorporation of eukaryotic genomes into the nucleoprotein structure of chromatin is central to the proper regulation of all forms of DNA metabolism, from gene transcription control to genome replication and repair (Papamichos-Chronakis and Peterson, 2012; Rando and Winston, 2012; Rivera *et al.*, 2014). The base unit of chromatin, the nucleosome, consists of 147bp of DNA wrapped approximately 1.7 times around an octamer of histone proteins—two H2A/H2B heterodimers flanking a central heterotetramer of H3 and H4 (Luger *et al.*, 1997a). Despite sharing this common base unit, genomic loci can exhibit very distinct sets of emergent properties. The cell imposes these distinct states onto the chromatin fiber by targeting three key activities to genomic loci: ATP-dependent chromatin remodeling (Clapier and Cairns, 2009), histone variant incorporation (Bönisch and Hake, 2012), and histone post-translational modification (Bannister and Kouzarides, 2011). Other chromatin-associated proteins can read the resulting chromatin landscape and specifically bind to loci, thereby associating their own unique properties with the locus (Musselman *et al.*, 2012).

One paradigm for such a chromatin state is silent heterochromatin. First discovered cytologically by the density of its nucleic acid staining, heterochromatin is a generally repressive domain (Heitz E., 1928). Heterochromatin contains genomic loci that are less transcriptionally active, less

frequently recombined, less sterically accessible, and replicated later during S phase than their euchromatic counterparts (Grewal and Jia, 2007). Heterochromatin plays key roles in organismal development, by repressing expression of certain developmental and cell identity loci (Laugesen and Helin, 2014). Heterochromatin also promotes genome stability, by repressing recombination between the repetitive sequences it often contains (Peng and Karpen, 2007, 2009).

The most well-studied heterochromatin system is budding yeast Sir (silent information regulator) heterochromatin. There are three main Sir proteins: Sir2p, Sir3p, and Sir4p. Sir2p is the founding member of the sirtuin class of NAD-dependent histone deacetylase enzymes (Imai *et al.*, 2000). Sir4p forms a stable heterodimer with Sir2p, and via Sir4p's locus-specific interactions with sequence-specific binding factors, Sir4p helps Sir2p deacetylate histones at heterochromatic loci (Luo *et al.*, 2002; Hsu *et al.*, 2013). This deacetylation creates a high-affinity binding site for the third Sir protein, Sir3p (Onishi *et al.*, 2007; Buchberger *et al.*, 2008). Chromatin bound by purified Sir2p, Sir3p and Sir4p is repressed for both recombination and transcription *in vitro* (Johnson *et al.*, 2009; Sinha *et al.*, 2009; Johnson *et al.*, 2013). While much work has been done on the molecular biology of heterochromatin proteins (Simon and Kingston, 2009; Grunstein and Gasser, 2013), not much is known about cellular means to circumvent heterochromatin structure—for example, when a cell must repair or replicate its genome.

Prior work from our lab has identified physical interactions between the SWI/SNF core ATPase subunit Swi2p and the heterochromatin structural protein Sir3p. These interactions are required for the ability of SWI/SNF to evict Sir3p from a chromatin fiber, an ability that is involved in DNA replication and silent chromatin establishment *in vivo* (Manning and Peterson, 2014). However, establishment of silent Sir chromatin domains *in vivo* requires Sir2p and Sir4p in addition to Sir3p. Sir4p in particular exhibits strong interactions with both Sir3p and Sir2p (Chang *et al.*, 2003; Liou *et al.*, 2005), can bind to histones H3 and H4 (Hecht, Andreas *et al.*, 1995), and interacts with DNA exiting the nucleosome (Kueng *et al.*, 2012). Disruptions of several of these Sir4p interactions weaken heterochromatin silencing *in vivo*. These data suggest a structural role for Sir4p, and by extension its associated Sir2p, in the heterochromatin fiber. Therefore, a more relevant heterochromatin substrate for SWI/SNF activity would be a chromatin fiber bearing all three Sir proteins.

In this work, we find that SWI/SNF complex exhibits a novel heterochromatin disruption activity when faced with a Sir2p/Sir4p-bound chromatin substrate. This activity results in the eviction of Sir proteins from chromatin, and separates Sir3p and Sir2p from Sir4p. Furthermore, this activity stimulates the eviction of histone dimers from nucleosomes. We discover that this activity involves SWI/SNF subunits outside of the Swi2p catalytic core. Finally, we find that SWI/SNF requires a heterochromatin substrate with higher levels of Sir proteins and functional H4 tail nucleosomal contacts, resembling *in*

vivo Sir heterochromatin, in order to perform this heterochromatin disruption activity.

Results

SWI/SNF disrupts Sir-nucleosome structure

In order to investigate the effect of SWI/SNF on chromatin that bears all three core Sir proteins, we first sought to recreate a Sir2p/Sir3p/Sir4p-nucleosome substrate *in vitro*. First, purified recombinant histone octamers were reconstituted by stepwise salt dialysis onto DNA templates bearing nucleosome positioning sequences (Dechassa *et al.*, 2010). We generated dinucleosomes separated by a 30bp linker as well as core mononucleosomes bearing no flanking DNA. Then, purified Sir2p/4p and Sir3p were mixed at equimolar ratios, and preincubated together. These Sir proteins were titrated on to the chromatin substrates. The binding reactions were subjected to native PAGE analysis, and the DNA was visualized by fluorescent staining. At an equimolar nucleosome: Sir protein ratio, chromatin substrates are bound by Sir proteins and migrate as discrete complexes (Figure 16A).

Next, we asked what effect SWI/SNF enzyme had on these Sir-nucleosome complexes. Chromatin substrates, either with or without equimolar ratios of Sir proteins as described above, were incubated in the presence and absence of SWI/SNF and ATP, then subjected to native PAGE. In the absence of

Figure 16: SWI/SNF disrupts Sir nucleosome structure. (A) Increasing amounts of Sir proteins were bound to mononucleosome or dinucleosome templates, then subjected to Native PAGE. Nucleic acid was visualized by fluorescent stain. **(B)** Nucleosomes were either bound to Sir proteins as above, or not bound to Sir proteins, then incubated with SWI/SNF in the presence or absence of ATP. These reactions were then subjected to Native PAGE. Nucleic acid was visualized by fluorescent stain. **(C)** Radiolabeled mononucleosome was treated as in the left half of panel (B), but was incubated with 1µg competitor supercoiled plasmid DNA prior to loading and running on Native Page. Radiolabel was exposed and visualized.

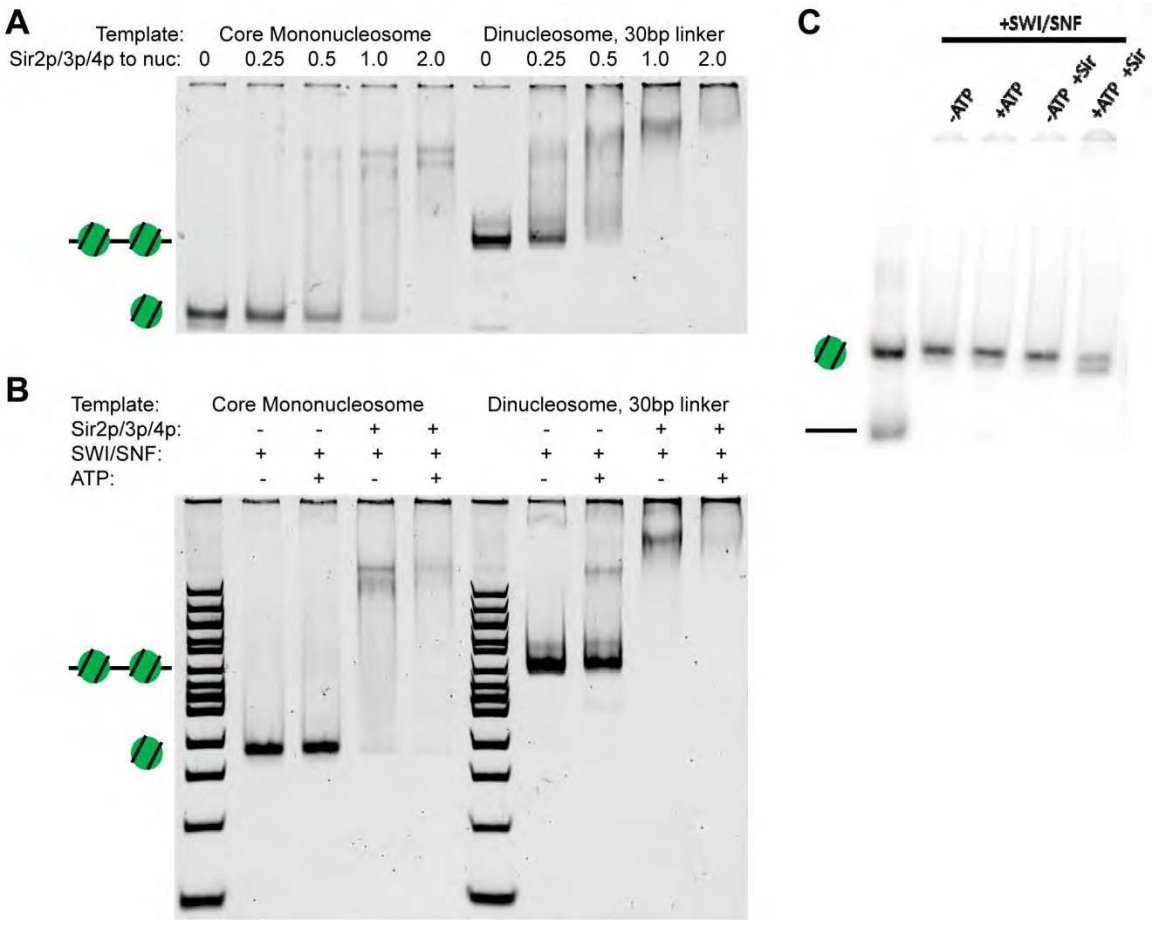
A
Template:
Core Mononucleosome
Dinucleosome, 30bp linker
Sir2p/3p/4p to nuc:
0
0.25
0.5
1.0
2.0
0
0.25
0.5
1.0
2.0
B
Template:
Core Mononucleosome
Dinucleosome, 30bp linker
Sir2p/3p/4p:
SWI/SNF:
ATP:
C
+SWI/SNF
-ATP
+ATP
-ATP +Sir
+ATP +Sir

Sir proteins, SWI/SNF does not significantly shift core mononucleosomes, regardless of whether or not ATP is also present (Figure 16B, lanes 2 and 3). Similarly, dinucleosome substrates are largely unshifted by SWI/SNF in the absence of Sir proteins, although evidence of chromatin remodeling is visible in the presence of ATP (Figure 16B, lanes 7 and 8). The absence of a SWI/SNF-dependent shift in these assays is consistent with two factors: the substoichiometric concentration of SWI/SNF (5nM) compared to nucleosomes (30nM), and the absence of linker DNA on the core mononucleosomes to allow nucleosome repositioning. Even in the presence of Sir proteins, no SWI/SNF-dependent shift is seen in the absence of ATP (Figure 16B, lanes 4 and 9). However, inclusion of both SWI/SNF and ATP disrupts Sir-nucleosome complexes (Figure 16B, lanes 5 and 10).

We hypothesized that this disruption activity incurs changes in the underlying chromatin template. To investigate this possibility, core mononucleosome DNA was radiolabeled by end-fill prior to nucleosomal reconstitution. Then, following reaction as above, an excess of unlabeled supercoiled plasmid DNA was added to compete SWI/SNF and Sir proteins off of chromatin. These reactions were subjected to native PAGE analysis; after, the gels were dried, exposed to a storage phosphor screen, and scanned on a Storm scanner. There is no apparent change in the core mononucleosome in the presence of SWI/SNF complex, whether or not ATP is present (Figure 16C, lanes 1 and 2). The presence of SWI/SNF and Sir proteins without ATP (Figure 16C,

lane 3) has no effect, however, once ATP and Sir proteins are present, SWI/SNF catalyzes formation of a faster-migrating chromatin species (Figure 16C, lane 4).

SWI/SNF evicts Sir proteins and histone proteins from chromatin

In line with our prior work on SWI/SNF and Sir3p, we hypothesized that components of the Sir heterochromatin fiber were being evicted by SWI/SNF complex during this ATP-dependent disruption activity. To test this hypothesis, we modified the biotinylated chromatin capture assay. Purified Sir3p and Sir2p/4p were preincubated together, then bound to nucleosomal array molecules. These arrays were made of recombinant histone octamers reconstituted by salt dialysis onto DNA molecules containing twelve tandem copies of the 208bp '5S' nucleosome positioning sequence. Included in these reconstitutions were a low proportion of octamers (15%, approximately two octamers per array) that contained biotinylated H2A C-terminal tails. The Sir-nucleosome array was then incubated with chromatin remodeling enzyme in the presence of ATP. Reactions were captured on streptavidin-coated magnetic beads as before. Supernatant (U) and bead-bound (B) fractions were subjected to SDS-PAGE and western blotting. Strikingly, SWI/SNF, but not RSC, evicts Sir2p, Sir3p and Sir4p into the supernatant in a concentration-dependent manner (Figure 17A). Histone H3 is also detected in the supernatant; this contrasts with our prior work, where no histone eviction is seen in heterochromatin eviction assays with Sir3p alone (Manning and Peterson, 2014).

Figure 17: SWI/SNF subunits are required for Sir disruption. (A) Chromatin capture assay where Sir2p/4p+Sir3p-bound biotinylated chromatin molecules were incubated with increasing amounts of the given chromatin remodeling enzyme and ATP, then captured on streptavidin-coated magnetic beads. The resulting bead-bound “B” and unbound “U” fractions were subjected to SDS-PAGE and western analysis. **(B)** As in A, but with different SWI/SNF complexes. **(C)** Chromatin capture assay where Sir3p-bound biotinylated chromatin molecules were incubated with increasing amounts of the chromatin remodeling enzymes from (B) and ATP, then captured on streptavidin-coated magnetic beads.

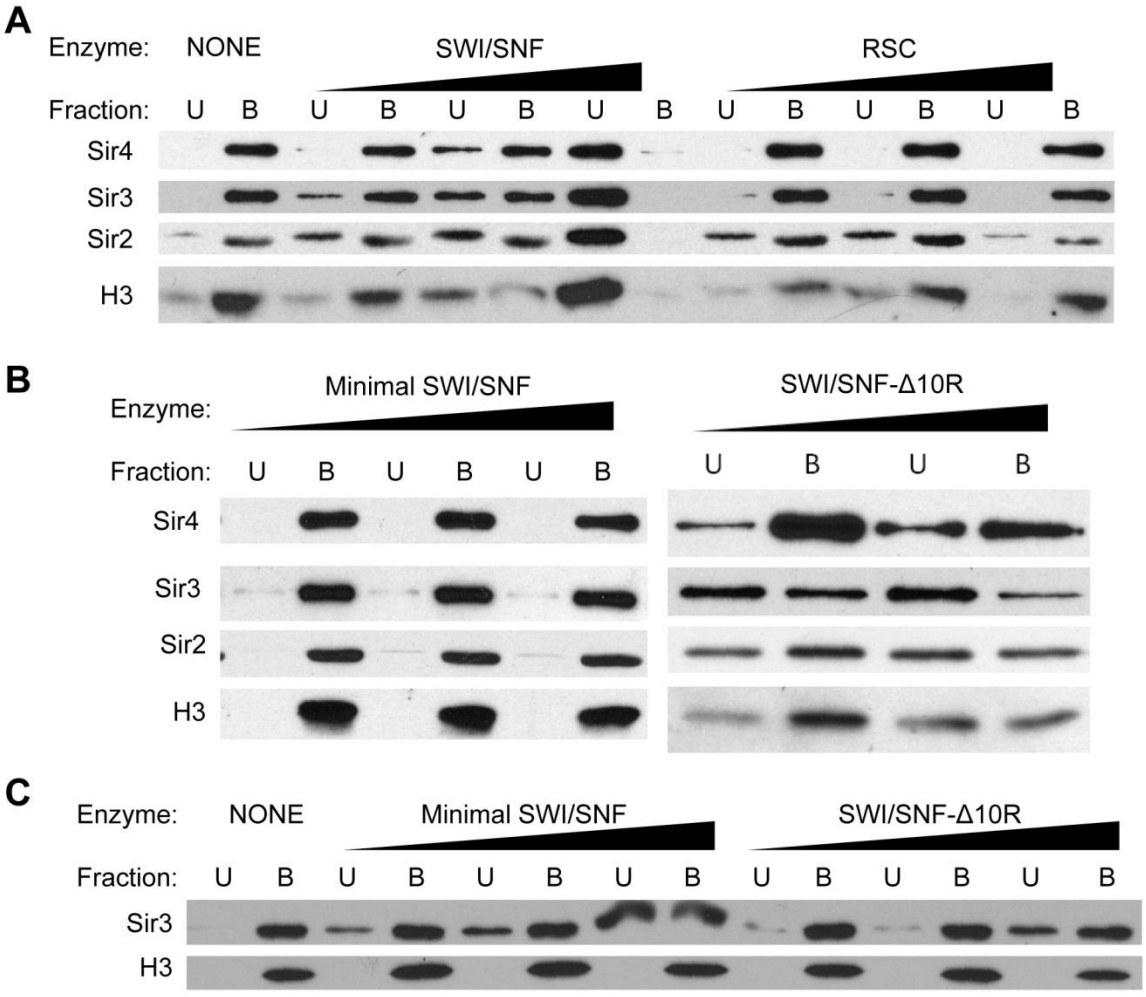
A
Enzyme:
NONE
SWI/SNF
RSC
Fraction:
U B U B U B U B U B U B U B
Sir4
Sir3
Sir2
H3
B
Enzyme:
Minimal SWI/SNF
SWI/SNF-Δ10R
Fraction:
U B U B U B U B U B
Sir4
Sir3
Sir2
H3
C
Enzyme:
NONE
Minimal SWI/SNF
SWI/SNF-Δ10R
Fraction:
U B U B U B U B U B U B U B
Sir3
H3

To determine which components of SWI/SNF complex are required for this novel Sir-histone eviction activity, we repeated this assay using various SWI/SNF complexes. First, we tested the SWI/SNF-Δ10R complex, which prior work established was competent for chromatin remodeling, but specifically defective at Sir3p protein eviction (Figure 17C right). Surprisingly, SWI/SNF-Δ10R was able to evict Sir proteins and histones from the bead-bound fraction (Figure 17B right), albeit at a slightly slower rate than wild-type SWI/SNF complex. Next, we tested the "Minimal SWI" core subcomplex, which contains Swi2p, Arp7p, Arp9p and Rtt102p, and is purified from *swi3ΔSANT* (where Swi3p lacks aa555-565) mutant yeast strains (Boyer *et al.*, 2002; Yang *et al.*, 2007). This complex is competent for chromatin remodeling activities and Sir3p eviction (Figure 17C left), but is unable to evict any proteins from the Sir chromatin fiber (Figure 17B left). Taken together, these data imply that a SWI/SNF subunit outside of the Minimal SWI subcomplex plays a role that is crucial to this Sir-chromatin disruption activity.

To test whether a non-core subunit SWI/SNF was acting as a histone chaperone, we next asked whether DNA leaves the bead-bound fraction along with Sir and histone proteins. We found that Sir3p and Sir2p are the first molecules to leave the bead-bound fraction; later, Sir4p, histone H3, and DNA leave the bead-bound fraction (Figure 18A). However, Sir4p and histone H3 leave the bead-bound fraction earlier than DNA does. These data are consistent with a model wherein Sir proteins and histone proteins are evicted from DNA

Figure 18: SWI/SNF evicts Sir proteins and histones sequentially from DNA. **(A)** Repeat experiment of Figure 17A, where half of each fraction was also phenol/chloroform extracted and ethanol precipitated, then visualized on an agarose gel by fluorescent staining for nucleic acid. **(B)** Chromatin capture assay with Sir2p/4p+Sir3p where the DNA template either is not (left) or is (right) covalently biotinylated, in addition to the biotinylated H2A in the chromatin molecule.

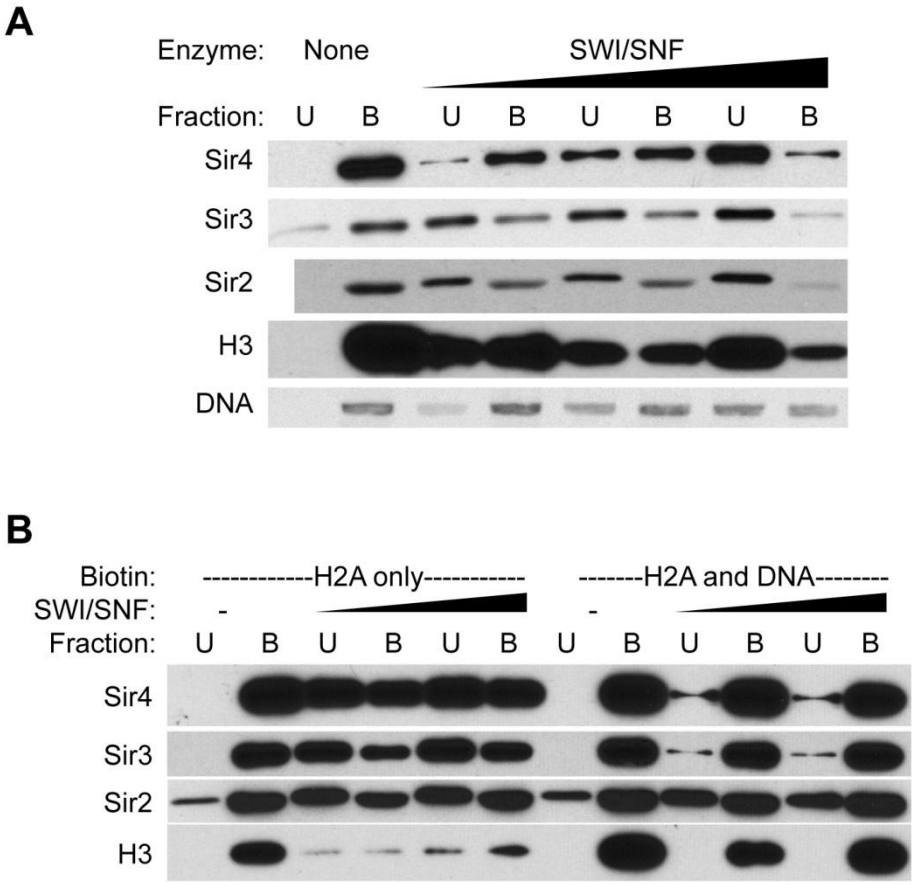
A
Enzyme:
None
SWI/SNF
Fraction:
U
B
U
B
U
B
U
B
Sir4
Sir3
Sir2
H3
DNA
B
Biotin:
----------H2A only----------
-------H2A and DNA--------
SWI/SNF:
-
-
Fraction:
U
B
U
B
U
B
U
B
U
B
U
B
Sir4
Sir3
Sir2
H3

throughout the reaction, but a DNA molecule only leaves the bead-bound fraction once all biotinylated H2A molecules on it have left.

To test this model, the chromatin capture assay was repeated with different chromatin substrates. Linear pUC19 DNA and biotinylated linear pUC19 generated by PCR were reconstituted with octamers as before. Notably, more Sir protein is captured in the bead-bound fraction when the DNA is biotinylated (Figure 8B, right set of lanes). While Sir protein is still seen in the unbound supernatant fraction, no appreciable histone H3 eviction is seen in the reactions with biotinylated DNA. These findings argue against whole octamer eviction, and suggest that Sir proteins promote the H2A/H2B dimer eviction activity of SWI/SNF complex (Vicent *et al.*, 2004; Yang *et al.*, 2007).

Sir nucleosomes might stimulate SWI/SNF's dimer eviction activity by tightly binding to SWI/SNF complex and increasing the time wherein SWI/SNF is translocating DNA into a nucleosome. Processive SWI/SNF translocation on the linear chromatin substrates used here might then result in translocation of chromatin off of the end of the DNA (Dechassa *et al.*, 2010). To test this model, identical biotinylated chromatin reconstitutions were made on either linearized or supercoiled pUC19 DNA, bound to Sir proteins, reacted with SWI/SNF complex and captured on streptavidin beads. Both linearized and supercoiled chromatin templates were competent substrates for this reaction (Figure 19), demonstrating that SWI/SNF removes histones and Sir proteins from topologically continuous DNA.

Figure 19: Sir disruption activity does not require DNA ends. Chromatin capture assay with Sir2p/4p+Sir3p where the DNA template either is linearized plasmid (left) or supercoiled plasmid (right).

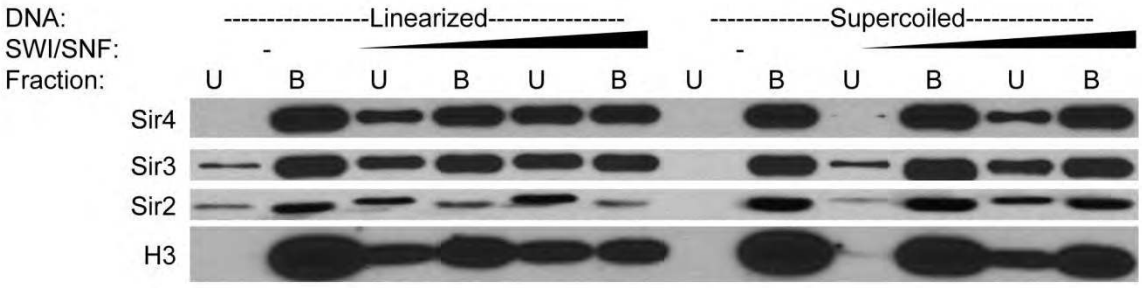
DNA:
----------Linearized----------
----------Supercoiled----------
SWI/SNF:
-
-
Fraction:
U B U B U B U B U B U B
Sir4
Sir3
Sir2
H3

Sir2p and Sir4p are required for Sir and histone eviction by SWI/SNF

Next, we sought to characterize how the Sir proteins contribute to this reaction. First, we hypothesized that a critical amount of Sir proteins was required in order for the reaction to occur. By titrating increasing amounts of Sir proteins into the chromatin capture assay, we found that low concentrations of Sir proteins are unable to induce this reaction. Strikingly, increasing the amount of Sir proteins present, from one Sir2p/4p+Sir3p per six nucleosomes up to one per three nucleosomes, sharply stimulates the eviction reaction (Figure 20A). This apparently cooperative stimulation implies that the relevant substrate for this reaction is a higher-order superstructure of consecutive Sir-bound nucleosomes.

We postulated that, if heterochromatin superstructure was a prerequisite to stimulate this SWI/SNF eviction activity, then disrupting heterochromatin superstructure should prevent the activity (Ling *et al.*, 1996). To test this hypothesis, we constructed biotinylated chromatin arrays as before, with octamers that either contained or lacked the N-terminal tail of histone H4. This histone tail is absolutely required for heterochromatic silencing *in vivo*. Surprisingly, Sir proteins bind well to nucleosomal arrays lacking the H4 tail, however no Sir or histone eviction activity is observed in the absence of the H4 tail (Figure 20B). To determine which of the Sir proteins were required for this evicrion reaction to happen, the chromatin capture assay was repeated in the presence and absence of Sir3p and Sir2/4p. Sir3p is dispensible for this SWI/SNF-catalyzed reaction, but Sir2p/4p is absolutely required (Figure 20C).

Figure 20: Sir chromatin requirements for SWI/SNF disruption. (A) Chromatin capture where increasing amounts (0, 1, 2, 4 molecules of Sir2p/4p+Sir3p per 12-nucleosome chromatin molecule) of Sir proteins were bound to chromatin, reacted with a fixed concentration of SWI/SNF complex, then captured on beads. **(B)** Chromatin capture assay with Sir2p/4p+Sir3p where the nucleosomes contain H4 that either has (left) or lacks (right) its N-terminal tail. **(C)** Chromatin capture assay with the indicated presence '+' or absence '-' of the indicated proteins.

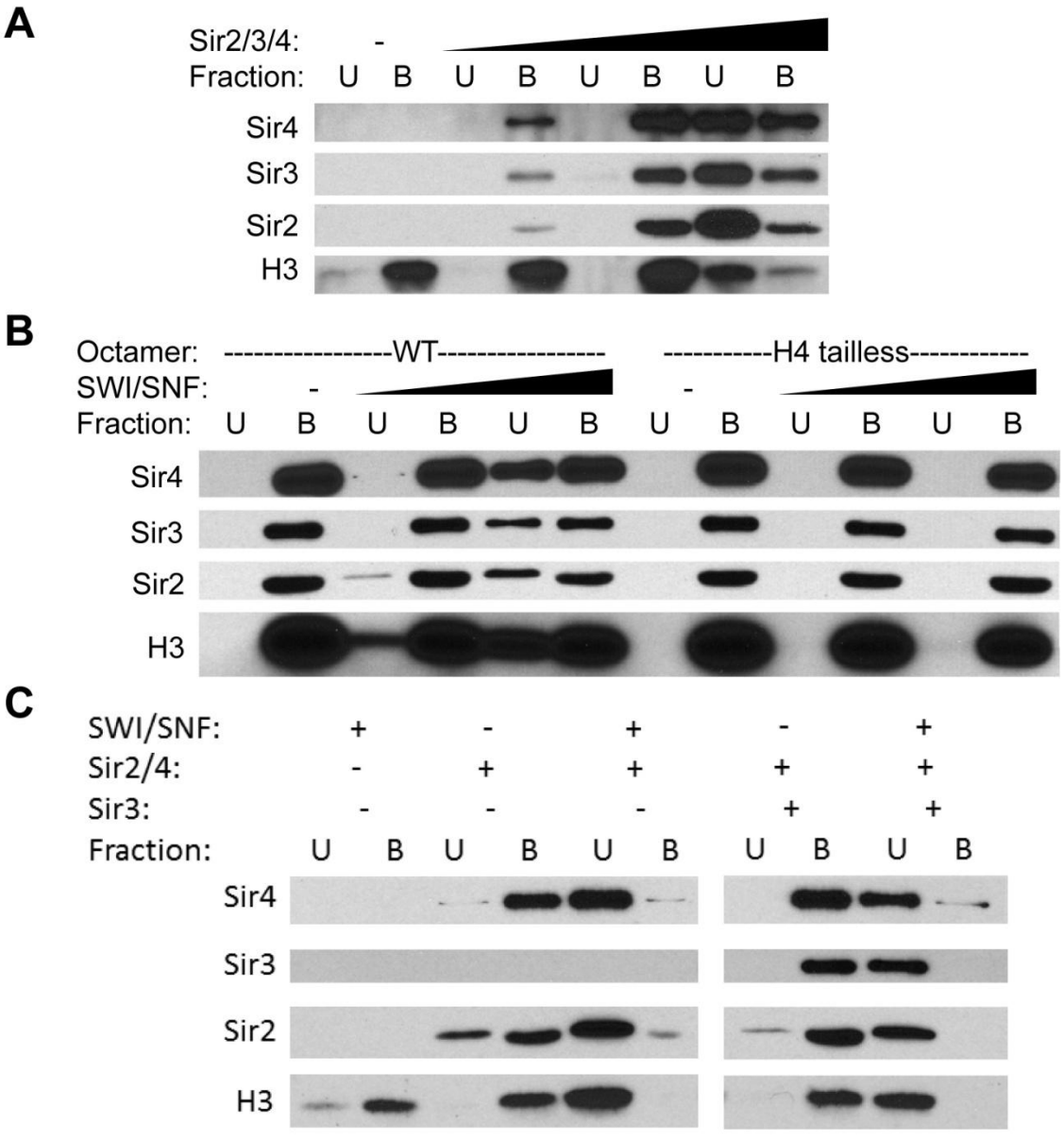
A
Sir2/3/4: -
Fraction: U B U B U B U B
Sir4
Sir3
Sir2
H3
B
Octamer: ----------WT---------- ----------H4 tailless----------
SWI/SNF: - -
Fraction: U B U B U B U B U B U B
Sir4
Sir3
Sir2
H3
C
SWI/SNF: + - + - +
Sir2/4: - + + + +
Sir3: - - - + +
Fraction: U B U B U B U B U B
Sir4
Sir3
Sir2
H3

Our prior work with SWI/SNF and Sir3p identified novel physical interactions between Sir3p and Swi2p that were required for SWI/SNF-catalyzed Sir3p eviction. Given this new reaction's requirement for Sir2p/4p, we hypothesized that physical interactions also exist between Sir2p/4p and Swi2p. To test this hypothesis, regions of Swi2p (Figure 21A top panel) were recombinantly expressed as GST-fusion proteins, then assayed for their ability to interact with purified Sir2p/4p complex. First, we found that the HSA domain (aa588-663) of Swi2p could interact with Sir2p/4p (Figure 21A middle panel). Notably, the 10-amino acid deletion "Δ10," which ablates interaction of the Swi2p HSA domain with the Sir3p AAA+ domain, has no effect on binding Sir2p/Sir4p (Figure 21A bottom panel). Second, the N-terminal ATPase lobe (aa836-924) of Swi2p was able to interact with Sir2p/4p (Figure 21A top panel, Figure 21B). An additional interaction was detected between Sir2p/4p and the C-terminal bromodomain (aa1321-1703) of Swi2p.

Discussion

Sir heterochromatin that bears all three necessary Sir proteins presents a significant barrier to metabolic processes, such as transcription or DNA repair, that must access heterochromatic DNA (Johnson *et al.*, 2009; Sinha *et al.*, 2009). Here, we discover and characterize a novel heterochromatin disruption activity present in the chromatin remodeling enzyme SWI/SNF. Unlike our prior work with

Figure 21. Regions of Swi2p interact with Sir2p/4p. (A) Top: schematic of the Swi2p protein regions used as GST-fusions below. Middle: equal mass of each Swi2p region's GST fusion was assayed for ability to pull down Sir2p/4p onto glutathione beads by incubation, coprecipitation, followed by SDS-PAGE and western analysis to detect Sir2p/4p. Bottom: as middle, but with various regions of the Swi2p HSA domain. **(B)** As above, but assaying GST-fusion fragments of the Swi2p ATPase domain for interaction with Sir2p/4p.

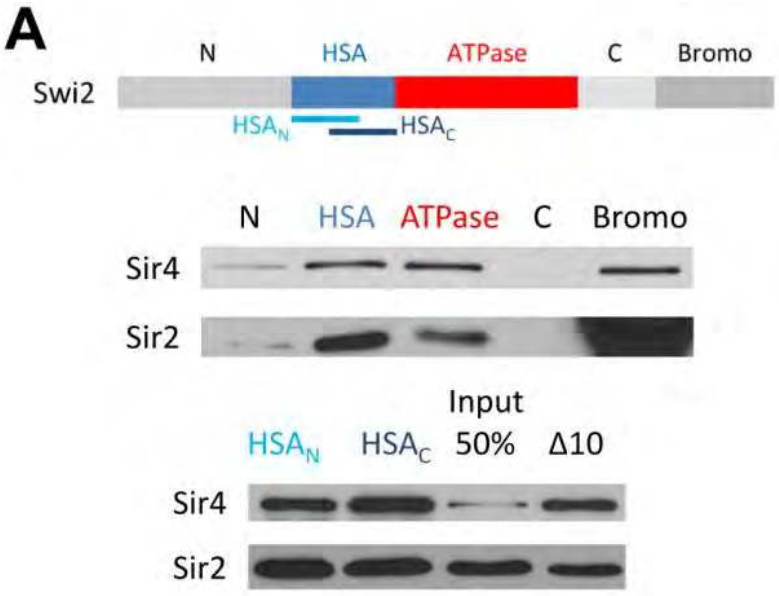
A
N
HSA
ATPase
C
Bromo
Swi2
HSA$_N$
HSA$_C$
N HSA ATPase C Bromo
Sir4
Sir2
Input
HSA$_N$ HSA$_C$ 50% Δ10
Sir4
Sir2

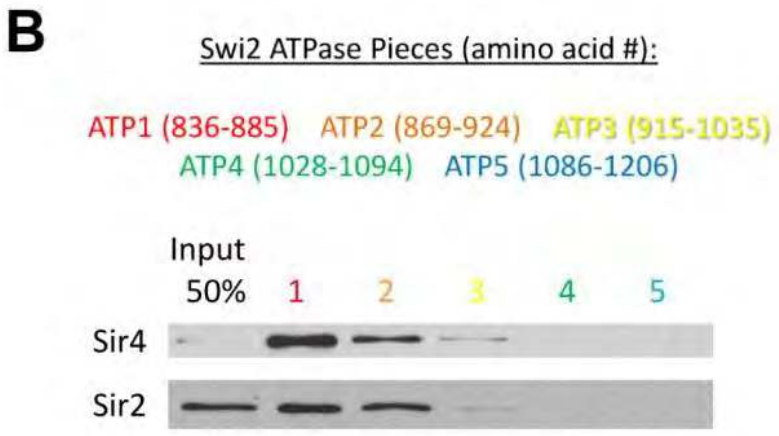
B
Swi2 ATPase Pieces (amino acid #):
ATP1 (836-885) ATP2 (869-924) ATP3 (915-1035)
ATP4 (1028-1094) ATP5 (1086-1206)
Input
50% 1 2 3 4 5
Sir4
Sir2

Swi2p and Sir3p, we find this disruption activity displaces both Sir proteins and histones from chromatin. It is also contingent upon the presence of ATP and holo-SWI/SNF complex, and is activated on chromatin bound by Sir2p and Sir4p.

Substrate requirements for this heterochromatin disruption also include the H4 N-terminal tail, which is required for silencing *in vivo* (Ling *et al.*, 1996), and a cooperative sensitivity to the concentration of Sir proteins on the substrate. Surprisingly, the Sir proteins bind very well even to nucleosomes lacking the H4 tail. This result, of Sir binding well to a substrate that is ultimately unable to silence, resembles what is seen at subtelomeric heterochromatin. There, H3K79-methylated nucleosomes bind to Sir proteins, and Sir proteins ChIP at these loci, but the chromatin remains actively transcribed both *in vivo* and *in vitro* (Kitada *et al.*, 2012; Xue *et al.*, 2015). These data are all consistent with Sir proteins being competent to bind nucleosomes in more than one manner, where not all of the potential binding modes can establish a silent structure. For example, Sir2p/4p complex can bind to acetylmimic H4K16Q nucleosomes (Oppikofer *et al.*, 2011), but Sir3p cannot (Buchberger *et al.*, 2008). However, Sir3p might still associate with the H4K16Q chromatin through its interactions with Sir2p/4p, although not in a manner that is compatible with transcriptional silencing. Taken together, these substrate requirements mimic what SWI/SNF might encounter at properly silenced Sir-regulated loci *in vivo*.

One model for the SWI/SNF heterochromatin disruption activity that is consistent with our data (figure 18A) begins when SWI/SNF interacts with a Sir-

bound nucleosome. SWI/SNF complex forms multiple interactions with the Sir proteins and with the nucleosome. Following ATP hydrolysis and DNA translocation, SWI/SNF complex evicts Sir3p and Sir2p from chromatin. Then, after further DNA translocation, the nucleosome is sufficiently destabilized for Sir4p and the H2A/H2B dimer to be evicted by SWI/SNF (Figure 22).

An alternative model that circumvents a two-step eviction mechanism is the simultaneous eviction of all three Sir proteins and the H2A/H2B dimer, followed by rebinding of Sir4p to DNA via its N-terminal DNA binding domain (Kueng *et al.*, 2012). At some rate, Sir3p and Sir2p may rebind to Sir4 as well. If Sir4p or Sir3p molecules on separate arrays dimerize (Chang *et al.*, 2003), then arrays whose biotinylated histone dimers had been evicted by SWI/SNF would still be captured on the streptavidin beads by bridging with arrays that retain biotinylated histone dimers. Such array-array bridging explains the delayed apparent histone H3 eviction. Furthermore, this would also provide an explanation for the inability of the reaction products in Figure 16B to enter the gel, which is notable because Sir-nucleosome complexes on their own enter the gel. SWI/SNF binding alone is unlikely to explain this phenomenon, since SWI/SNF is present at a fivefold lower concentration than Sir nucleosomes in those reactions.

Association of Sir2p/4p with nucleosomes regulates how SWI/SNF remodels nucleosomes, as seen in the chromatin mobility shift in lane 4 of Figure 16C. This shift most likely represents altered position of the nucleosome along

Figure 22: Model for Sir chromatin disruption by SWI/SNF. See text for description. ATP hydrolysis and DNA translocation are indicated by the 12-pointed star.

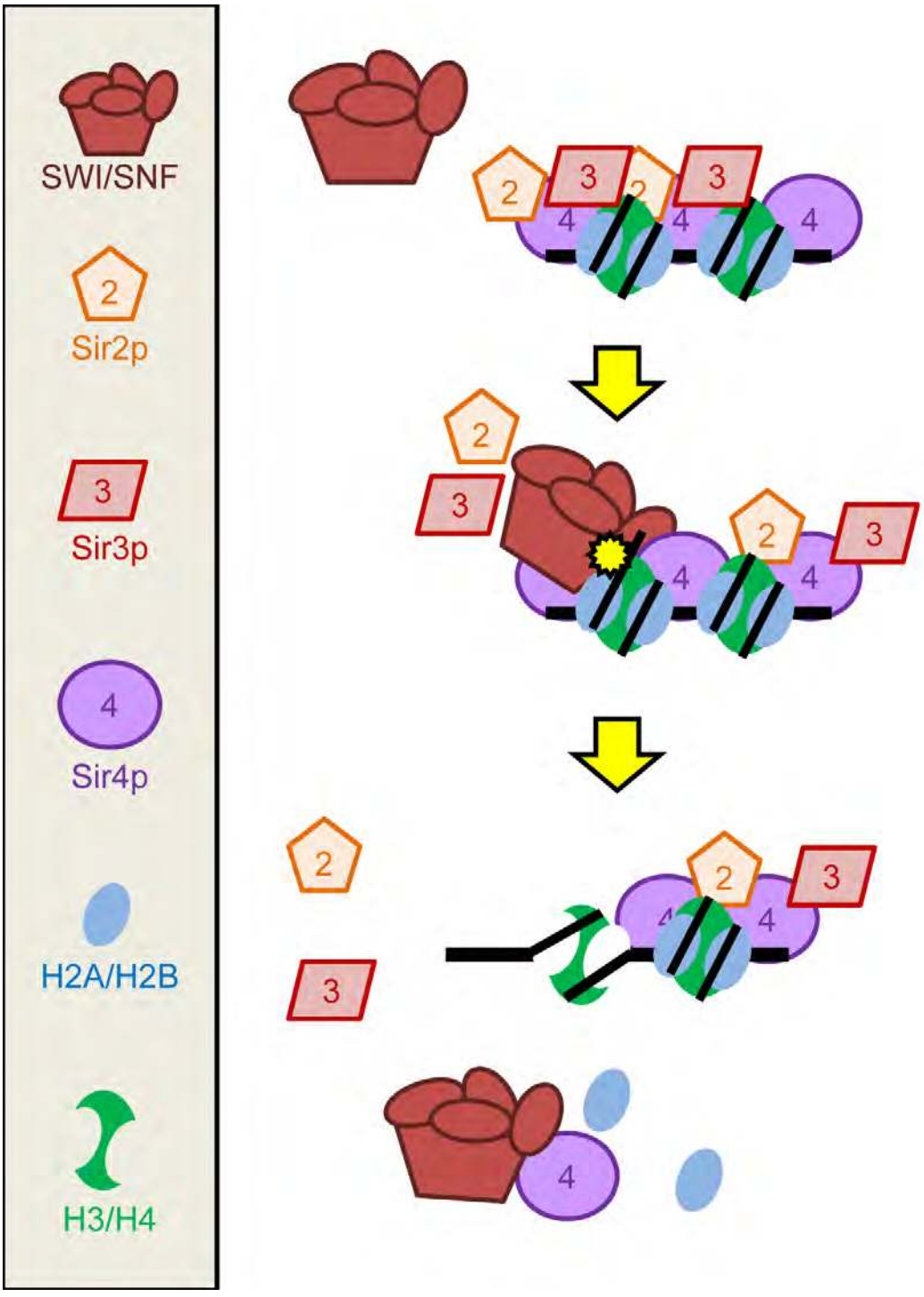
SWI/SNF
2
Sir2p
3
Sir3p
4
Sir4p
H2A/H2B
H3/H4

DNA, which on the core mononucleosomes used here would mean the nucleosome is partially translocated off of the DNA fragment. Alternatively, this remodeled product might migrate faster in the gel because it lacks one histone dimer, and thereby has a larger net negative charge.

Many chromatin remodeling reactions are regulated by cues hidden in the chromatin substrate (Clapier and Cairns, 2012; Watanabe *et al.*, 2013; Swygert and Peterson, 2014; Hwang *et al.*, 2014), however, this would be the first example of a chromatin-bound nonhistone protein acting as such a reaction-instructing substrate cue. There are three models that can explain how Sir2p/4p direct histone dimer eviction by SWI/SNF. First, while SWI/SNF has been shown in some cases to evict dimers from the nucleosome it is remodeling (Vicent *et al.*, 2004; Yang *et al.*, 2007), other data has shown that SWI/SNF has the ability to disrupt and evict histones from neighboring nucleosomes (Dechassa *et al.*, 2010). Perhaps neighboring nucleosomes that are held together in the silencing structure of Sir proteins represent a more stable barrier than free nucleosomes. When SWI/SNF binds to these Sir proteins and remodels the underlying chromatin, more destabilization could build up than would occur with free nucleosomes, resulting in the energy necessary to displace multiple histones and Sir proteins simultaneously. As a second model, since Sir2p/4p interacts with regions on Swi2p that are known to regulate SWI/SNF activity (Figure 21) (Smith *et al.*, 2003; Szerlong *et al.*, 2008), perhaps Sir2p/4p directs the outcome of the

remodeling reaction toward dimer eviction. Finally, Sir2p/4p might act as a chaperone to stabilize histone dimers away from the nucleosome.

Another interesting result from this Sir disruption reaction is the state of the remodeled heterochromatin. First, Sir3p and Sir2p are evicted from chromatin, and Sir2p appears to be separated from Sir4p as well. Since Sir4p has been shown to stimulate Sir2p's deacetylase activity (Hsu *et al.*, 2013), the resulting Sir2p would be less catalytically active, and also would no longer be tethered to loci by Sir4p's interactions. Second, Sir4p and H2A/H2B dimers are also evicted from chromatin. As a result, the underlying chromatin would be comprised of hexamers and/or tetramers. The DNA and proteins within incomplete nucleosome structures are more accessible than those within octameric chromatin. These two conditions in the remodeled product would presumably inhibit immediate full repressive heterochromatin formation, increasing the dynamic accessibility of the underlying DNA to cellular processes.

Materials and Methods

Protein purification

Proteins for the experiments in this chapter, including Sir2p-HA/Sir4p-TAP and Minimal Swi2p-TAP, were all purified, modified, and assembled as described in Chapter II of this thesis. Tailless Xenopus H4 octamer was a kind gift of Dr.

Nicholas Adkins (University of Massachusetts Medical School). GST fusion protein pulldown was performed as described in Chapter II of this thesis.

DNA generation

DNA substrates were generated as described in Chapter II of this thesis. Mononucleosome and dinucleosome template DNA were generated by NEB Taq PCR (Chapter II of this thesis) using the plasmid 601b-30-603 (see Appendix 2, gift from Dr. Blaine Bartholomew, University of Texas MD Anderson Cancer Center) and the primers listed in Appendix 1. Radiolabeled mononucleosome was generated by digesting mononucleosome PCR product with EcoRI followed by Klenow end fill-in (Chapter II of this thesis). Linear pUC19 plasmid templates with or without biotinylation were generated by NEB Phusion PCR (Chapter II of this thesis) using linearized pUC19 plasmid (NEB #N3041S) and the primers listed in Appendix 1.

Sir chromatin gel shift assay

All native PAGE minigels were poured in 0.5XTBE, 4% 37.5:1 acrylamide:bis, and run in 0.5XTBE at 120V for 30 minutes. Samples were all loaded in 5% v/v glycerol (final).

Equimolar purified Sir2p/Sir4p and purified Sir3p were preincubated in buffer 'TTF' (two three four;' 25mM Tris pH=7.4, 50mM NaCl, 1.75mM $MgCl_2$, 1mM DTT, 0.05% TWEEN-20) for 10 minutes at 22°C. Then, equal volumes of

Sir2p/Sir4p in TTF buffer and chromatin in TTF buffer (stoichiometry as given in Figure 16A) were mixed and incubated for 10 minutes at 22°C as 10µl reactions.

Where appropriate, Sir chromatin in TTF buffer was subsequently mixed four parts to one with purified chromatin remodeling enzyme (buffer TTF, ±25nM SWI/SNF, ±5mM MgATP) at final concentrations of 5nM enzyme, 1mM MgATP, and 30nM nucleosome. Reaction proceeded for 10 minutes at 22°C. For figure 1C, prior to gel loading, reactions were stopped by supplementing 1ug of supercoiled competitor plasmid DNA and 50mM EDTA, and incubating for 10 minutes at 22°C prior to loading.

Sir chromatin capture assay

Biotinylated arrays were constructed as described (Swygert *et al.*, 2014). Unless otherwise noted, 208 5S-12 DNA templates were used for reconstitutions. Sir nucleosome binding and remodeling reaction proceeded exactly as for the native gel shift experiments, except at final concentrations of 30nM nucleosome, 15nM Sir proteins (unless experimentally varied), and a 0/1/2/4nM gradient of chromatin remodeling enzyme (2nM/4nM enzyme for two-point gradient, 2nM enzyme if no gradient is varied). Following remodeling, arrays were captured and samples were subjected to SDS-PAGE and western blotting (as performed in Chapter II of this thesis).

Chapter IV: Conclusions

The context of this research

The proper function and preservation of the eukaryotic genome require that the genome be stored within chromatin. Chromatin fundamentally alters the accessibility of DNA sequences to the cellular machineries that carry out the transcription, repair and replication of DNA (Papamichos-Chronakis and Peterson, 2012; Rando and Winston, 2012; Venkatesh and Workman, 2015). While all chromatin shares the common core nucleosome subunit, even simple microscopy readily reveals the heterogeneity of nuclear chromatin (Heitz E., 1928). Cells create this heterogeneity via a plethora of molecular mechanisms that modify the chromatin fiber. Histones and DNA are post-translationally modified (Bannister and Kouzarides, 2011); histones are translocated along DNA, evicted, or exchanged for variant versions (Clapier and Cairns, 2009). The resulting variegated chromatin landscape is read by other factors, which bind to loci of interest and associate their own activites with those loci (Musselman *et al.*, 2012). The genomic locations of these molecular mechanisms and chromatin landscapes can vary from organism to organism, and even between different cells within the same organism (Steffen and Ringrose, 2014). Importantly, these diverse aspects of the chromatin fiber serve to regulate the activity and modification of genes contained within the underlying DNA (Woodcock and Ghosh, 2010).

With the development of genome-wide data generation and analysis techniques, detailed pictures can be drawn concerning the chromatin state, associated proteins, and spatial proximity of gene loci. While some chromatin features signify process-relevant information—H3K36 methylation over active gene bodies (Carrozza *et al.*, 2005), or DNA damage-induced phosphorylation of serine 129 on the H2A C-terminal tail (Downs *et al.*, 2000)—many chromatin features speak to the existence of overarching regulatory chromatin superstructures. Indeed, Hidden Markov model analysis of chromatin features and associated proteins predict that five to six distinct chromatin environments exist *in vivo* (Filion *et al.*, 2010; Rao *et al.*, 2014). These distinct chromatin environments correlate with transcriptional and replicative regulation of the underlying gene loci (Pope *et al.*, 2014). While these types of chromatin are constrained in a linear sense to contiguous domains by boundary factors like CTCF, two chromatin domains that share common features and proteins are more likely to share spatial proximity with one another than two dissimilar but linearly adjacent loci are (Lieberman-Aiden *et al.*, 2009; Rao *et al.*, 2014). This proximity potentially reflects these domains' common association with the various self-interacting molecules responsible for creating these domains.

These five or six chromatin environments are congruent with prior data if they are considered as subclasses of the two main types of chromatin domains that had already been extensively characterized: active and open euchromatin, and repressive and closed heterochromatin. An additional feature captured as

two of these chromatin environments is the existence of both constitutive and facultative heterochromatin. Constitutive heterochromatin is present in all cell types, whereas facultative heterochromatin may silence gene loci in one cell type but not another. Both types of heterochromatin, despite employing different molecular machinery, rely upon the themes of heterochromatin establishment that were discussed in the introduction to this thesis. First, chromatin modifying enzymes are recruited to a nucleation site. Then, iterative binding of proteins that read this modification, and their protein-protein interactions that increase the range of the modifying enzyme, result in spreading of the heterochromatin domain in a DNA sequence-independent manner. These domains spread outwards until they encounter boundary factors or activities (Grewal and Jia, 2007; Hathaway *et al.*, 2012; Grunstein and Gasser, 2013).

Heterochromatic loci are transcribed less, undergo recombination less, and replicate later during S phase than their euchromatic counterparts. Heterochromatin plays key roles in the maintenance of genome stability, during organism development and cell differentiation, maintaining cell type identity, and restricting the activity of transposable genetic elements. These roles are thought to be filled by a repressive superstructure formed by heterochromatin proteins bound to chromatin. Key to this repressive superstructure are abundant protein-protein interactions—between heterochromatin proteins themselves, via homodimerization or heterodimerization, as well as between the heterochromatin proteins and their optimally modified chromatin substrates.

The most well-understood model system for heterochromatin formation and regulation is the Sir heterochromatin of *S. cerevisiae*. Here, the three main Sir proteins Sir2p, Sir3p, and Sir4p direct silent chromatin formation at both the silent *HM* loci and at telomeres. Sir4p interacts with proteins at silencer elements, and stimulates the Sir2p histone deacetylase to deacetylate histone lysines around the silencer locus. Deacetylation of H4K16 creates a high-affinity binding site for Sir3p, whose N-terminal BAH domain interacts with a large region on the surface of the nucleosome (Armache *et al.*, 2011). Sir3p can also bind to Sir4p, and in so doing is thought to increase the range of Sir2p's catalytic activities. Iterative deacetylation and binding thus directs Sir spreading outwards. Sir3p is thought to be the primary structural determinant of Sir heterochromatin, as its overexpression alone results in the expansion of silent chromatin domains, whereas overexpression of Sir4p disrupts silencing (Hecht *et al.*, 1996; Strahl-Bolsinger *et al.*, 1997; Cockell *et al.*, 1998).

Despite the heritable stable, repressive nature of heterochromatin, there are events that necessitate quick access of trans factors to the underlying DNA. At least once per cell cycle, all heterochromatic DNA must be replicated. Moreover, genomic lesions that damage the fidelity or stability of heterochromatic DNA must be made accessible to the myriad of repair pathways a cell employs if they are to be repaired. Such access must be thorough enough to grant access, yet transient and dynamic such that the silent chromatin state is not lost. The only such means of access discovered thus far are post-translational

modifications on heterochromatin proteins that remove them from chromatin in response to stresses (Ai *et al.*, 2002; Bolderson *et al.*, 2012). However, unless the activity of the corresponding modifying enzyme is spatially or temporally restricted, such activity would affect heterochromatin stability globally.

There is also circumstantial evidence suggesting that ATP-dependent chromatin remodeling enzymes are tools that cells use to access heterochromatic DNA. These large, multi-subunit enzymes use the power of ATP hydrolysis to translocate DNA, reposition nucleosomes along DNA, exchange or evict histone dimers, or evict histone octamers from DNA. These enzymes were first discovered and studied in the context of transcriptional activation, but subsequently have been implicated in regulating many aspects of chromatin structure and the majority of a cell's DNA molecular biology. By nature, these enzymes function to regulate chromatin structure in order to change the primary effect of chromatin, differential DNA accessibility. These enzymes adapt a common DNA translocation mechanism into a variety of application-specific outcomes via regulatory domains and subunits that recognize substrate cues or chaperone reaction intermediates (Clapier and Cairns, 2009; Narlikar *et al.*, 2013).

In particular, the SWI/SNF chromatin remodeling enzyme family has a number of ties to heterochromatin regulation. This conserved enzyme complex is a potent tumor suppressor in humans (Kadoch *et al.*, 2013), and acts biochemically via nucleosome sliding and histone dimer and octamer eviction

(Liu *et al.*, 2011). As a member of the transcriptionally activating trithorax group of developmental chromatin regulators, SWI/SNF complex represents an opposing phenotype to the heterochromatic Polycomb group proteins (Steffen and Ringrose, 2014). This opposition is borne out at floral patterning genes in *A. thaliana*, where SWI/SNF is required to inactivate Polycomb-mediated transcriptional silencing (Wu *et al.*, 2012; Li *et al.*, 2015). Polycomb group proteins and SWI/SNF-B complex cooperate in human cells to silence transcription around genomic lesions (Kakarougkas *et al.*, 2014). In *S. cerevisiae*, SWI/SNF has been implicated in nucleotide excision repair at Sir loci (Gong *et al.*, 2006), and ectopically tethered SWI/SNF complex is sufficient to act as a barrier against Sir heterochromatin spreading (Oki *et al.*, 2004). Finally, earlier work implied that SWI/SNF was required for yeast mating type switching, for recombination into heterochromatin (Chai *et al.*, 2005; Sinha *et al.*, 2009), and not just for transcriptional activation of the *HO* endonuclease (Stern *et al.*, 1984).

The most direct evidence for SWI/SNF disrupting the repressive structure of heterochromatin is *in vitro* work that reconstitutes the early steps of homologous recombination. In these assays, the recombinase Rad51p was sufficient to search through a chromatinized donor plasmid for homology to an oligonucleotide, and to form a protein-stabilized joint at the locus (Sinha and Peterson, 2008). However, prebinding Sir3p to the chromatin substrate was sufficient to block this homology search reaction. SWI/SNF complex was uniquely able to revert the Sir3p-stimulated inhibition, and even able to rescue

homology search in the presence of all three Sir proteins. Central to this rescue appeared to be an ATP-dependent Sir3p eviction activity that was also unique to SWI/SNF complex (Sinha *et al.*, 2009). However, no mechanistic details, substrate requirements, or *in vivo* contexts were known for this Sir antagonism.

Insight, speculation, and next steps for this research

We set out to uncover the mechanism behind the Sir3p eviction activity of SWI/SNF complex. Using coprecipitation and far western blotting techniques, we succeeded in identifying and characterizing a pair of interactions between Sir3p and the core ATPase subunit of SWI/SNF, Swi2p. We found that the extended alpha-helical HSA region of Swi2p contacts the C-terminal end of the Sir3p AAA^+ domain. The interaction regions in these domains are immediately adjacent to numerous other protein-protein interaction sites. According to structural data, the ten HSA amino acids that are required for Sir3p binding lie immediately between the HSA binding sites for the two regulatory Arp proteins (Schubert *et al.*, 2013). Similarly, the region of the AAA^+ domain required to bind the HSA sits structurally adjacent to Sir3p alpha helices that bind to the Sir4p C-terminus (Ehrentraut *et al.*, 2011). Moreover, this region of Sir3p is immediately followed by a wH homodimerization domain (Oppikofer *et al.*, 2013a). We speculate that this HSA-AAA^+ interaction could facilitate disruption of protein-protein interactions in both SWI/SNF and Sir chromatin. Indeed, in chapter three of this thesis, there is notable eviction of Sir3p from chromatin prior to eviction of Sir4p. Destabilizing

the Sir3p-Sir3p/Sir4p interactions would weaken heterochromatin superstructure, assisting SWI/SNF in remodeling heterochromatin.

The second interaction between Swi2p and Sir3p occurs between their respective functional nucleosome-binding domains: the Swi2p ATPase domain, and the Sir3p BAH domain. This interaction is intriguing because both of these domains seem to be in the same place on the nucleosome at the same time. The BAH domain binds atop the H4 tail two superhelical turns from the nucleosomal dyad, right where strong crosslinking is seen between the ATPase domain of SWI/SNF and nucleosomal DNA (Dechassa *et al.*, 2008; Armache *et al.*, 2011). The first RecA-like fold of the Swi2p ATPase domain is involved in binding Sir3p, specifically by a relatively divergent sequence patch at its N-terminal face. Swapping these residues with the corresponding residues from the Sth1p ATPase is sufficient to break this interaction.

Interestingly, the same residues from Sth1p that are unable to interact with the Sir3p BAH domain are able to interact with the BAH domain of Orc1p, whereas the Swi2p sequence interacts with both Orc1p and Sir3p BAH domains. This specificity can be traced to a feature of the BAH domains—the poorly conserved gating regions that surround the evolutionarily conserved core fold (Callebaut *et al.*, 1999; Oliver *et al.*, 2005). By sequentially deleting the gating regions of the Sir3p BAH, interaction with Sth1p was restored. Since the silencing properties of the Sir3p BAH domain subfunctionalized after its divergence from ancestral Orc1p (Hickman and Rusche, 2010; Hickman *et al.*,

2011), we postulate that the gating modules of the Sir3p BAH domain and the N-terminal residues of the Swi2p ATPase domain might have co-evolved to generate this specificity. We wondered whether this ‘core fold gating’ model was present not only in the Orc1p-like class of BAH domains, but also in the PBRM1/Rsc1p/Rsc2p-like class as well. We found that deleting the gating regions of the Rsc2p BAH domain also allowed that domain to interact with SWI/SNF.

BAH domains are quite abundant in chromatin-associated proteins. In addition to RSC/hSWI/SNF-B remodeling enzymes, mammalian NuRD chromatin remodeling enzymes—members of the CHD family—possess BAH domain-containing MTA1/2/3 subunits. The NuRD complex functions in many aspects of genome regulation, and overexpression the MTA1 subunit is found in high-grade cancers (Lai and Wade, 2011). The silencing-associated BAHD1 and DNMT1 proteins also bear BAH domains, as does the trithorax-group histone methyltransferase Ash1 (Byrd and Shearn, 2003; Song *et al.*, 2011). Given the ubiquity of BAH domains in chromatin-associated proteins, it is possible that Swi2p-like ATPase domains have evolved to recognize BAH domains as protein motifs that regulate their activities.

Consistent with this hypothesis, H3 tail peptides are known to bind to Rsc2p BAH domains, and this association affects the 3D conformation of the whole RSC complex (Leschziner *et al.*, 2007; Skiniotis *et al.*, 2007; Chambers *et al.*, 2013). Evidence also exists that BAH domains dictate particular activities of

RSC complexes *in vivo* (Chambers *et al.*, 2012). A model for BAH-ATPase regulation, based on the ISWI AutoN regulation model, is consistent with these data: when an H3 tail is not present, the Rsc2p BAH domain binds the Sth1p ATPase domain and holds RSC in a closed conformation that precludes nucleosome remodeling. Inclusion of the H3 tail competes the Rsc2p BAH domain away from its ATPase contact, opening up the complex for nucleosome binding. This mechanism would allow the BAH domain of Rsc1p/Rsc2p to direct activities of the RSC complex as a whole; indirect evidence suggesting this has already been published (Chambers *et al.*, 2012). While such modes of regulation are speculative at this point, given the central role of BAH-domain containing proteins in transcriptional control, development, genome stability and tumor suppression, research remains to be done on BAH-directed chromatin regulation.

Interaction of Sir3p with both the HSA domain and the ATPase domain suggests that these Sir3p interactions may directly regulate the Swi2p ATPase. Evidence reinforcing this suggestion comes from study of HSA domains and chromatin remodeling activity. Both SWI/SNF and Ino80 family remodeling enzymes have HSA domains, and both families have actin or actin-related proteins that bind to these domains (Szerlong *et al.*, 2008). In the context of the Ino80 family, inactivation of the HSA-Arp module confers defects in DNA binding (Shen *et al.*, 2003; Watanabe *et al.*, 2015). Disruption of this module in SWI/SNF family results in defective ATPase activity, but this defect can be suppressed by other mutations in the ATPase subunit, specifically in the region following the

HSA domain and at a region within the ATPase domain (Szerlong *et al.*, 2008). These data suggest that the HSA module may function in SWI/SNF family enzymes to relieve an intrinsic ATPase autoinhibition activity. Sir3p's contacts in the HSA domain and ATPase domain suggest that Sir3p can directly regulate SWI/SNF activities, but additional work must be done to investigate this hypothesis.

We also generate a mutant allele of *SWI2*, *swi2-Δ10R*, that disrupts both of the Swi2p-Sir3p contacts. We validate that this mutant allele is a surprisingly faithful separation-of-function mutant using a combination of biochemistry and yeast genetics. With the exception of a 50% reduction in Arp7p/Arp9p/Rtt102p content following complex purification via a stringent TAP protocol, the SWI/SNF-Δ10R complex possessed identical subunit composition to wild-type SWI/SNF complex. More importantly, the SWI/SNF-Δ10R ATPase properties and chromatin remodeling activities were indistinguishable from normal SWI/SNF. Importantly, we showed that SWI/SNF-Δ10R complex demonstrated a specific defect in evicting Sir3p from chromatin.

SWI/SNF complex is involved in a myriad of chromatin regulatory pathways, and as a result full null mutants of SWI/SNF subunits have complex, severe growth phenotypes (Neigeborn and Carlson, 1984; Peterson and Herskowitz, 1992). Our separation-of-function mutant is uniquely able to reveal which specific processes require SWI/SNF to regulate heterochromatin *in vivo*. Validating this logic, we found no large transcriptional defects in *swi2-Δ10R*

mutants either by RNA-seq or by RT-qPCR. Instead, we found that *swi2-Δ10R* cells grew slower than wild-type cells in the presence of the RNR inhibitor hydroxyurea. This defect was not due to defective RNR gene expression in response to HU (Sharma and Reese, 2003), but it could be rescued by also deleting Sir3p. Together with data showing that Sir proteins ChIP to and transcriptionally silence impaired replication forks (Dubarry *et al.*, 2011), we hypothesize that SWI/SNF is required to evict Sir proteins in order for replication to proceed normally. Future work could illuminate the mechanism by which SWI/SNF is brought to these replication forks.

Another result that we found was, consistent with earlier full *swi2Δ* data, SWI/SNF is required for the proper establishment of subtelomeric heterochromatin (Dror and Winston, 2004). Our data shows that eviction of Sir3p by SWI/SNF is involved in this process. This involvement could be either direct or indirect. If indirect, then SWI/SNF actively evicts Sir3p elsewhere in the genome—for example, at ectopic loci or stressed replication forks (Dubarry *et al.*, 2011; Radman-Livaja *et al.*, 2011). The stability of subtelomeric silencing is impaired by the shortage of Sir3p that results when Sir3p stays at these other loci. If direct, then SWI/SNF may be required to evict Sir3p in order for the underlying chromatin to achieve a state compatible with silencing. For example, Sir3p binding may impair enzymes that generate silencing-compatible nucleosome spacing.

We began this research with the hypothesis, based on context above, that SWI/SNF would be required to disrupt Sir heterochromatin during the homologous recombination phase of yeast mating type switching. Consistent with prior literature (Neigeborn and Carlson, 1984; Peterson and Herskowitz, 1992; Stern *et al.*, 1984), but contradicting one specific study (Chai *et al.*, 2005), we found that *swi2Δ* mutants were very slow growing and had severe galactose induction defects, but were ultimately able to switch mating types in systems with ectopically expressed *HO* endonuclease. One explanation for these data is that the original, lost *snf5Δ* isolate used in the aforementioned study (Chai *et al.*, 2005) possessed suppressor mutations as a byproduct of its haploid PCR transformation method of generation. However, this is not the only viable explanation. In an earlier figure in the same paper, an independently created *snf5Δ* strain was compared to a *swi2Δ* strain, and the *snf5Δ* strain was significantly more defective at general euchromatic HR repair than the *swi2Δ* strain. In this explanation, deletion of *SNF5* would result in disassembly of SWI/SNF complex into subcomplexes, including the minimal Swi2p/Arp7p/Arp9p/Rtt102p subcomplex. Minimal SWI/SNF subcomplex might function as a dominant negative regulator of HR repair *in vivo*, and it would not form if the *SWI2* gene were deleted instead. Further research would need to be done to clarify this situation, the simplest test being testing whether additional deletion of *SWI2* is sufficient to rescue the HR defect of *snf5Δ* yeast.

Properly silenced Sir chromatin *in vivo* requires all three main Sir proteins, Sir2p, Sir3p, and Sir4p. In this work, we also discovered and characterized a novel Sir disruption activity that SWI/SNF activates when its substrate bears Sir2p and Sir4p. This activity requires the H4 tail and is cooperatively activated by Sir proteins, both of which are hallmarks of silent chromatin *in vivo* as well. This disruption activity ejects all three Sir proteins from chromatin, and appears to separate Sir2p and Sir3p from Sir4p. Finally, this disruption activity drives eviction of histone H2A/H2B dimers from chromatin.

Surprisingly, the Sir2p/4p heterodimer appears to interact with the same regions of Swi2p that Sir3p interacts with—the first RecA lobe of the ATPase domain, and the HSA domain. Deletion of the ten HSA amino acids that disrupt Sir3p binding has no effect on Sir2p/4p binding to the HSA, which could explain why the SWI/SNF-Δ10R mutant complex was still competent for Sir2p/4p-stimulated Sir disruption. As with Sir3p, there is a possibility that Sir2p/4p binds to regulatory regions on Swi2p in order to direct reaction outcome, in this case also activating SWI/SNF's H2A/H2B dimer eviction activity. In contrast to the Sir3p eviction activity, the Sir2p/4p-stimulated Sir disruption activity requires SWI/SNF subunits outside of the minimal SWI subcomplex. Identifying which subunits are responsible for this new eviction activity could create new paradigms for chromatin remodeling mechanism.

The existence of multiple activities for SWI/SNF, and the dependence of these activities on the Sir proteins that are present on the substrate, may indicate

that different forms of heterochromatin exist in the nucleus (Strahl-Bolsinger *et al.*, 1997). It is easy to imagine that Sir3p BAH domain binding to the H4 tail is mutually exclusive with Sir2p binding the H4 tail to deacetylate H4K16Ac. Indeed, purification of endogenous Sir2p/4p from yeast yields very little Sir3p (Moazed *et al.*, 1997; Ghidelli, 2001). Similarly, the influence of H3K79Me on Sir3p BAH domain and AAA domain nucleosome binding happens independent of one another (Armache *et al.*, 2011; Ehrentraut *et al.*, 2011). Overexpression of Sir3 reveals preferential binding to some heterochromatin loci over others (Radman-Livaja *et al.*, 2011). Particular aspects of Sir heterochromatin—silencing dependence on Sir1p, Abf1p, or the ORC complex, for example—vary depending on whether heterochromatin is telomeric or silencer-nucleated (Grunstein and Gasser, 2013; Oppikofer *et al.*, 2013b). Finally, binding of Sir proteins to H4 tailless nucleosomes here, or to H3K79Me nucleosomes *in vivo*, results in structures that are competent for binding but incompetent for spreading (Kitada *et al.*, 2012). Perhaps each of these putatively distinct heterochromatin contexts requires different activities from SWI/SNF—just Sir3p eviction, or Sir2p/4p-dependent histone dimer eviction, or both activities, might be applied depending on the Sir context of the locus.

Sir2p/4p also interacts with the bromodomain of Swi2p. This interaction could indicate the presence of acetylated lysines on Sir2p/4p. As an alternative, speculative hypothesis, it has been shown that acetylation of Swi2p, near its AT-hooks DNA binding region, by the Gcn5p histone acetyltransferase stimulates

dissociation of SWI/SNF from chromatin (Kim *et al.*, 2010; Dutta *et al.*, 2014). Perhaps Sir2p/Sir4p can bind to the region of Swi2p containing this acetylation site. Then, in the cases where Swi2p is acetylated, Sir2p can deacetylate Swi2p to antagonize SWI/SNF dissociation. The exact mechanism of the Sir disruption reaction warrants further investigation, as identifying its mechanism would provide keys for identifying other substrate cues that grant chromatin remodeling enzymes alternate activities.

Why would a yeast cell specifically employ SWI/SNF complex to dynamically regulate access to Sir heterochromatin? As mentioned above, after the yeast whole genome duplication, duplication of Orc1p and Snf2p afforded extra copies of these loci that might have subfunctionalized together to regulate silent genetic information. Additionally, SWI/SNF complex is present at a much lower copy number in the cell than other enzymes like RSC, Ino80 or ISWI (Ghaemmaghami *et al.*, 2003), therefore there is less SWI/SNF that could aberrantly derepress heterochromatic loci. Moreover, the SWI/SNF family of chromatin remodeling enzymes is the only family that is known to evict histone dimers and octamers from chromatin (Vicent *et al.*, 2004; Yang *et al.*, 2007; Dechassa *et al.*, 2010; Brown *et al.*, 2011), implying that this particular family of enzymes might have the unique amount of applicable power necessary to disrupt heterochromatin superstructure. Finally, a factor might exist that serves to recruit SWI/SNF to heterochromatin when needed.

While Sir heterochromatin is not conserved in metazoans, the basic themes of heterochromatin as discussed in this thesis are conserved, albeit manifested in different proteins. SWI/SNF complex is absolutely conserved in metazoans. There is circumstantial evidence that metazoan SWI/SNF acts to antagonize facultative heterochromatin during development, as described in the first section of this chapter. There is also evidence that SWI/SNF interacts with components of constitutive heterochromatin—the human core subunit's HSA domain interacts with the chromoshadow domain of heterochromatin protein 1, a protein-protein interaction domain vaguely analogous to the C-terminus of Sir3p (Lavigne *et al.*, 2009). Therefore, future research may bear out that the themes of dynamically regulating heterochromatin outlined here are evolutionarily conserved.

Concluding Remarks

Many rules have exceptions for practical purposes. In this work, we have characterized mechanisms that sidestep the static repressive rule of heterochromatin. We identified physical interactions between heterochromatin proteins and ATP-dependent chromatin remodeling enzymes, and investigated how these physical interactions guide the remodeling reaction to novel outcomes. We disrupted these physical interactions, and used these disruption mutants to discern novel roles for the SWI/SNF complex in genome regulation. I am optimistic that continuing these veins of research will lead to new conserved

paradigms of chromatin regulation. These paradigms will augment our appreciation, both in terms of flexibility and power, of the structure that houses our genomes.

Appendix 1: Oligonucleotide Sequences

Name	Description	Sequence
Making 282bp-Mid601 from CP1024		
282-601MID UP		GATCCTCTAGAGTCGGGAGCTC
282-601MID DOWN		TGACCAAGGAAAGCATGATTCTTCAC
Making Mononucleosomes and Dinucleosomes from CP1462		
601-603 F	Common UP	GCCAGTGAATTCCAGGATGT
601-603 DI R	Dinuc DOWN	GATCTGCCCAGTTCGCG
601 MO R	Mono DOWN	CCGAGAGAATCCCGGTG
Linear pUC19 DNA PCR, ±Biotinylated End		
pUC19 Biot	Biotinyl UP	/5Bio/AACGTCGTGACTGGGAAAAC
pUC19 F	Normal UP	AACGTCGTGACTGGGAAAAC
pUC19 R	Common DOWN	AGCTTGGCGTAATCATGGTC
Mating Type Confirmation:		
MAT DOWN		AGTCACATCAAGATCGTTTATGG
ALPHA UP		GCACGGAATATGGGACTACTTCG
A UP		ACTCCACTTCAAGTAAGAGTTTG
HML DOWN		TGGAACACAGAAAAGAGCAGTG
HMR DOWN		GATTAAGAGAAAATGTCACTACA
***MAT* qPCR Primers:**		
MAT Down		GGTTAAGATAAGAACAAAGAATGATGCT
DSB MATa UP		CTTTTAGTTTCAGCTTTCCG
SI MATα UP		GCAGCACGGAATATGGGACT
SI MATa UP		GTCGGGTTTTTCTTTTAGTTTCA
ACT1 F		CTTTCAACGTTCCAGCCTTC
ACT1 R		CCAGCGTAAATTGGAACGAC
RNR3 F	MR226	TGAACAAAAGGCGGCATCTG
RNR3 R	MR227	TGTTTCCGTTGGAACTGCTG
Deletion Primers:		
MR030	up for *sir3Δ*	TTAAGAAAGTTGTTTTGTTCTAACAATTGGATTAGCTAAAcggatccccgggttaattaa
MR031	down for *sir3Δ*	CATAGGCATATCTATGGCGGAAGTGAAAATGAATGTTGGTGGgcataggccactagtggatc
MR045	*MX* down	GTATTCTGGGCCTCCATGTC
MR078	*SIR3* 3`UTR R	ACATCTAGTCATTTTGGGTATATTATCGCG
MR079	*SIR3* C term F	TTGTTGTGGTGCTCGAGGAGCCCAGTGC
MR011	up for *swi2Δ*	TCAGCTATTCTGTTGTTTCTCTAATCGCGACTTTCTGCTATTTTCACGACTTTCGATTAATTATCTGCCCGGATCCCCGGGTTAATTAA
MR012	down for *swi2Δ*	ATAAAAAAAAGAGGGATTAATGTTTGTCTACGTATAAACGAATAAGTACTTATATTGCTTTAGGAAGGTAGAATTCGAGCTCGTTTAAAC
MR074	*SWI2* 5`UTR F	CCTGAGGCGGTAGGACAATA
MR075	*SWI2* ORF R	TTGCTAAATTGACGCTGTGG
Generating GST Fusion Proteins:		
GST-SIR3BAH-UP		CAGATAGGATCCCCATGGCTAAAACATTGAAAG
GST-SIR3BAH-DOWN		CGGTAGGAATTCCCTGGTACAGATACTCTTTTC
SIR3U1UP		CAGATAGGATCCCCGTGAGTGGGCAGAAGACA
SIR3U1DOWN		CGGTAGGAATTCCCAGATGTCTTCTCTGGCTT
SIR3U2UP		CAGATAGGATCCCCTCACCTACAGATTCTTCG
SIR3U2 DOWN		CTGGGAATTCCAGGTTTTCC
GST-SIR3AAA-UP		CAGATAGGATCCCCAACGCTGATATAAATTTAG
GST-SIR3AAA-		CGGTAGGAATTCCCTCCGTTAATAGCTTCTGAG

DOWN		
GST-SIR3MID-UP		CAGATAGGATCCCCCCAAAGATGATTGATTTCGC
GST-SIR3MID-DOWN		CGGTAGGAATTCCCCAATTCATTCTTGTCCACC
GST-SIR3END-UP		CAGATAGGATCCCCAAGAACGTAGCCAACGTAAG
GST-SIR3END-DOWN		CGGTAGGAATTCCCTTCATCCATCGAAAAGGCG
SWI2N-UP		CAGATAGGATCCCCAACCGCTGCTATTTAAGA
SWI2N-DOWN		CGGTAGGAATTCCCCGATTCTGTTTGCGTGAT
SWI2HSA-UP		CAGATAGGATCCCCGGTCCATCTAGTGTACAT
SWI2HSA-N-DOWN		CGGTAGGAATTCCCATCGTTCGCCTTTAAAGC
SWI2HSA-C-UP		CAGATAGGATCCCCCATGAATTACTTAAGTTAG
SWI2HSA-DOWN		CGGTAGGAATTCCCCGAAACCATCCACTGTAA
SWI2ATP-UP		CAGATAGGATCCCCGCGAAATGGGCTCCTACC
SWI2ATP-DOWN		CGGTAGGAATTCCCAACTTCATTCTTCTGACC
SWI2C-UP		CAGATAGGATCCCCTCAGTTGAAGAAGTTATC
SWI2C-DOWN		CGGTAGGAATTCCCAGACAAGAAATCATCGTC
SWI2BROMO-UP		CAGATAGGATCCCCAGTGAATTACCTGATATT
SWI2BROMO-DOWN		CGGTAGGAATTCCCCTATACACTCGCTTCTGT
HSAC1 UP		CAGATAGGATCCCCGCCAGATTAAAGTCGATG
HSAC2 UP		CAGATAGGATCCCCAGAAGACAAGATAAAAAG
HSAC3 UP		CAGATAGGATCCCCCTCATTGCTACGCATACT
HSAC4 UP		CAGATAGGATCCCCGCTGAAAAAAAGGCAAAAG
HSAN1 DOWN		CGGTAGGAATTCCCAGCTCTCTTTTGCTCATC
HSAN2 DOWN		CGGTAGGAATTCCCGAGTCTATGGCCAAACTTC
HSAN3 DOWN		CGGTAGGAATTCCCTCTATTATATTGATTGATG
HSAN4 DOWN		CGGTAGGAATTCCCGGCCACTGCCTCAGTCTTC
SWI2ATP2UP		CAGATAGGATCCCCGTTCTGACTACCTTTGAG
SWI2ATP3UP		CAGATAGGATCCCCCATGCAGATTATAGATTA
SWI2ATP4UP		CAGATAGGATCCCCCGTCGTCTTTTTATCGGT
SWI2ATP5UP		CAGATAGGATCCCCGCTGGTAAATTTGAACTA
SWI2ATP1DOWN		CGGTAGGAATTCCCCTTGGATAAAAGTGCTCT
SWI2ATP2DOWN		CGGTAGGAATTCCCACCTGTCAAAATTAATCT
SWI2ATP3DOWN		CGGTAGGAATTCCCACCGATAAAAAGACGACG
SWI2ATP4DOWN		CGGTAGGAATTCCCTCTATCTAATAGTTCAAA
SIR3BAHΔ187DOWN		CGGTAGGAATTCCCAATTGGTACAAACTTTTCCG
SIR3BAHΔ153DOWN		CGGTAGGAATTCCCTATCTGTCCAACTGCAATG
SIR3BAHΔ128DOWN		CGGTAGGAATTCCCTACTTCGTTGAAAAATTTATC
SIR3BAHΔ98DOWN		CGGTAGGAATTCCCTTTGAGTTCAAACCATCTCA
STH1ATP1UP		CAGATAGGATCCCCTGGACTTTAGAATTTGAA
STH1ATP1DOWN		CGGTAGGAATTCCCTTTTGATAAAAGAGATTT
ORC1BAH UP		CAGATAGGATCCCCATGGCAAAAACGTTGAAGG
ORC1BAH DOWN		CGGTAGGAATTCCCCTTTTGAGGACCTCTTTTG
RSC2BAH UP		CAGATAAGATCTCCGATGAAGTCATTGTAAATAATATATC
RSC2BAH DOWN		CGGTAGCAATTGCCGGGGGAAGGATATTTGAAG
RSC2CT1 DOWN		CGGTAGCAATTGCCAAGAGCATTTGCTGTTG
Amplification of FLAG-tagged domains:		
SWI2HSAFLAGUP		CAGATACATATGCATGAATTACTTAAGTTAG
SWI2HSAFLAGDOW		CGGTAGGGATCCTTACTTATCGTCATCGTCTTTATAATCCTTGTCATCGTCATC

N		TTTGTAGTCATCGTTCGCCTTTAAAGCCTG
BAH-FLAGUP		CAGATACATATGGCTAAAACATTGAAAG
BAH-FLAGDOWN		CGGTAGGGATCCTTACTTATCGTCATCGTCTTTATAATCCTTGTCATCGTCATC TTTGTAGTCCCCACTCACTGGTACAGA
***STH1* ATPase lobe 1 amplification:**		
STHATP123UP		GATTCGGGTACCTTAAAAGAGTATCAATTACGA
STHATP123DOWN		CACAGGCACCGGTGTTGGCAAATGGAGTATTAAACC
Site-directed mutagenesis of *SWI2*:		
SWI2HSA-10 S		CGATGAATAAATCCGCCAAGAATAAAAGGTTG
SWI2HSA-10 AS		CAACCTTTTATTCTTGGCGGATTTATTCATCG
C-terminal TAP tag for CP1414:		
TAP-Xho UP		CAGATACTCGAGCATGGAAAAGAGAAGATGGAAAAAG
TAP-Xho DOWN		CGGTAGCTCGAGGTTGACTTCCCCGCGGAATTC

Appendix 2: Plasmids

ID #	Backbone	Description
CP126	pGEX-3X	Plasmid for IPTG-inducing expression of N-terminally GST-tagged fusion proteins in DE3 E. coli
CP137	YCp50	pGAL-HO; Gal-inducible HO endonuclease expression from YCp50 (GAL10 promoter->HO; CEN/ARS, URA3)
CP337	pRS315	SWI2 in pRS315 (~6300bp Sau3AI-partial piece with ~1kb 5`UTR, ORF, and ~300bp 3`UTR)
CP426	pBS SK-	208-12 array; cut out with HhaI to digest backbone
CP589	pBS SK-	208-11 array; cut out with NotI, HindII, and use HhaI to digest backbone
CP717	pET	xH2A expression
CP718	pET	xH2B expression
CP719	pET	xH3 expression
CP720	pET	xH4 expression
CP967	pFA6a	pAG25; for cerevisiae gene deletion cassette template; NatMX4 cassette
CP969	pFA6a	pAG32; for cerevisiae gene deletion cassette template; HphMX4 cassette
CP999	pFA6a	Plasmid for c-terminally tap-tagging
CP1024	pGEM-3Z	601 NPS mono plasmid
CP1109	pET	xH2AS113C expression
CP1163	pDM641	pGal1-HA-Sir2/Leu plasmid derived from pRS315
CP1164	pDM654	pGal1-TAP-Sir4/Ura plasmid derived from pRS315
CP1165	pDM1009	pGal1/10-Sir3-FLAG/Leu plasmid derived from pRS425
CP1210	pMK43	C-terminal AID-tag with KanMX
CP1211	pMK76	StuI-Linearizable URA3-integrable AtTIR1
CP1250	pRS410	Yeast CEN/ARS Plasmid; KanMX; Addgene # 11258
CP1253	pMK43	C-terminal AID-tag with HphMX
CP1406	pRS410	pRS410 cut KpnI-SalI, SWI2 C-terminus inserted (CP337 KpnI-SalI)
CP1407	pRS410	CP1406 cut KpnI-AgeI, STH1 ATPase lobe I inserted (aa#468-665; KpnI-SgrAI; 52 divergent AAs converted)
CP1408	pRS410	pRS410 cut NgoMIV-KpnI, SWI2 N-terminus inserted (CP337 NgoMIV-KpnI)
CP1409	pRS410	CP1408, site-directed mutagenesis HSAΔ10 (aa#613-622 deleted)
CP1410	pRS410	SWI2 in pRS410 CP1408 cut KpnI-SalI, SWI2 C-terminus inserted (CP337 KpnI-SalI)
CP1413	pRS410	SWI2 'Δ10R' in pRS410 CP1409 cut KpnI-SalI, STH1-SWI2 chimera ATPase C-term inserted (CP1407 KpnI-SalI)
CP1414	pRS410	CP1407 cut XhoI-BamHI with 4xpA-CTAP inserted (PCR from CP999 with in-frame XhoI inserted; XhoI-BglII)
CP1415	pRS410	SWI2 'Δ10R'-TAP in pRS410 CP1414 cut NaeI-AgeI with SWI2 HSA10 N-terminus inserted

		(CP1413 NaeI-AgeI)
CP1416	pGEX-3X	GST-SWI2 N (aa#1-390)
CP1417	pGEX-3X	GST-SWI2 HSA (aa#361-780)
CP1418	pGEX-3X	GST-SWI2 HSAN (aa#316-663)
CP1419	pGEX-3X	GST-SWI2 HSAC (aa#588-780)
CP1420	pGEX-3X	GST-SWI2 ATP (aa#836-1206)
CP1421	pGEX-3X	GST-SWI2 C (aa#1216-1440)
CP1422	pGEX-3X	GST-SWI2 BROMO (aa#1321-1703)
CP1423	pGEX-3X	GST-SWI2 HSA (aa#588-663)
CP1424	pGEX-3X	GST-SWI2 HSAN1 (aa#588-648)
CP1425	pGEX-3X	GST-SWI2 HSAN2 (aa#588-633)
CP1426	pGEX-3X	GST-SWI2 HSAN3 (aa#588-618)
CP1427	pGEX-3X	GST-SWI2 HSAN4 (aa#588-603)
CP1428	pGEX-3X	GST-SWI2 HSAC1 (aa#603-663)
CP1429	pGEX-3X	GST-SWI2 HSAC2 (aa#618-663)
CP1430	pGEX-3X	GST-SWI2 HSAC3 (aa#633-663)
CP1431	pGEX-3X	GST-SWI2 HSAC4 (aa#648-663)
CP1432	pGEX-3X	GST-SWI2 HSAΔ10 (CP1423 with 613- 622 deleted)
CP1433	pGEX-3X	GST-SWI2 ATP1 (aa#836-885)
CP1434	pGEX-3X	GST-SWI2 ATP2 (aa#869-924)
CP1435	pGEX-3X	GST-SWI2 ATP3 (aa#915-1035)
CP1436	pGEX-3X	GST-SWI2 ATP4 (aa#1028-1094)
CP1437	pGEX-3X	GST-SWI2 ATP5 (aa#1086-1206)
CP1438	pGEX-3X	GST-STH1 ATP1 (aa#539-588)
CP1439	pGEX-3X	GST-SIR3 BAH (aa#1-214)
CP1440	pGEX-3X	GST-SIR3 U1 (aa#214-350)
CP1441	pGEX-3X	GST-SIR3 U2 (aa#300-440)
CP1442	pGEX-3X	GST-SIR3 MID (aa#460-730)
CP1443	pGEX-3X	GST-SIR3 AAA (aa#530-845)
CP1444	pGEX-3X	GST-SIR3 END (aa#790-970)
CP1445	pGEX-3X	GST-SIR3 BAH1 (aa#1-186)
CP1446	pGEX-3X	GST-SIR3 BAH2 (aa#1-152)
CP1447	pGEX-3X	GST-SIR3 BAH3 (aa#1-127)
CP1448	pGEX-3X	GST-SIR3 BAH4 (aa#1-97)
CP1449	pGEX-3X	GST-ORC1 BAH (*S. cerevisiae* aa#1-214)
CP1450	pGEX-3X	GST-RSC2 BAH (aa#401-557)
CP1451	pGEX-3X	GST-RSC2 BAHCT-1 (aa#401-642)
CP1452	pET3a	SIR3 BAH-FLAG (aa#1-214)
CP1453	pET3a	SWI2 HSA-FLAG (aa#588-663)
CP1460	pGEX6P-1	GST-ORC1 BAH (*H. sapiens* aa#1-185)
CP1461	pGEM-3Z	601b NPS - 6bp linker – 603 NPS - $GAL4^{P}$
CP1462	pGEM-3Z	601b NPS - 30bp linker – 603 NPS - $GAL4^{P}$
CP1463	pGEM-3Z	601b NPS - 50bp linker – 603 NPS - $GAL4^{P}$
CP1464	pGEM-3Z	601b NPS - 70bp linker – 603 NPS - $GAL4^{P}$

Appendix 3: Yeast Strains

Strain #	Source	*MAT*	Genotype
CY57		MAT_{α}	*swi2Δ::*His^{+} *lys2-801*^{A} *ade2-101*^{o} *trp1-Δ1 his3-Δ200 leu2-Δ1 ura3-52*
CY118		MAT_{A}	*swi2Δ::*His^{+} from CY57 background BUT Trp^{+}
CY384		MAT_{A}	α tester

CY385		MAT_{α}	A tester
CY915	JKM179	MAT_{α}	*Δho Δhml::ADE1 Δhmr::ADE1 ade1-100 leu2,3-112 lys5 trp1::hisG ura3-52 ade3::GAL::HO*
CY924	JKM154	MAT_{A}	*Δho ade1-100 leu2,3-112 lys5 trp1::hisG ura3-52 ade3::GAL::HO*
CY971	W303	MAT_{a}	*swi2Δ::HIS3 leu2-3,112 trp1-1 can1-100 ura3-1 ade2-1 his3-11,15*
CY1274	WDHY668	$MAT_{A/\alpha}$	*ura3-52 trp1 leu2-Δ1 his3-Δ200 pep4Δ::HIS3 prb1-Δ1.6R can1*
CY1496		$MAT_{A/\alpha}$	CY1274 with *[CP1165]*
CY1497		$MAT_{A/\alpha}$	CY1274 with *[CP1163 and CP1164]*
CY1503	BY4741	MAT_{A}	*RSC2-TAP*
CY1504	BY4741	MAT_{A}	*ISW2-FLAG*
CY1552	BY4741	MAT_{A}	*SWI2-TAP*
CY1752	W303	$MAT_{A/\alpha}$	*swi2Δ::HIS3/SWI2 sir3Δ::HphMX/SIR3*
CY1754	L1088	MAT_{A}	*ura3Δ0 leu2Δ0 TEL-VR::URA3*
CY1755	L1089	MAT_{A}	*ura3-52 leu2Δ0 snf2Δ::LEU2 TEL-VR::URA3*
CY1760		$MAT_{A/\alpha}$	CY915 and CY924 mated; *swi2Δ::NatMX/SWI2*
CY1761		MAT_{α}	*swi2Δ::NatMX* segregant from CY1760 with HML_{α} HMR_{A}
CY1762		MAT_{α}	*swi2Δ::NatMX* segregant from CY1760 with HML_{α} HMR_{A}
CY1765		MAT_{A}	CY924 with *URA3::atTIR1* (CP1211 StuI-linearized)
CY1766		MAT_{A}	CY1765 with *SWI2-AID::HphMX*
CY2041			*swi2Δ::HIS3* segregant from CY1752
CY2332		MAT_{α}	CY57 with *sir3Δ::HphMX [CP1410 (SWI2 in pRS410)]*
CY2333		MAT_{α}	CY57 with *sir3Δ::HphMX [CP1413 (Δ10R in pRS410)]*

Bibliography

Ai, W., Bertram, P.G., Tsang, C.K., Chan, T.-F., and Zheng, X.F.S. (2002). Regulation of Subtelomeric Silencing during Stress Response. Molecular Cell *10*, 1295–1305.

Allahverdi, A., Yang, R., Korolev, N., Fan, Y., Davey, C.A., Liu, C.-F., and Nordenskiold, L. (2011). The effects of histone H4 tail acetylations on cation-induced chromatin folding and self-association. Nucleic Acids Research *39*, 1680–1691.

Altaf, M., Auger, A., Monnet-Saksouk, J., Brodeur, J., Piquet, S., Cramet, M., Bouchard, N., Lacoste, N., Utley, R.T., Gaudreau, L., *et al.* (2010). NuA4-dependent Acetylation of Nucleosomal Histones H4 and H2A Directly Stimulates Incorporation of H2A.Z by the SWR1 Complex. Journal of Biological Chemistry *285*, 15966–15977.

Aparicio, O.M., Billington, B.L., and Gottschling, D.E. (1991). Modifiers of position effect are shared between telomeric and silent mating-type loci in S. cerevisiae. Cell *66*, 1279–1287.

Arents, G., Burlingame, R.W., Wang, B.C., Love, W.E., and Moudrianakis, E.N. (1991). The nucleosomal core histone octamer at 3.1 A resolution: a tripartite protein assembly and a left-handed superhelix. Proc. Natl. Acad. Sci. U.S.A. *88*, 10148–10152.

Armache, K.-J., Garlick, J.D., Canzio, D., Narlikar, G.J., and Kingston, R.E. (2011). Structural Basis of Silencing: Sir3 BAH Domain in Complex with a Nucleosome at 3.0 A Resolution. Science *334*, 977–982.

Arnaudo, N., Fernández, I.S., McLaughlin, S.H., Peak-Chew, S.Y., Rhodes, D., and Martino, F. (2013). The N-terminal acetylation of Sir3 stabilizes its binding to the nucleosome core particle. Nature Structural & Molecular Biology *20*, 1119–1121.

Auble, D.T. (2009). The dynamic personality of TATA-binding protein. Trends in Biochemical Sciences *34*, 49–52.

Bannister, A.J., and Kouzarides, T. (2011). Regulation of chromatin by histone modifications. Cell Research *21*, 381–395.

Bazett-Jones, D.P., Côté, J., Landel, C.C., Peterson, C.L., and Workman, J.L. (1999). The SWI/SNF complex creates loop domains in DNA and polynucleosome arrays and can disrupt DNA-histone contacts within these domains. Molecular and Cellular Biology *19*, 1470–1478.

Bell, S.P. (2002). The origin recognition complex: from simple origins to complex functions. Genes Dev. *16*, 659–672.

Bell, S.P., Mitchell, J., Leber, J., Kobayashi, R., and Stillman, B. (1995). The multidomain structure of Orc1p reveals similarity to regulators of DNA replication and transcriptional silencing. Cell *83*, 563–568.

Belmont, A.S. (1994). Visualization of G1 chromosomes: a folded, twisted, supercoiled chromonema model of interphase chromatid structure. The Journal of Cell Biology *127*, 287–302.

Bolderson, E., Savage, K.I., Mahen, R., Pisupati, V., Graham, M.E., Richard, D.J., Robinson, P.J., Venkitaraman, A.R., and Khanna, K.K. (2012). Kruppel-associated Box (KRAB)-associated Co-repressor (KAP-1) Ser-473 Phosphorylation Regulates Heterochromatin Protein 1 (HP1-) Mobilization and DNA Repair in Heterochromatin. Journal of Biological Chemistry *287*, 28122–28131.

Bönisch, C., and Hake, S.B. (2012). Histone H2A variants in nucleosomes and chromatin: more or less stable? Nucl. Acids Res. gks865.

Boyer, L.A., Langer, M.R., Crowley, K.A., Tan, S., Denu, J.M., and Peterson, C.L. (2002). Essential role for the SANT domain in the functioning of multiple chromatin remodeling enzymes. Mol. Cell *10*, 935–942.

Brockdorff, N. (2013). Noncoding RNA and Polycomb recruitment. RNA *19*, 429–442.

Brookes, E., and Shi, Y. (2014). Diverse Epigenetic Mechanisms of Human Disease. Annual Review of Genetics *48*, 237–268.

Brown, C.R., Mao, C., Falkovskaia, E., Law, J.K., and Boeger, H. (2011). In Vivo Role for the Chromatin-remodeling Enzyme SWI/SNF in the Removal of Promoter Nucleosomes by Disassembly Rather Than Sliding. Journal of Biological Chemistry *286*, 40556–40565.

Buchberger, J.R., Onishi, M., Li, G., Seebacher, J., Rudner, A.D., Gygi, S.P., and Moazed, D. (2008). Sir3-Nucleosome Interactions in Spreading of Silent Chromatin in Saccharomyces cerevisiae. Molecular and Cellular Biology *28*, 6903–6918.

Byrd, K.N., and Shearn, A. (2003). ASH1, a Drosophila trithorax group protein, is required for methylation of lysine 4 residues on histone H3. PNAS *100*, 11535–11540.

Cairns, B.R., Lorch, Y., Li, Y., Zhang, M., Lacomis, L., Erdjument-Bromage, H., Tempst, P., Du, J., Laurent, B., and Kornberg, R.D. (1996). RSC, an essential, abundant chromatin-remodeling complex. Cell *87*, 1249–1260.

Callebaut, I., Courvalin, J.-C., and Mornon, J.-P. (1999). The BAH (bromo-adjacent homology) domain: a link between DNA methylation, replication and transcriptional regulation. FEBS Letters *446*, 189–193.

Canzio, D., Larson, A., and Narlikar, G.J. (2014). Mechanisms of functional promiscuity by HP1 proteins. Trends in Cell Biology *24*, 377–386.

Carrozza, M.J., Li, B., Florens, L., Suganuma, T., Swanson, S.K., Lee, K.K., Shia, W.-J., Anderson, S., Yates, J., Washburn, M.P., *et al.* (2005). Histone H3 methylation by Set2 directs deacetylation of coding regions by Rpd3S to suppress spurious intragenic transcription. Cell *123*, 581–592.

Chai, B., Huang, J., Cairns, B.R., and Laurent, B.C. (2005). Distinct roles for the RSC and Swi/Snf ATP-dependent chromatin remodelers in DNA double-strand break repair. Genes Dev. *19*, 1656–1661.

Chambers, A.L., Brownlee, P.M., Durley, S.C., Beacham, T., Kent, N.A., and Downs, J.A. (2012). The Two Different Isoforms of the RSC Chromatin Remodeling Complex Play Distinct Roles in DNA Damage Responses. PLoS ONE *7*, e32016.

Chambers, A.L., Pearl, L.H., Oliver, A.W., and Downs, J.A. (2013). The BAH domain of Rsc2 is a histone H3 binding domain. Nucleic Acids Research *41*, 9168–9182.

Chang, J.-F., Hall, B.E., Tanny, J.C., Moazed, D., Filman, D., and Ellenberger, T. (2003). Structure of the coiled-coil dimerization motif of Sir4 and its interaction with Sir3. Structure *11*, 637–649.

Chiolo, I., Minoda, A., Colmenares, S.U., Polyzos, A., Costes, S.V., and Karpen, G.H. (2011). Double-Strand Breaks in Heterochromatin Move Outside of a Dynamic HP1a Domain to Complete Recombinational Repair. Cell *144*, 732–744.

Clapier, C.R., and Cairns, B.R. (2009). The Biology of Chromatin Remodeling Complexes. Annual Review of Biochemistry *78*, 273–304.

Clapier, C.R., and Cairns, B.R. (2012). Regulation of ISWI involves inhibitory modules antagonized by nucleosomal epitopes. Nature *492*, 280–284.

Cockell, M., Gotta, M., Palladino, F., Martin, S.G., and Gasser, S.M. (1998). Targeting Sir Proteins to Sites of Action: A General Mechanism for Regulated Repression. Cold Spring Harbor Symposia on Quantitative Biology *63*, 401–412.

Collart, M.A., and Oliviero, S. (2001). Preparation of Yeast RNA. In Current Protocols in Molecular Biology, (John Wiley & Sons, Inc.),.

Connelly, J.J., Yuan, P., Hsu, H.-C., Li, Z., Xu, R.-M., and Sternglanz, R. (2006). Structure and Function of the Saccharomyces cerevisiae Sir3 BAH Domain. Molecular and Cellular Biology *26*, 3256–3265.

Corpet, A., and Almouzni, G. (2009). Making copies of chromatin: the challenge of nucleosomal organization and epigenetic information. Trends in Cell Biology *19*, 29–41.

Cote, J., Quinn, J., Workman, J.L., and Peterson, C.L. (1994). Stimulation of GAL4 derivative binding to nucleosomal DNA by the yeast SWI/SNF complex. Science *265*, 53–60.

Dechassa, M.L., Zhang, B., Horowitz-Scherer, R., Persinger, J., Woodcock, C.L., Peterson, C.L., and Bartholomew, B. (2008). Architecture of the SWI/SNF-Nucleosome Complex. Molecular and Cellular Biology *28*, 6010–6021.

Dechassa, M.L., Sabri, A., Pondugula, S., Kassabov, S.R., Chatterjee, N., Kladde, M.P., and Bartholomew, B. (2010). SWI/SNF Has Intrinsic Nucleosome Disassembly Activity that Is Dependent on Adjacent Nucleosomes. Molecular Cell *38*, 590–602.

Delmas, V., Stokes, D.G., and Perry, R.P. (1993). A mammalian DNA-binding protein that contains a chromodomain and an SNF2/SWI2-like helicase domain. PNAS *90*, 2414–2418.

Dixon, J.R., Selvaraj, S., Yue, F., Kim, A., Li, Y., Shen, Y., Hu, M., Liu, J.S., and Ren, B. (2012). Topological domains in mammalian genomes identified by analysis of chromatin interactions. Nature *485*, 376–380.

Dorigo, B. (2004). Nucleosome Arrays Reveal the Two-Start Organization of the Chromatin Fiber. Science *306*, 1571–1573.

Downs, J.A., Lowndes, N.F., and Jackson, S.P. (2000). A role for Saccharomyces cerevisiae histone H2A in DNA repair. Nature *408*, 1001–1004.

Dror, V., and Winston, F. (2004). The Swi/Snf Chromatin Remodeling Complex Is Required for Ribosomal DNA and Telomeric Silencing in Saccharomyces cerevisiae. Molecular and Cellular Biology *24*, 8227–8235.

Dubarry, M., Loiodice, I., Chen, C.L., Thermes, C., and Taddei, A. (2011). Tight protein-DNA interactions favor gene silencing. Genes & Development *25*, 1365–1370.

Dürr, H., Körner, C., Müller, M., Hickmann, V., and Hopfner, K.-P. (2005). X-Ray Structures of the Sulfolobus solfataricus SWI2/SNF2 ATPase Core and Its Complex with DNA. Cell *121*, 363–373.

Dürr, H., Flaus, A., Owen-Hughes, T., and Hopfner, K.-P. (2006). Snf2 family ATPases and DExx box helicases: differences and unifying concepts from high-resolution crystal structures. Nucl. Acids Res. *34*, 4160–4167.

Dutta, A., Gogol, M., Kim, J.-H., Smolle, M., Venkatesh, S., Gilmore, J., Florens, L., Washburn, M.P., and Workman, J.L. (2014). Swi/Snf dynamics on stress-responsive genes is governed by competitive bromodomain interactions. Genes Dev. *28*, 2314–2330.

Edmondson, D.G., and Dent, S.Y.R. (2001). Identification of Protein Interactions by Far Western Analysis. In Current Protocols in Protein Science, (John Wiley & Sons, Inc.),.

Ehrentraut, S., Hassler, M., Oppikofer, M., Kueng, S., Weber, J.M., Mueller, J.W., Gasser, S.M., Ladurner, A.G., and Ehrenhofer-Murray, A.E. (2011). Structural basis for the role of the Sir3 AAA+ domain in silencing: interaction with Sir4 and unmethylated histone H3K79. Genes & Development *25*, 1835–1846.

Elfring, L.K., Deuring, R., McCallum, C.M., Peterson, C.L., and Tamkun, J.W. (1994). Identification and characterization of Drosophila relatives of the yeast transcriptional activator SNF2/SWI2. Mol. Cell. Biol. *14*, 2225–2234.

Filion, G.J., van Bemmel, J.G., Braunschweig, U., Talhout, W., Kind, J., Ward, L.D., Brugman, W., de Castro, I.J., Kerkhoven, R.M., Bussemaker, H.J., *et al.* (2010). Systematic Protein Location Mapping Reveals Five Principal Chromatin Types in Drosophila Cells. Cell *143*, 212–224.

Fox, C.A. (1997). The Origin Recognition Complex, SIR1, and the S Phase Requirement for Silencing. Science *276*, 1547–1551.

Fox, C.A., Loo, S., Dillin, A., and Rine, J. (1995). The origin recognition complex has essential functions in transcriptional silencing and chromosomal replication. Genes Dev. *9*, 911–924.

Furuyama, T., Banerjee, R., Breen, T.R., and Harte, P.J. (2004). SIR2 is required for polycomb silencing and is associated with an E(Z) histone methyltransferase complex. Curr. Biol. *14*, 1812–1821.

Ghaemmaghami, S., Huh, W.-K., Bower, K., Howson, R.W., Belle, A., Dephoure, N., O'Shea, E.K., and Weissman, J.S. (2003). Global analysis of protein expression in yeast. Nature *425*, 737–741.

Ghidelli, S. (2001). Sir2p exists in two nucleosome-binding complexes with distinct deacetylase activities. The EMBO Journal *20*, 4522–4535.

Goldstein, A.L., and McCusker, J.H. (1999). Three new dominant drug resistance cassettes for gene disruption in Saccharomyces cerevisiae. Yeast *15*, 1541–1553.

Gong, F., Fahy, D., and Smerdon, M.J. (2006). Rad4–Rad23 interaction with SWI/SNF links ATP-dependent chromatin remodeling with nucleotide excision repair. Nature Structural & Molecular Biology *13*, 902–907.

Gottlieb, S., and Esposito, R.E. (1989). A new role for a yeast transcriptional silencer gene, SIR2, in regulation of recombination in ribosomal DNA. Cell *56*, 771–776.

Gottschling, D.E., Aparicio, O.M., Billington, B.L., and Zakian, V.A. (1990). Position effect at S. cerevisiae telomeres: Reversible repression of Pol II transcription. Cell *63*, 751–762.

Gozani, O., and Shi, Y. (2014). Histone Methylation in Chromatin Signaling. In Fundamentals of Chromatin, J.L. Workman, and S.M. Abmayr, eds. (New York, NY: Springer New York), pp. 213–256.

Grewal, S.I.S., and Jia, S. (2007). Heterochromatin revisited. Nat Rev Genet *8*, 35–46.

Grunstein, M., and Gasser, S.M. (2013). Epigenetics in Saccharomyces cerevisiae. Cold Spring Harbor Perspectives in Biology *5*, a017491–a017491.

Hansen, J.C. (2002). Conformational Dynamics of the Chromatin Fiber in Solution: Determinants, Mechanisms, and Functions. Annual Review of Biophysics and Biomolecular Structure *31*, 361–392.

Hansen, J.C., Ausio, J., Stanik, V.H., and Van Holde, K.E. (1989). Homogeneous reconstituted oligonucleosomes, evidence for salt-dependent folding in the absence of histone H1. Biochemistry *28*, 9129–9136.

Hansen, J.C., van Holde, K.E., and Lohr, D. (1991). The mechanism of nucleosome assembly onto oligomers of the sea urchin 5 S DNA positioning sequence. J. Biol. Chem. *266*, 4276–4282.

Hathaway, N.A., Bell, O., Hodges, C., Miller, E.L., Neel, D.S., and Crabtree, G.R. (2012). Dynamics and Memory of Heterochromatin in Living Cells. Cell *149*, 1447–1460.

Hauk, G., and Bowman, G.D. (2011). Structural insights into regulation and action of SWI2/SNF2 ATPases. Current Opinion in Structural Biology *21*, 719–727.

Hauk, G., McKnight, J.N., Nodelman, I.M., and Bowman, G.D. (2010). The Chromodomains of the Chd1 Chromatin Remodeler Regulate DNA Access to the ATPase Motor. Molecular Cell *39*, 711–723.

Hayes, J.J., Tullius, T.D., and Wolffe, A.P. (1990). The structure of DNA in a nucleosome. Proc Natl Acad Sci U S A *87*, 7405–7409.

Hecht, A., Strahl-Bolsinger, S., and Grunstein, M. (1996). Spreading of transcriptional repressor SIR3 from telomeric heterochromatin. Nature *383*, 92–96.

Hecht, Andreas, Laroche, Thierry, Strahl-Bolsinger, Sabine, Gasser, Susan M., and Grunstein, Michael (1995). Histone H3 and H4 N-termini interact with SIR3 and SIR4 proteins: A molecular model for the formation of heterochromatin in yeast. Cell *80*, 583–592.

Heitz E. (1928). Das Heterochromatin der Moose. Jahrb Wiss Botanik *1928*, 762–818.

Herskowitz, I., and Jensen, R.E. (1991). Putting the HO gene to work: Practical uses for mating-type switching. In Methods in Enzymology, G.R.F. Christine Guthrie, ed. (Academic Press), pp. 132–146.

Hickman, M.A., and Rusche, L.N. (2010). Transcriptional silencing functions of the yeast protein Orc1/Sir3 subfunctionalized after gene duplication. Proceedings of the National Academy of Sciences *107*, 19384–19389.

Hickman, M.A., Froyd, C.A., and Rusche, L.N. (2011). Reinventing Heterochromatin in Budding Yeasts: Sir2 and the Origin Recognition Complex Take Center Stage. Eukaryotic Cell *10*, 1183–1192.

Horn, P.J., and Peterson, C.L. (2002). Chromatin Higher Order Folding--Wrapping up Transcription. Science *297*, 1824–1827.

Hsu, H.-C., Stillman, B., and Xu, R.-M. (2005). Structural basis for origin recognition complex 1 protein–silence information regulator 1 protein interaction in epigenetic silencing. Proceedings of the National Academy of Sciences of the United States of America *102*, 8519–8524.

Hsu, H.-C., Wang, C.-L., Wang, M., Yang, N., Chen, Z., Sternglanz, R., and Xu, R.-M. (2013). Structural basis for allosteric stimulation of Sir2 activity by Sir4 binding. Genes & Development *27*, 64–73.

Hughes, A.L., and Rando, O.J. (2015). Comparative Genomics Reveals Chd1 as a Determinant of Nucleosome Spacing in Vivo. G3 (Bethesda).

Hwang, W.L., Deindl, S., Harada, B.T., and Zhuang, X. (2014). Histone H4 tail mediates allosteric regulation of nucleosome remodelling by linker DNA. Nature *512*, 213–217.

Imai, S., Armstrong, C.M., Kaeberlein, M., and Guarente, L. (2000). Transcriptional silencing and longevity protein Sir2 is an NAD-dependent histone deacetylase. Nature *403*, 795–800.

Iwafuchi-Doi, M., and Zaret, K.S. (2014). Pioneer transcription factors in cell reprogramming. Genes Dev. *28*, 2679–2692.

Jaskelioff, M., Gavin, I.M., Peterson, C.L., and Logie, C. (2000). SWI-SNF-mediated nucleosome remodeling: role of histone octamer mobility in the persistence of the remodeled state. Molecular and Cellular Biology *20*, 3058–3068.

Javaid, S., Manohar, M., Punja, N., Mooney, A., Ottesen, J.J., Poirier, M.G., and Fishel, R. (2009). Nucleosome remodeling by hMSH2-hMSH6. Mol Cell *36*, 1086–1094.

Johnson, A., Li, G., Sikorski, T.W., Buratowski, S., Woodcock, C.L., and Moazed, D. (2009). Reconstitution of Heterochromatin-Dependent Transcriptional Gene Silencing. Molecular Cell *35*, 769–781.

Johnson, A., Wu, R., Peetz, M., Gygi, S.P., and Moazed, D. (2013). Heterochromatic Gene Silencing by Activator Interference and a

Transcription Elongation Barrier. Journal of Biological Chemistry *288*, 28771–28782.

Johnson, L.M., Kayne, P.S., Kahn, E.S., and Grunstein, M. (1990). Genetic evidence for an interaction between SIR3 and histone H4 in the repression of the silent mating loci in Saccharomyces cerevisiae. Proceedings of the National Academy of Sciences *87*, 6286–6290.

Kadoch, C., and Crabtree, G.R. (2013). Reversible Disruption of mSWI/SNF (BAF) Complexes by the SS18-SSX Oncogenic Fusion in Synovial Sarcoma. Cell *153*, 71–85.

Kadoch, C., Hargreaves, D.C., Hodges, C., Elias, L., Ho, L., Ranish, J., and Crabtree, G.R. (2013). Proteomic and bioinformatic analysis of mammalian SWI/SNF complexes identifies extensive roles in human malignancy. Nature Genetics *45*, 592–601.

Kakarougkas, A., Ismail, A., Chambers, A.L., Riballo, E., Herbert, A.D., Künzel, J., Löbrich, M., Jeggo, P.A., and Downs, J.A. (2014). Requirement for PBAF in Transcriptional Repression and Repair at DNA Breaks in Actively Transcribed Regions of Chromatin. Molecular Cell.

Kelley, L.A., and Sternberg, M.J.E. (2009). Protein structure prediction on the Web: a case study using the Phyre server. Nat. Protocols *4*, 363–371.

Kim, J.-H., Saraf, A., Florens, L., Washburn, M., and Workman, J.L. (2010). Gcn5 regulates the dissociation of SWI/SNF from chromatin by acetylation of Swi2/Snf2. Genes & Development *24*, 2766–2771.

Kimura, A., Umehara, T., and Horikoshi, M. (2002). Chromosomal gradient of histone acetylation established by Sas2p and Sir2p functions as a shield against gene silencing. Nature Genetics *32*, 370–377.

King, D.A., Hall, B.E., Iwamoto, M.A., Win, K.Z., Chang, J.F., and Ellenberger, T. (2006). Domain Structure and Protein Interactions of the Silent Information Regulator Sir3 Revealed by Screening a Nested Deletion Library of Protein Fragments. Journal of Biological Chemistry *281*, 20107–20119.

Kitada, T., Kuryan, B.G., Tran, N.N.H., Song, C., Xue, Y., Carey, M., and Grunstein, M. (2012). Mechanism for epigenetic variegation of gene expression at yeast telomeric heterochromatin. Genes & Development *26*, 2443–2455.

Klemm, R.D., Austin, R.J., and Bell, S.P. (1997). Coordinate Binding of ATP and Origin DNA Regulates the ATPase Activity of the Origin Recognition Complex. Cell *88*, 493–502.

Kornberg, R.D. (1977). Structure of Chromatin. Annual Review of Biochemistry *46*, 931–954.

Kruger, W., Peterson, C.L., Sil, A., Coburn, C., Arents, G., Moudrianakis, E.N., and Herskowitz, I. (1995). Amino acid substitutions in the structured domains of histones H3 and H4 partially relieve the requirement of the yeast SWI/SNF complex for transcription. Genes Dev. *9*, 2770–2779.

Kueng, S., Tsai-Pflugfelder, M., Oppikofer, M., Ferreira, H.C., Roberts, E., Tsai, C., Roloff, T.-C., Sack, R., and Gasser, S.M. (2012). Regulating Repression: Roles for the Sir4 N-Terminus in Linker DNA Protection and Stabilization of Epigenetic States. PLoS Genetics *8*, e1002727.

Kuo, A.J., Song, J., Cheung, P., Ishibe-Murakami, S., Yamazoe, S., Chen, J.K., Patel, D.J., and Gozani, O. (2012). The BAH domain of ORC1 links H4K20me2 to DNA replication licensing and Meier-Gorlin syndrome. Nature *484*, 115–119.

Kwon, H., Imbalzano, A.N., Khavari, P.A., Kingston, R.E., and Green, M.R. (1994). Nucleosome disruption and enhancement of activator binding by a human SW1/SNF complex. Nature *370*, 477–481.

Lai, A.Y., and Wade, P.A. (2011). Cancer biology and NuRD: a multifaceted chromatin remodelling complex. Nature Reviews Cancer *11*, 588–596.

Lau, A., Blitzblau, H., and Bell, S.P. (2002). Cell-cycle control of the establishment of mating-type silencing in S. cerevisiae. Genes Dev. *16*, 2935–2945.

Laugesen, A., and Helin, K. (2014). Chromatin Repressive Complexes in Stem Cells, Development, and Cancer. Cell Stem Cell *14*, 735–751.

Lavigne, M., Eskeland, R., Azebi, S., Saint-André, V., Jang, S.M., Batsché, E., Fan, H.-Y., Kingston, R.E., Imhof, A., and Muchardt, C. (2009). Interaction of HP1 and Brg1/Brm with the Globular Domain of Histone H3 Is Required for HP1-Mediated Repression. PLoS Genetics *5*, e1000769.

van Leeuwen, F., Gafken, P.R., and Gottschling, D.E. (2002). Dot1p modulates silencing in yeast by methylation of the nucleosome core. Cell *109*, 745–756.

Lenstra, T.L., Benschop, J.J., Kim, T., Schulze, J.M., Brabers, N.A.C.H., Margaritis, T., van de Pasch, L.A.L., van Heesch, S.A.A.C., Brok, M.O., Groot Koerkamp, M.J.A., *et al.* (2011). The Specificity and Topology of Chromatin Interaction Pathways in Yeast. Molecular Cell *42*, 536–549.

Leschziner, A.E., Saha, A., Wittmeyer, J., Zhang, Y., Bustamante, C., Cairns, B.R., and Nogales, E. (2007). Conformational flexibility in the chromatin remodeler RSC observed by electron microscopy and the orthogonal tilt reconstruction method. Proceedings of the National Academy of Sciences *104*, 4913–4918.

Lewis, E.B. (1978). A gene complex controlling segmentation in Drosophila. *276*, 565.

Li, G., and Widom, J. (2004). Nucleosomes facilitate their own invasion. Nat Struct Mol Biol *11*, 763–769.

Li, C., Chen, C., Gao, L., Yang, S., Nguyen, V., Shi, X., Siminovitch, K., Kohalmi, S.E., Huang, S., Wu, K., *et al.* (2015). The Arabidopsis SWI2/SNF2 Chromatin Remodeler BRAHMA Regulates Polycomb Function during Vegetative Development and Directly Activates the Flowering Repressor Gene SVP. PLoS Genet *11*, e1004944.

Lieberman-Aiden, E., van Berkum, N.L., Williams, L., Imakaev, M., Ragoczy, T., Telling, A., Amit, I., Lajoie, B.R., Sabo, P.J., Dorschner, M.O., *et al.* (2009). Comprehensive mapping of long range interactions reveals folding principles of the human genome. Science *326*, 289–293.

Ling, X., Harkness, T.A., Schultz, M.C., Fisher-Adams, G., and Grunstein, M. (1996). Yeast histone H3 and H4 amino termini are important for nucleosome assembly in vivo and in vitro: redundant and position-independent functions in assembly but not in gene regulation. Genes Dev. *10*, 686–699.

Liou, G.-G., Tanny, J.C., Kruger, R.G., Walz, T., and Moazed, D. (2005). Assembly of the SIR Complex and Its Regulation by O-Acetyl-ADP-Ribose, a Product of NAD-Dependent Histone Deacetylation. Cell *121*, 515–527.

Liu, N., Balliano, A., and Hayes, J.J. (2011). Mechanism(s) of SWI/SNF-Induced Nucleosome Mobilization. Chembiochem *12*, 196–204.

Logie, C., and Peterson, C.L. (1997). Catalytic activity of the yeast SWI/SNF complex on reconstituted nucleosome arrays. The EMBO Journal *16*, 6772–6782.

Lohr, D., and Holde, K.E.V. (1979). Organization of spacer DNA in chromatin. PNAS *76*, 6326–6330.

Lu, P.Y.T., and Kobor, M.S. (2014). Maintenance of Heterochromatin Boundary and Nucleosome Composition at Promoters by the Asf1 Histone Chaperone and SWR1-C Chromatin Remodeler in Saccharomyces cerevisiae. Genetics *197*, 133–145.

Lu, X., Simon, M.D., Chodaparambil, J.V., Hansen, J.C., Shokat, K.M., and Luger, K. (2008). The effect of H3K79 dimethylation and H4K20 trimethylation on nucleosome and chromatin structure. Nature Structural & Molecular Biology *15*, 1122–1124.

Luger, K., Mäder, A.W., Richmond, R.K., Sargent, D.F., and Richmond, T.J. (1997a). Crystal structure of the nucleosome core particle at 2.8 Å resolution. Nature *389*, 251–260.

Luger, K., Rechsteiner, T.J., Flaus, A.J., Waye, M.M., and Richmond, T.J. (1997b). Characterization of nucleosome core particles containing histone proteins made in bacteria. Journal of Molecular Biology *272*, 301–311.

Luo, K., Vega-Palas, M.A., and Grunstein, M. (2002). Rap1–Sir4 binding independent of other Sir, yKu, or histone interactions initiates the assembly of telomeric heterochromatin in yeast. Genes Dev *16*, 1528–1539.

Manning, B.J., and Peterson, C.L. (2013). Releasing the brakes on a chromatin-remodeling enzyme. Nature Structural & Molecular Biology *20*, 5–7.

Manning, B.J., and Peterson, C.L. (2014). Direct interactions promote eviction of the Sir3 heterochromatin protein by the SWI/SNF chromatin remodeling enzyme. PNAS *111*, 17827–17832.

Meneghini, M.D., Wu, M., and Madhani, H.D. (2003). Conserved histone variant H2A.Z protects euchromatin from the ectopic spread of silent heterochromatin. Cell *112*, 725–736.

Mizuguchi, G. (2004). ATP-Driven Exchange of Histone H2AZ Variant Catalyzed by SWR1 Chromatin Remodeling Complex. Science *303*, 343–348.

Moazed, D., Kistler, A., Axelrod, A., Rine, J., and Johnson, A.D. (1997). Silent information regulator protein complexes in Saccharomyces cerevisiae: A SIR2/SIR4 complex and evidence for a regulatory domain in SIR4 that inhibits its interaction with SIR3. PNAS *94*, 2186–2191.

Moretti, P., Freeman, K., Coodly, L., and Shore, D. (1994). Evidence that a complex of SIR proteins interacts with the silencer and telomere-binding protein RAP1. Genes & Development *8*, 2257–2269.

Morgan, M.A., and Shilatifard, A. (2015). Chromatin signatures of cancer. Genes Dev. *29*, 238–249.

Mueller-Planitz, F., Klinker, H., Ludwigsen, J., and Becker, P.B. (2012). The ATPase domain of ISWI is an autonomous nucleosome remodeling machine. Nature Structural & Molecular Biology *20*, 82–89.

Muller, P., Park, S., Shor, E., Huebert, D.J., Warren, C.L., Ansari, A.Z., Weinreich, M., Eaton, M.L., MacAlpine, D.M., and Fox, C.A. (2010). The conserved bromo-adjacent homology domain of yeast Orc1 functions in the selection of DNA replication origins within chromatin. Genes & Development *24*, 1418–1433.

Musselman, C.A., Lalonde, M.-E., Côté, J., and Kutateladze, T.G. (2012). Perceiving the epigenetic landscape through histone readers. Nature Structural & Molecular Biology *19*, 1218–1227.

Narendra, V., Rocha, P.P., An, D., Raviram, R., Skok, J.A., Mazzoni, E.O., and Reinberg, D. (2015). CTCF establishes discrete functional chromatin domains at the Hox clusters during differentiation. Science *347*, 1017–1021.

Narlikar, G.J., Sundaramoorthy, R., and Owen-Hughes, T. (2013). Mechanisms and Functions of ATP-Dependent Chromatin-Remodeling Enzymes. Cell *154*, 490–503.

Neigeborn, L., and Carlson, M. (1984). Genes affecting the regulation of SUC2 gene expression by glucose repression in Saccharomyces cerevisiae. Genetics *108*, 845–858.

Nishimura, K., Fukagawa, T., Takisawa, H., Kakimoto, T., and Kanemaki, M. (2009). An auxin-based degron system for the rapid depletion of proteins in nonplant cells. Nat Meth *6*, 917–922.

Norris, A., and Boeke, J.D. (2010). Silent information regulator 3: the Goldilocks of the silencing complex. Genes & Development *24*, 115–122.

Oki, M., Valenzuela, L., Chiba, T., Ito, T., and Kamakaka, R.T. (2004). Barrier Proteins Remodel and Modify Chromatin To Restrict Silenced Domains. Molecular and Cellular Biology *24*, 1956–1967.

Olins, A.L., and Olins, D.E. (1974). Spheroid Chromatin Units (v Bodies). Science *183*, 330–332.

Oliver, A.W., Jones, S.A., Roe, S.M., Matthews, S., Goodwin, G.H., and Pearl, L.H. (2005). Crystal structure of the proximal BAH domain of the polybromo protein. Biochem J *389*, 657–664.

Onishi, M., Liou, G.-G., Buchberger, J.R., Walz, T., and Moazed, D. (2007). Role of the Conserved Sir3-BAH Domain in Nucleosome Binding and Silent Chromatin Assembly. Molecular Cell *28*, 1015–1028.

Oppikofer, M., Kueng, S., Martino, F., Soeroes, S., Hancock, S.M., Chin, J.W., Fischle, W., and Gasser, S.M. (2011). A dual role of H4K16 acetylation in the establishment of yeast silent chromatin. The EMBO Journal *30*, 2610–2621.

Oppikofer, M., Kueng, S., Keusch, J.J., Hassler, M., Ladurner, A.G., Gut, H., and Gasser, S.M. (2013a). Dimerization of Sir3 via its C-terminal winged helix domain is essential for yeast heterochromatin formation. The EMBO Journal *32*, 437–449.

Oppikofer, M., Kueng, S., and Gasser, S.M. (2013b). SIR–nucleosome interactions: Structure–function relationships in yeast silent chromatin. Gene *527*, 10–25.

Papamichos-Chronakis, M., and Peterson, C.L. (2012). Chromatin and the genome integrity network. Nature Reviews Genetics *14*, 62–75.

Papamichos-Chronakis, M., Watanabe, S., Rando, O.J., and Peterson, C.L. (2011). Global Regulation of H2A.Z Localization by the INO80 Chromatin-Remodeling Enzyme Is Essential for Genome Integrity. Cell *144*, 200–213.

Pâques, F., and Haber, J.E. (1999). Multiple Pathways of Recombination Induced by Double-Strand Breaks in Saccharomyces cerevisiae. Microbiol. Mol. Biol. Rev. *63*, 349–404.

Patel, A., McKnight, J.N., Genzor, P., and Bowman, G.D. (2011). Identification of Residues in Chromodomain Helicase DNA-Binding Protein 1 (Chd1) Required for Coupling ATP Hydrolysis to Nucleosome Sliding. Journal of Biological Chemistry *286*, 43984–43993.

Patel, A., Chakravarthy, S., Morrone, S., Nodelman, I.M., McKnight, J.N., and Bowman, G.D. (2013). Decoupling nucleosome recognition from DNA binding dramatically alters the properties of the Chd1 chromatin remodeler. Nucleic Acids Research *41*, 1637–1648.

Peng, J.C., and Karpen, G.H. (2007). H3K9 methylation and RNA interference regulate nucleolar organization and repeated DNA stability. Nature Cell Biology *9*, 25–35.

Peng, J.C., and Karpen, G.H. (2009). Heterochromatic Genome Stability Requires Regulators of Histone H3 K9 Methylation. PLoS Genetics *5*, e1000435.

Peterson, C.L., and Herskowitz, I. (1992). Characterization of the yeast SWI1, SWI2, and SWI3 genes, which encode a global activator of transcription. Cell *68*, 573–583.

Peterson, C.L., Kruger, W., and Herskowitz, I. (1991). A functional interaction between the C-terminal domain of RNA polymerase II and the negative regulator SIN1. Cell *64*, 1135–1143.

Peterson, C.L., Dingwall, A., and Scott, M.P. (1994). Five SWI/SNF gene products are components of a large multisubunit complex required for transcriptional enhancement. PNAS *91*, 2905–2908.

Pope, B.D., Ryba, T., Dileep, V., Yue, F., Wu, W., Denas, O., Vera, D.L., Wang, Y., Hansen, R.S., Canfield, T.K., *et al.* (2014). Topologically associating domains are stable units of replication-timing regulation. Nature *515*, 402–405.

Poulose, N., and Raju, R. (2015). Sirtuin regulation in aging and injury. Biochim. Biophys. Acta.

Radman-Livaja, M., Ruben, G., Weiner, A., Friedman, N., Kamakaka, R., and Rando, O.J. (2011). Dynamics of Sir3 spreading in budding yeast: secondary recruitment sites and euchromatic localization. The EMBO Journal *30*, 1012–1026.

Rando, O.J., and Winston, F. (2012). Chromatin and Transcription in Yeast. Genetics *190*, 351–387.

Rao, S.S.P., Huntley, M.H., Durand, N.C., Stamenova, E.K., Bochkov, I.D., Robinson, J.T., Sanborn, A.L., Machol, I., Omer, A.D., Lander, E.S., *et al.* (2014). A 3D Map of the Human Genome at Kilobase Resolution Reveals Principles of Chromatin Looping. Cell *159*, 1665–1680.

Rine, J., and Herskowitz, I. (1987). Four genes responsible for a position effect on expression from HML and HMR in Saccharomyces cerevisiae. Genetics *116*, 9–22.

Rivera, C., Gurard-Levin, Z.A., Almouzni, G., and Loyola, A. (2014). Histone lysine methylation and chromatin replication. Biochimica et Biophysica Acta (BBA) - Gene Regulatory Mechanisms *1839*, 1433–1439.

Robinson, P.J.J., Fairall, L., Huynh, V.A.T., and Rhodes, D. (2006). EM measurements define the dimensions of the “30-nm” chromatin fiber: Evidence for a compact, interdigitated structure. Proc Natl Acad Sci U S A *103*, 6506–6511.

Roy, R., Meier, B., McAinsh, A.D., Feldmann, H.M., and Jackson, S.P. (2004). Separation-of-function Mutants of Yeast Ku80 Reveal a Yku80p-Sir4p Interaction Involved in Telomeric Silencing. Journal of Biological Chemistry *279*, 86–94.

Ruault, M., De Meyer, A., Loiodice, I., and Taddei, A. (2011). Clustering heterochromatin: Sir3 promotes telomere clustering independently of silencing in yeast. The Journal of Cell Biology *192*, 417–431.

Rudner, A.D., Hall, B.E., Ellenberger, T., and Moazed, D. (2005). A Nonhistone Protein-Protein Interaction Required for Assembly of the SIR Complex and Silent Chromatin. Mol Cell Biol *25*, 4514–4528.

Rusche, L.N., Kirchmaier, A.L., and Rine, J. (2003). The Establishment, Inheritance, and Function of Silenced Chromatin in Saccharomyces cerevisiae. Annual Review of Biochemistry *72*, 481–516.

Schiestl, R.H., and Gietz, R.D. (1989). High efficiency transformation of intact yeast cells using single stranded nucleic acids as a carrier. Current Genetics *16*, 339–346.

Schubert, H.L., Wittmeyer, J., Kasten, M.M., Hinata, K., Rawling, D.C., Heroux, A., Cairns, B.R., and Hill, C.P. (2013). Structure of an actin-related subcomplex of the SWI/SNF chromatin remodeler. Proceedings of the National Academy of Sciences *110*, 3345–3350.

Schwarz, P.M., Felthauser, A., Fletcher, T.M., and Hansen, J.C. (1996). Reversible oligonucleosome self-association: dependence on divalent cations and core histone tail domains. Biochemistry *35*, 4009–4015.

Sen, P., Ghosh, S., Pugh, B.F., and Bartholomew, B. (2011). A new, highly conserved domain in Swi2/Snf2 is required for SWI/SNF remodeling. Nucleic Acids Research *39*, 9155–9166.

Sen, P., Vivas, P., Dechassa, M.L., Mooney, A.M., Poirier, M.G., and Bartholomew, B. (2013). The SnAC Domain of SWI/SNF Is a Histone

Anchor Required for Remodeling. Molecular and Cellular Biology *33*, 360–370.

Sexton, T., and Cavalli, G. (2015). The Role of Chromosome Domains in Shaping the Functional Genome. Cell *160*, 1049–1059.

Sexton, T., Yaffe, E., Kenigsberg, E., Bantignies, F., Leblanc, B., Hoichman, M., Parrinello, H., Tanay, A., and Cavalli, G. (2012). Three-Dimensional Folding and Functional Organization Principles of the Drosophila Genome. Cell *148*, 458–472.

Sharma, V.M., and Reese, J.C. (2003). SWI/SNF-dependent chromatin remodeling of RNR3 requires TAFIIs and the general transcription machinery. Genes & Development *17*, 502–515.

Shen, X., Mizuguchi, G., Hamiche, A., and Wu, C. (2000). A chromatin remodelling complex involved in transcription and DNA processing. Nature *406*, 541–544.

Shen, X., Ranallo, R., Choi, E., and Wu, C. (2003). Involvement of Actin-Related Proteins in ATP-Dependent Chromatin Remodeling. Molecular Cell *12*, 147–155.

Shogren-Knaak, M. (2006). Histone H4-K16 Acetylation Controls Chromatin Structure and Protein Interactions. Science *311*, 844–847.

Simon, J.A., and Kingston, R.E. (2009). Mechanisms of Polycomb gene silencing: knowns and unknowns. Nature Reviews Molecular Cell Biology.

Singleton, M.R., Dillingham, M.S., and Wigley, D.B. (2007). Structure and Mechanism of Helicases and Nucleic Acid Translocases. Annual Review of Biochemistry *76*, 23–50.

Sinha, M., and Peterson, C.L. (2008). A Rad51 Presynaptic Filament Is Sufficient to Capture Nucleosomal Homology during Recombinational Repair of a DNA Double-Strand Break. Molecular Cell *30*, 803–810.

Sinha, M., and Peterson, C.L. (2009). Chromatin dynamics during repair of chromosomal DNA double-strand breaks. Epigenomics *1*, 371–385.

Sinha, M., Watanabe, S., Johnson, A., Moazed, D., and Peterson, C.L. (2009). Recombinational Repair within Heterochromatin Requires ATP-Dependent Chromatin Remodeling. Cell *138*, 1109–1121.

Sirinakis, G., Clapier, C.R., Gao, Y., Viswanathan, R., Cairns, B.R., and Zhang, Y. (2011). The RSC chromatin remodelling ATPase translocates DNA with high force and small step size. The EMBO Journal *30*, 2364–2372.

Skiniotis, G., Moazed, D., and Walz, T. (2007). Acetylated Histone Tail Peptides Induce Structural Rearrangements in the RSC Chromatin Remodeling Complex. J. Biol. Chem. *282*, 20804–20808.

Smith, C.L., and Peterson, C.L. (2005). A Conserved Swi2/Snf2 ATPase Motif Couples ATP Hydrolysis to Chromatin Remodeling. Molecular and Cellular Biology *25*, 5880–5892.

Smith, C.L., Horowitz-Scherer, R., Flanagan, J.F., Woodcock, C.L., and Peterson, C.L. (2003). Structural analysis of the yeast SWI/SNF chromatin remodeling complex. Nature Structural Biology *10*, 141–145.

Song, J., Rechkoblit, O., Bestor, T.H., and Patel, D.J. (2011). Structure of DNMT1-DNA Complex Reveals a Role for Autoinhibition in Maintenance DNA Methylation. Science *331*, 1036–1040.

Steffen, P.A., and Ringrose, L. (2014). What are memories made of? How Polycomb and Trithorax proteins mediate epigenetic memory. Nat Rev Mol Cell Biol *15*, 340–356.

Stern, M., Jensen, R., and Herskowitz, I. (1984). Five SWI genes are required for expression of the HO gene in yeast. Journal of Molecular Biology *178*, 853–868.

Strahl-Bolsinger, S., Hecht, A., Luo, K., and Grunstein, M. (1997). SIR2 and SIR4 interactions differ in core and extended telomeric heterochromatin in yeast. Genes & Development *11*, 83–93.

Sugawara, N., and Haber, J.E. (2012). Monitoring DNA Recombination Initiated by HO Endonuclease. In DNA Repair Protocols, L. Bjergbæk, ed. (Humana Press), pp. 349–370.

Suto, R.K., Clarkson, M.J., Tremethick, D.J., and Luger, K. (2000). Crystal structure of a nucleosome core particle containing the variant histone H2A.Z. Nat Struct Mol Biol *7*, 1121–1124.

Swygert, S.G., and Peterson, C.L. (2014). Chromatin dynamics: Interplay between remodeling enzymes and histone modifications. Biochimica et Biophysica Acta (BBA) - Gene Regulatory Mechanisms *1839*, 728–736.

Swygert, S.G., Manning, B.J., Senapati, S., Kaur, P., Lindsay, S., Demeler, B., and Peterson, C.L. (2014). Solution-state conformation and stoichiometry of yeast Sir3 heterochromatin fibres. Nat Commun *5*.

Szerlong, H., Saha, A., and Cairns, B.R. (2003). The nuclear actin-related proteins Arp7 and Arp9: a dimeric module that cooperates with architectural proteins for chromatin remodeling. The EMBO Journal *22*, 3175–3187.

Szerlong, H., Hinata, K., Viswanathan, R., Erdjument-Bromage, H., Tempst, P., and Cairns, B.R. (2008). The HSA domain binds nuclear actin-related proteins to regulate chromatin-remodeling ATPases. Nature Structural & Molecular Biology *15*, 469–476.

Taddei, A., Hediger, F., Neumann, F.R., Bauer, C., and Gasser, S.M. (2004). Separation of silencing from perinuclear anchoring functions in yeast Ku80, Sir4 and Esc1 proteins. The EMBO Journal *23*, 1301–1312.

Takahashi, Y.-H., Schulze, J.M., Jackson, J., Hentrich, T., Seidel, C., Jaspersen, S.L., Kobor, M.S., and Shilatifard, A. (2011). Dot1 and Histone H3K79 Methylation in Natural Telomeric and HM Silencing. Molecular Cell *42*, 118–126.

Tatchell, K., and Van Holde, K.E. (1977). Reconstitution of chromatin core particles. Biochemistry *16*, 5295–5303.

Thakar, A., Gupta, P., Ishibashi, T., Finn, R., Silva-Moreno, B., Uchiyama, S., Fukui, K., Tomschik, M., Ausio, J., and Zlatanova, J. (2009). H2A.Z and H3.3 histone variants affect nucleosome structure: biochemical and biophysical studies. Biochemistry *48*, 10852–10857.

Tran, H.G., Steger, D.J., Iyer, V.R., and Johnson, A.D. (2000). The chromo domain protein Chd1p from budding yeast is an ATP-dependent chromatin-modifying factor. The EMBO Journal *19*, 2323–2331.

Trapnell, C., Roberts, A., Goff, L., Pertea, G., Kim, D., Kelley, D.R., Pimentel, H., Salzberg, S.L., Rinn, J.L., and Pachter, L. (2012). Differential gene and transcript expression analysis of RNA-seq experiments with TopHat and Cufflinks. Nature Protocols *7*, 562–578.

Triolo, T., and Sternglanz, R. (1996). Role of interactions between the origin recognition complex and SIR1 in transcriptional silencing. Nature *381*, 251.

Tsukamoto, Y., Kato, J., and Ikeda, H. (1997). Silencing factors participate in DNA repair and recombination in Saccharomyces cerevisiae. Nature *388*, 900–903.

Tsukiyama, T., Daniel, C., Tamkun, J., and Wu, C. (1995). ISWI, a member of the SWI2/SNF2 ATPase family, encodes the 140 kDa subunit of the nucleosome remodeling factor. Cell *83*, 1021–1026.

Vary Jr., J.C., Fazzio, T.G., and Tsukiyama, T. (2003). Assembly of Yeast Chromatin Using ISWI Complexes. In Methods in Enzymology, C. David Allis and Carl Wu, ed. (Academic Press), pp. 88–102.

Venkatesh, S., and Workman, J.L. (2015). Histone exchange, chromatin structure and the regulation of transcription. Nat Rev Mol Cell Biol *16*, 178–189.

Vicent, G.P., Nacht, A.S., Smith, C.L., Peterson, C.L., Dimitrov, S., and Beato, M. (2004). DNA instructed displacement of histones H2A and H2B at an inducible promoter. Mol. Cell *16*, 439–452.

Wang, F., Li, G., Altaf, M., Lu, C., Currie, M.A., Johnson, A., and Moazed, D. (2013). Heterochromatin protein Sir3 induces contacts between the amino terminus of histone H4 and nucleosomal DNA. Proceedings of the National Academy of Sciences *110*, 8495–8500.

Watanabe, S., Resch, M., Lilyestrom, W., Clark, N., Hansen, J.C., Peterson, C., and Luger, K. (2010). Structural characterization of H3K56Q nucleosomes and nucleosomal arrays. Biochimica et Biophysica Acta (BBA) - Gene Regulatory Mechanisms *1799*, 480–486.

Watanabe, S., Radman-Livaja, M., Rando, O.J., and Peterson, C.L. (2013). A Histone Acetylation Switch Regulates H2A.Z Deposition by the SWR-C Remodeling Enzyme. Science *340*, 195–199.

Watanabe, S., Tan, D., Lakshminarasimhan, M., Washburn, M.P., Erica Hong, E.-J., Walz, T., and Peterson, C.L. (2015). Structural analyses of the chromatin remodelling enzymes INO80-C and SWR-C. Nat Commun *6*.

Weintraub, H., and Lente, F.V. (1974). Dissection of Chromosome Structure with Trypsin and Nucleases. PNAS *71*, 4249–4253.

Wollmann, P., Cui, S., Viswanathan, R., Berninghausen, O., Wells, M.N., Moldt, M., Witte, G., Butryn, A., Wendler, P., Beckmann, R., *et al.* (2011). Structure and mechanism of the Swi2/Snf2 remodeller Mot1 in complex with its substrate TBP. Nature *475*, 403–407.

Wong, H., Victor, J.-M., and Mozziconacci, J. (2007). An All-Atom Model of the Chromatin Fiber Containing Linker Histones Reveals a Versatile Structure Tuned by the Nucleosomal Repeat Length. PLoS ONE *2*.

Woodcock, C.L., and Ghosh, R.P. (2010). Chromatin Higher-order Structure and Dynamics. Cold Spring Harb Perspect Biol *2*, a000596.

Wu, M.-F., Sang, Y., Bezhani, S., Yamaguchi, N., Han, S.-K., Li, Z., Su, Y., Slewinski, T.L., and Wagner, D. (2012). SWI2/SNF2 chromatin remodeling ATPases overcome polycomb repression and control floral organ identity with the LEAFY and SEPALLATA3 transcription factors. Proceedings of the National Academy of Sciences *109*, 3576–3581.

Xue, Y., Van, C., Pradhan, S.K., Su, T., Gehrke, J., Kuryan, B.G., Kitada, T., Vashisht, A., Tran, N., Wohlschlegel, J., *et al.* (2015). The Ino80 complex prevents invasion of euchromatin into silent chromatin. Genes Dev. *29*, 350–355.

Yang, B., Britton, J., and Kirchmaier, A.L. (2008). Insights into the Impact of Histone Acetylation and Methylation on Sir Protein Recruitment, Spreading, and Silencing in Saccharomyces cerevisiae. Journal of Molecular Biology *381*, 826–844.

Yang, D., Fang, Q., Wang, M., Ren, R., Wang, H., He, M., Sun, Y., Yang, N., and Xu, R.-M. (2013). Nα-acetylated Sir3 stabilizes the conformation of a nucleosome-binding loop in the BAH domain. Nature Structural & Molecular Biology *20*, 1116–1118.

Yang, X., Zaurin, R., Beato, M., and Peterson, C.L. (2007). Swi3p controls SWI/SNF assembly and ATP-dependent H2A-H2B displacement. Nat Struct Mol Biol *14*, 540–547.

Yelagandula, R., Stroud, H., Holec, S., Zhou, K., Feng, S., Zhong, X., Muthurajan, U.M., Nie, X., Kawashima, T., Groth, M., *et al.* (2014). The Histone Variant H2A.W Defines Heterochromatin and Promotes Chromatin Condensation in Arabidopsis. Cell *158*, 98–109.

Zentner, G.E., and Henikoff, S. (2013). Mot1 Redistributes TBP from TATA-Containing to TATA-Less Promoters. Mol. Cell. Biol. *33*, 4996–5004.

Zhang, W., Sankaran, S., Gozani, O., and Song, J. (2015). A Meier-Gorlin Syndrome Mutation Impairs the ORC1-Nucleosome Association. ACS Chem. Biol.

Zhang, Y., Smith, C.L., Saha, A., Grill, S.W., Mihardja, S., Smith, S.B., Cairns, B.R., Peterson, C.L., and Bustamante, C. (2006). DNA Translocation and Loop Formation Mechanism of Chromatin Remodeling by SWI/SNF and RSC. Molecular Cell *24*, 559–568.

Ziv, Y., Bielopolski, D., Galanty, Y., Lukas, C., Taya, Y., Schultz, D.C., Lukas, J., Bekker-Jensen, S., Bartek, J., and Shiloh, Y. (2006). Chromatin relaxation in response to DNA double-strand breaks is modulated by a novel ATM- and KAP-1 dependent pathway. Nature Cell Biology *8*, 870–876.

Zofall, M., Persinger, J., Kassabov, S.R., and Bartholomew, B. (2006). Chromatin remodeling by ISW2 and SWI/SNF requires DNA translocation inside the nucleosome. Nature Structural & Molecular Biology *13*, 339–346.